7)

Independent Control of a Molten Stream Temperature and Mass Flow Rate

by
Kenneth Amoruso

B.S. in Electrical Engineering
Rensselaer Polytechnic Institute
(1987)

Submitted to the
Department of Mechanical Engineering
in Partial Fulfillment of the Requirements
for the Degree of

Master of Science in Mechanical Engineering

at the

Massachusetts Institute of Technology

June 1996

Signature of Author _____
Department of Mechanical Engineering
March 1996

Certified By _____
David E. Hardt
Professor of Mechanical Engineering
Thesis Supervisor

Accepted By _____
Ain A. Sonin
Chairman, Committee on Graduate Students
Department of Mechanical Engineering

Independent Control of a Molten Stream Temperature and Mass Flow Rate

by
Kenneth Amoruso

Submitted to the Department of Mechanical Engineering
March 1996 in partial fulfillment of the requirements for the
Degree of Master of Science in Mechanical Engineering.

Abstract

Welding process control, controlling the output variables of a process versus the machine parameters, has been the focus of much recent research. This research identified limitations in current welding processes that prevented true process control and devised a new process, called "stream welding", to overcome these limitations. Stream welding uses a molten steel stream, whose temperature and flow rate can be controlled independently, to melt the base metal.

This research proposes a scheme to independently control the temperature and flow rate of a molten tin stream. A previously developed arc furnace was used to hold, melt, and deliver the metal. A temperature control feedback loop controlled the temperature of the molten stream. An arc resistance control loop indirectly controlled the flow of the molten stream. With a constant arc resistance and thus a constant quantity of metal in the furnace, the flow will equal the feed used to replenish the furnace.

Both control schemes were implemented successfully with the stream temperature being controlled independently of the flow. However, the flow controller could not be operated for extended periods of time. For the controller to be used in practical applications, the furnace needs to be modified.

Thesis Advisor: David E. Hardt
Title: Professor of Mechanical Engineering

Acknowledgements

I would like to thank numerous people for their help in my research:

- Professor Hardt for his guidance and for providing me the opportunity to pursue my studies.

- Benny Budiman whose constant collaboration I could not have done without.

- Everyone in the lab Ryan Boas, Boyd Bucher, Mark Grodzinsky, Andrew Parris, David Sha, Torbin Thurow, Upendra Ummethela, Marko Valjavec, and Dan Walczyk who I could always go to for answers. I learned the most from them.

- Fred Cote and Gerry Wentworth for sharing their time and expertise in the machine shop.

- Jessica Baum for her assistance in administrative matters.

- Finally, my parents for their constant support.

Table of Contents

List of Figures

List of Tables

Chapter 1: Introduction[1]

1.1 Research Purpose

This research analytically and experimentally investigated a way to accurately deliver a superheated molten metal stream at a specified flow rate and temperature. Decoupling the temperature of a molten stream from its flow rate provides a means to independently vary the heat input and metal deposition rate in processes that require this to manipulate the output variables of interest. The investigation was a continuation of efforts begun by Lee (1993), Ratliff (1994) and Budiman (1995) to improve the Gas Metal Arc Welding (GMAW) process by using a molten stream of filler metal to melt the base metal. The heat input to the weld would come from only one source, the energy stored in the high temperature filler metal. The deposition rate and mode of mass transfer would be controlled by a filler metal delivery system.

1.2 Gas Metal Arc Welding

Arc welding is a widely used joining process. It uses heat from the arc to melt the metals to be joined. An ideal weld will have the same metallurgical and geometric properties as the surrounding base metal. Measurable output parameters such as bead height, bead depth, and the heat affected zone serve as indications of these properties. Figure 1.1 illustrates the different output parameters.

GMAW has many attributes that make it a desirable welding process. It can be used to weld most commercial metals and alloys. Its deposition rates are high and long welds can be deposited because the filler metal is fed continuously.

---

[1] The figures in this section are adapted from Ratliff (1994).

GMAW, shown in Figure 1.2, uses a gas shielded arc, generated by a constant potential power supply, to melt the continuously fed wire filler metal and base metal. The shielding gas prevents oxidation of the weld. The voltage droop characteristic of the power supply maintains the arc length independent of the wire feed rate resulting in a stable arc.

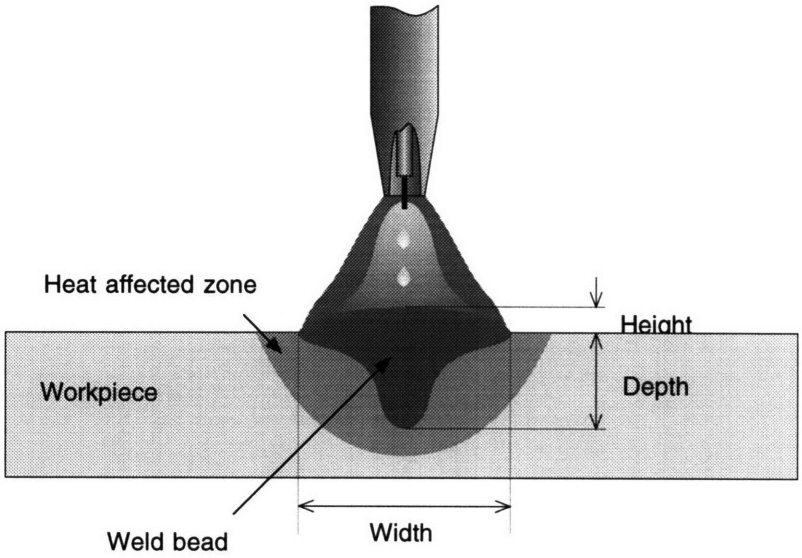

Figure 1.1 Welding Output Parameters

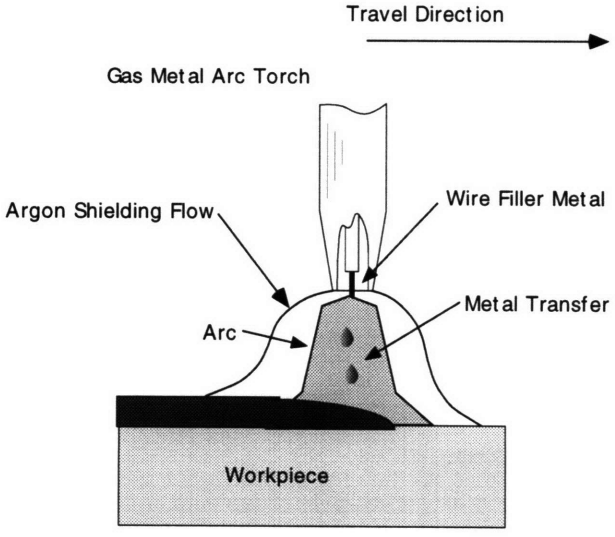

Figure 1.2 Gas Metal Arc Welding

There are several modes of mass transfer that occur in GMAW. Figure 1.3 shows the most common ones. Factors which determine the type of transfer are:

- the magnitude of the welding current
- the electrode size and composition
- the type of shielding gas
- the electrode extension.

Globular transfer typically occurs at low currents. It is characterized by large drops that are hard to control. Spray transfer, which occurs at higher currents, is characterized by smaller drops which makes splattering less likely. (O'Brien, 1991)

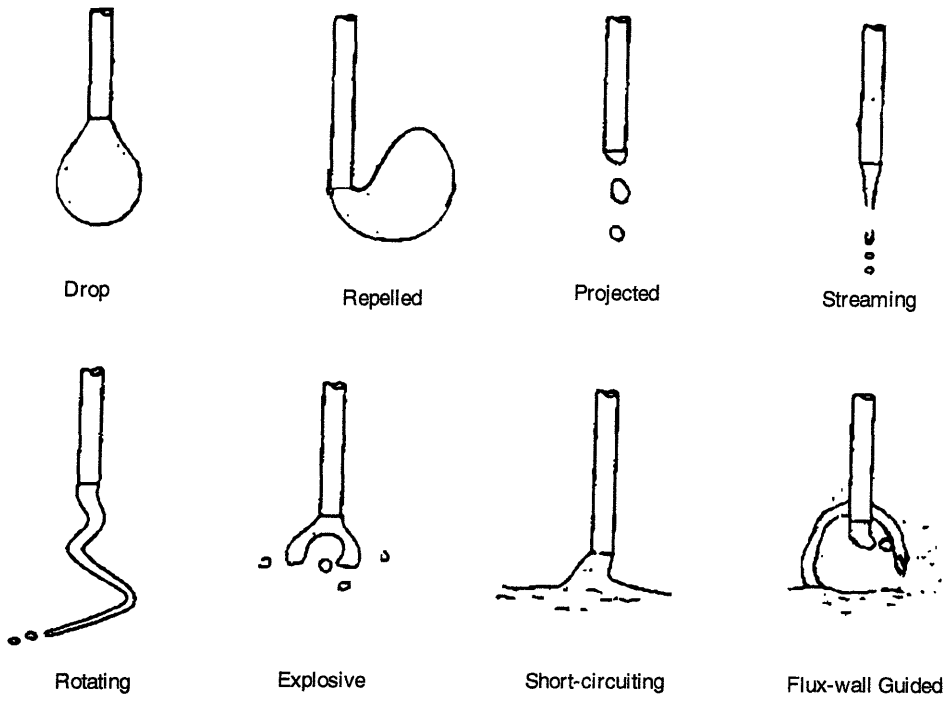

Figure 1.3 Modes of Metal Transfer

Three important GMAW parameters to be controlled are the heat input, the quantity of filler metal deposited in a weld, and the mode of filler metal transfer. They have a great impact on the metallurgical and geometric properties of a welded joint. The heat input affects the grain structure of a weld. The quantity of filler metal determines the bead height and width. The mode of filler metal transfer alters the quality of fusion and depth of penetration. Unfortunately, the three GMAW parameters are difficult to control independently. The arc current is a dominate factor in determining all three.

The equations for the heat input to a weld and the quantity of filler metal deposited onto a weld show that the arc current is a major factor for determining both. The heat input is given by:

$$P_{input} = \eta IV$$

where

P_{input} = the power transferred to the weld. (W)

η = the efficiency of the arc.

I = the arc current. (A)

V = the arc voltage. (V)

The quantity of filler metal deposited is given by:

$$WFS = aI + bLI^2$$

where

WFS = the wire feed rate. (mm/s)

a = the constant of proportionality for electrode heating. Its magnitude depends on such factors as polarity and electrode composition. (mm/s*A)

b = the constant of proportionality for electrical resistance heating. ($1/s*A^2$)

L = the electrode extension. (mm)

I = the arc current. (A)

With the arc length and voltage maintained constant, the only variable that determines the power and filler metal deposition rate is the arc current. Although, an equation is not given for the mode of filler metal transfer, the mode is also determined by the arc current.

1.3 Process Control

Process control is a means to increase the quality, reduce the cost, and increase the efficiency of a manufacturing process. The output variables of a process are controlled versus machine parameters, which ideally correlate to the output variables. To implement process control the output variables must be measurable or estimable and controllable. Hardt (1992) identified welding as a process whose output variables of interest have been measured with some success but which does not have a machine to manipulate independently the output variables.

Hale (1989) and Song (1992) attempted to conduct welding process control using GMAW. Hale tried to independently control the weld bead width, height, and depth. Song tried to independently control the weld bead width and depth. He used an estimator to determine the depth. Both came to the same conclusion. The parameters of GMAW are highly coupled in a complicated manner making effective and independent control of process outputs over a wide range impossible.

Doumanidis (1988) and Masmoudi (1992) attempted to reduce the coupling in GMAW output parameters through process modification. Doumanidis altered the heat distribution attainable in the weld by weaving the torch along the welding axis. Masmoudi accomplished the same by weaving the torch orthogonal to the welding axis. Both were able to increase the range over which process output variables could be controlled independently.

Hardt (1992) concluded that for ultimate process control in welding, the heat and mass flux distribution inputs need to be able to be manipulated independently. The success of Doumanidis and Masmoudi supports his

conclusion. Delivering molten metal at a specified flow rate and temperature is a way of doing this.

1.4 Stream Welding

Stream welding was devised as an alternative to GMAW. The concept involved decoupling the heat input, the filler metal deposition rate, and the mass transfer mode by using a stream of molten metal to conduct welding. Initial efforts in stream welding concentrated on developing the machine to be used in the process and analysis to verify that the machine could be used for welding. Research was conducted by primarily three people, Lee (1993), Ratliff (1994), and Budiman (1995).

Lee, the originator of the idea, devised the concept as an extension of spray welding (Singer, 1984) and thermal spraying (Passow, 1992). Spray welding produces a weld by preheating the base metal to above its solidus temperature, applying a filler metal in the form of a molten spray, and peening the result. The process suffers from the disadvantage of producing non-uniform spray droplets which makes the exact heat content of the spray and filler metal flow rate difficult to control. Advances in thermal spraying allow a uniform droplet spray to be formed by disturbing a molten metal stream. The heat content of a droplet is:

H_d = heat content of the solid + heat of fusion + heat content of the liquid

$$H_d = \int_{T_O}^{T_m} \rho_s C_s(T)dT + H_f + \int_{T_m}^{T_f} \rho_l C_l(T)dT$$

where

H_d = the heat content of the droplet. (J/mm^3)

T_o = the initial metal temperature. ($^\circ C$)

T_m = the melting point of the metal. (°C)

ρ_s = the density of the solid metal. (kg/mm^3)

$C_s(T)$ = the specific heat of the solid metal. (J/kg°C)

T = the temperature. (°C)

H_f = the heat of fusion. (J/mm^3)

T_f = the final temperature of the metal. (°C)

ρ_l = the density of the liquid metal. (kg/mm^3)

$C_l(T)$ = the specific heat of the liquid metal. (J/kg°C)

The mass flow rate, assuming spherical droplets of radius r, is:

$$\dot{m} = \tfrac{4}{3}\rho\pi r^3 f$$

where

$\dot{m}$ = the mass flow rate. (g/sec)

ρ = density of the molten metal. (g/m^3)

r = radius of droplet. (m)

f = frequency of droplets. (1/sec)

With the size and temperature of the droplets known, the exact heat content and flow rate of the spray can be determined and manipulated independently. Lee combined the idea of using molten metal to weld and being able to control the temperature and flow rate of a molten metal to develop stream welding. In stream welding the stream flow rate and heat content can be determined as in thermal spraying and the stream is used to weld as in spray welding.

Lee built the first prototype machine. The machine designed to implement the concept was a small arc furnace that melts and heats filler metal to a desired temperature. The arc furnace is pressurized to expel the filler metal onto a base metal. The arc furnace pressure controls the mass flow rate and the temperature of the molten metal controls the heat input. Figure 1.4 shows

the stream welding process. Lee demonstrated that welding could be conducted with a stream of tin, but only manual control was implemented.

Ratliff attempted to use steel in the arc furnace, but this eroded the graphite crucible used to hold the molten steel. The erosion made it difficult to contain the steel and led to weld contamination. Ratliff was able to achieve high temperatures in the furnace by increasing its efficiency. Steel was heated to temperatures in excess of 2000°C.

Ratliff and Budiman conducted heat transfer analyses to determine if there would be sufficient energy stored in a molten steel stream to melt a steel base. Their conclusions, which could not be verified because of the material limitation, were that the energy would not be enough.

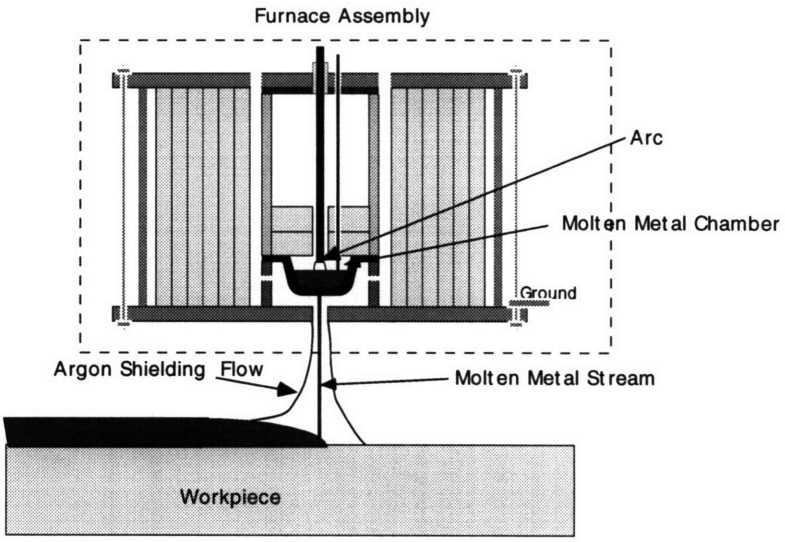

Figure 1.4 Arc Furnace Stream Welder

1.5 Molten Metal Stream Control

This research centers on a way to deliver a molten metal stream at a specified flow rate and temperature. Tin was used instead of steel to avoid crucible damage. The hope is that other applications can use this technology,

and that a material will eventually be developed that can hold molten steel so that experiments on stream welding can be conducted.

1.6 Thesis Outline

Chapter 2 goes into detail on the previous work on molten metal stream control, stream welding. It includes the specifics on the arc furnace design used to implement the idea, the initial experiments conducted to demonstrate the ability to use the stream for tin welding, the analysis of stream welding capabilities with steel, and the problems encountered when steel was used in the arc furnace. Chapter 3 covers the reasons for choosing tin as the metal to be controlled in this research. Chapter 4 describes the components of the proposed closed loop control scheme. Chapters 5 and 6 describe in detail the temperature and flow controllers. They are the two controllers used in the scheme. Chapter 5 discusses the temperature controller. It includes the requirements of the controller, dynamic models, simulated results, and experimental results. Chapter 6 discusses the flow controller. It includes the requirements of the controller, simulated results, experimental results, and limitations that prevented long term operation of the controller. Chapter 7 summarizes the progress made in this research. It also provides recommendations for future research.

Chapter 2: Previous Work on Molten Metal Stream Control[1]

2.1 Overview

Previous work on molten stream control resulted in an arc furnace that could be used to hold and deliver a molten metal other than steel and showed that a superheated steel stream could probably not melt a steel base. Three people conducted the previous research, Lee (1993), Ratliff (1994), and Budiman (1995). Lee built a prototype arc furnace in which tin was used and demonstrated that a superheated stream could be used to weld tin. His demonstration of the stream welding concept encouraged future research. Ratliff attempted to use steel in the furnace and conducted analyses on steel stream welding. He was successful in creating superheated steel in the furnace, but a crucible material could not be found to contain molten steel at high temperatures. His analysis indicated that melting of the base was not likely. Budiman conducted additional analyses on stream welding with steel. Using a different model than Ratliff, he demonstrated why welding would not occur.

2.2 The Arc Furnace

Lee developed the first prototype arc furnace, Figure 2.1, and conducted initial furnace tests. The furnace consisted of a crucible, a graphite support ring, a ceramic cylinder, thermal insulation and radiation shields, a Gas Tungsten Arc Welding (GTAW) torch, and a stainless steel shell.

The crucible holds the molten metal and has an orifice in its bottom through which the molten metal is expelled. Graphite was chosen as the crucible material, because it has a large hot strength, can withstand thermal

---

[1] The figures in this section are adapted from Ratliff (1994) and Budiman (1995).

shock, is electrically conductive so it can serve an one electrode for the arc, has a high melting point so exposure to high temperatures is not a problem, and can contain most molten materials (Campbell, 1967).

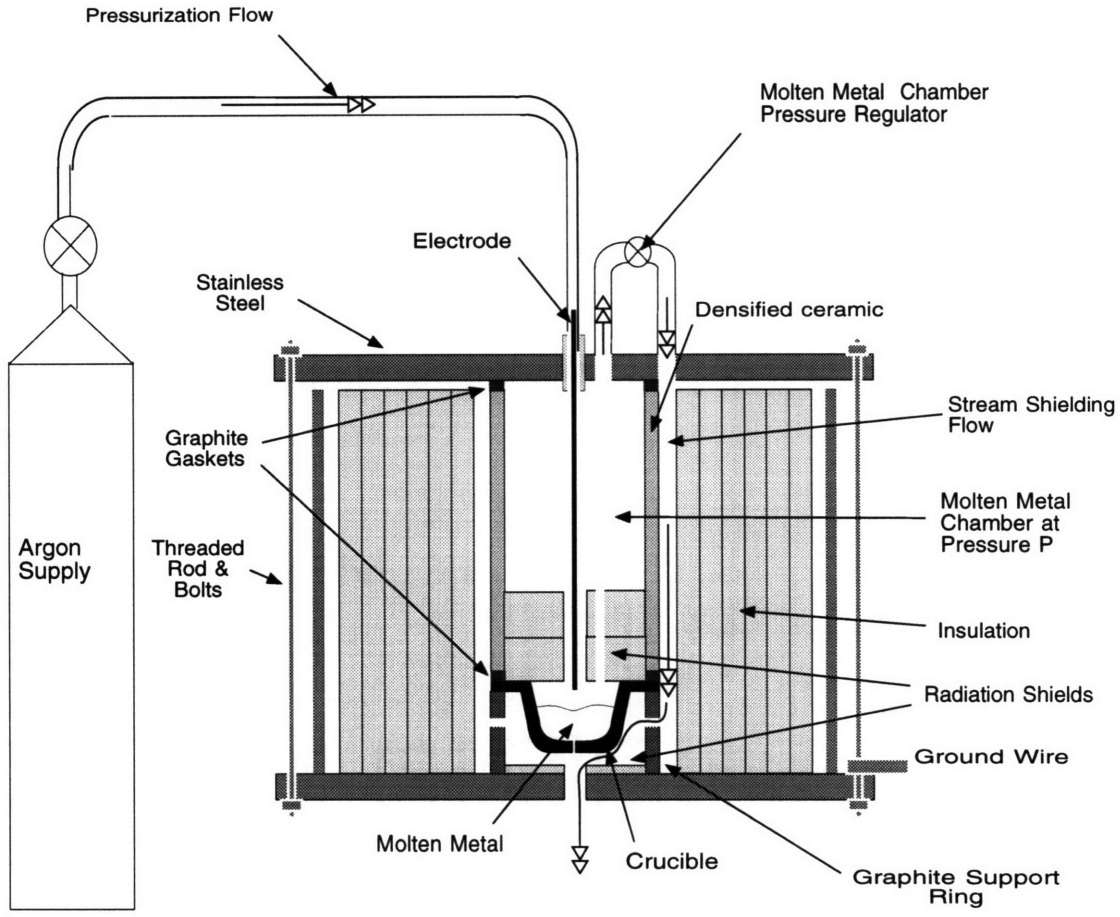

Figure 2.1 Lee's Prototype Arc Furnace Design

The graphite support ring supports the crucible and provides passages for argon flow. The argon provides shielding for the molten stream and for the graphite crucible which oxidizes at high temperatures. The argon first flows into the pressurized volume to maintain the desired pressure and then flows through the passages. The support ring was constructed of graphite because of its previously mentioned properties.

The ceramic cylinder provides a pressure chamber which can be pressurized to expel the tin. Mullite ceramic was chosen as the cylinder

material. It is strong under compression so that the stainless steel lid can be tightened to it. It is not conductive so the torch and stainless steel lid are not shorted to the crucible, and it has a high melting point, allowing it to be near the heat source.

The insulation and radiation shields allow for a large temperature differences between the molten metal and ambient with a reasonable amount of power input. Alumina was chosen as the insulation, and graphite as the radiation shields because their effective thermal conductivity is small. The amount of insulation was limited so that the response of the furnace to a temperature decrease would be reasonable.

The GTAW torch is the power source. Resistive heaters are the only other source that is less expensive, but the torch is more efficient. A GTAW power supply is a high density heat input. As much as 80% of the power can used for heating.

The stainless steel shell supports the internal components, and was chosen because of its cost and strength. It must be cooled by cooper coils because the maximum useful temperature of stainless steel is 950°C and because many of the components attached to the furnace can not withstand high temperatures.

Lee conducted a test of the arc furnace with tin. It was a success with the furnace operating as designed. It was able to attain high temperatures, over 1400°C. The time constant for an increase in temperature was 58 seconds, and the time constant for a decrease in temperature was 142 to 198 seconds.

2.3 Arc Furnace Modifications

Ratliff modified the original prototype design slightly to increase the maximum operating temperature of the furnace and to make control of the pressure in the furnace easier. He also recommended further improvements.

Ratliff's modifications included the adding of insulation, separating the argon used to pressurize the pressure chamber from the argon used for

shielding, and adding a keyhole in the bottom steel plate so that a pyrometer could be used to measure the crucible temperature. Figure 2.2 shows the furnace shielding and argon flow improvements. The insulation increased the maximum operating temperature of the furnace. Separating the argon flow made pressure control easier. The need for using a pyrometer to sense temperature will be discussed in the next section.

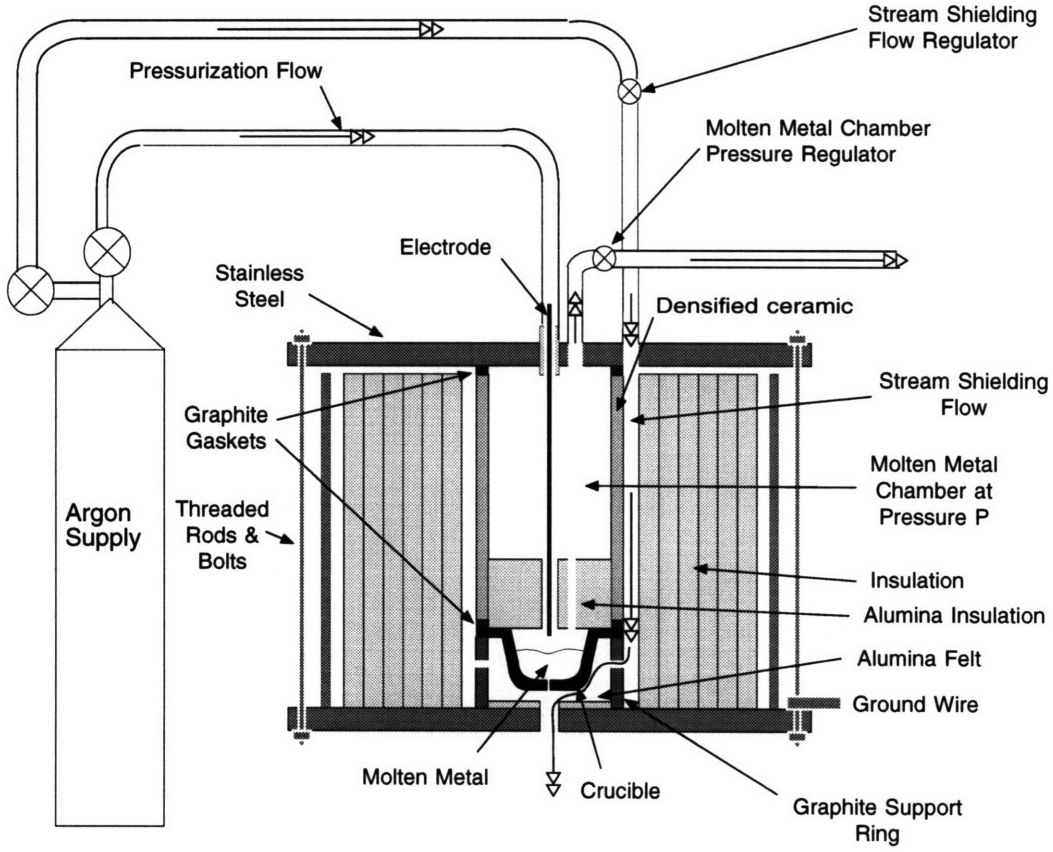

Figure 2.2 Ratliff's Furnace Redesign

Ratliff also recommended changing the GTAW torch attachment arrangement. The NPT fittings, used to attach the tubing for the argon to the furnace, clamped the torch as well. This made it difficult to remove the torch and prevented the fitting from sealing properly. His advice was followed in this research.

2.4 Temperature Controller

Ratliff designed a rudimentary temperature controller. The scheme is shown in Figure 2.3. It used a high bandwidth pyrometer, a 12 bit DT-2801 Data Acquisition and Control (DAQC) card, a personal computer, and a Hobart Cybertig III power supply.

The pyrometer senses the temperature of the tin. A pyrometer was chosen because thermocouples could not withstand the high temperatures and the harsh electrical environment of the arc furnace. A large temperature error was not expected between the a pyrometer reading and a contact sensor reading. Figure 2.4 was used by Ratliff to estimate that temperature difference. The circled changes in slope indicate a phase transformation of the steel. They should be occurring at approximately 1500°C. The measured temperature was 270°C lower.

The computer implemented the control law with the DAQC board converting the signals. A Proportional-integral-derivative (PID) controller was used. The control algorithm was:

$$G_c = K_p + K_i z/(z+1) + K_D(z-1)/z$$

where

K_P = 1300

K_i = 1

K_D = 500

The sampling period was 0.1 sec.

The Hobart power supply provided the power to change the tin temperature.

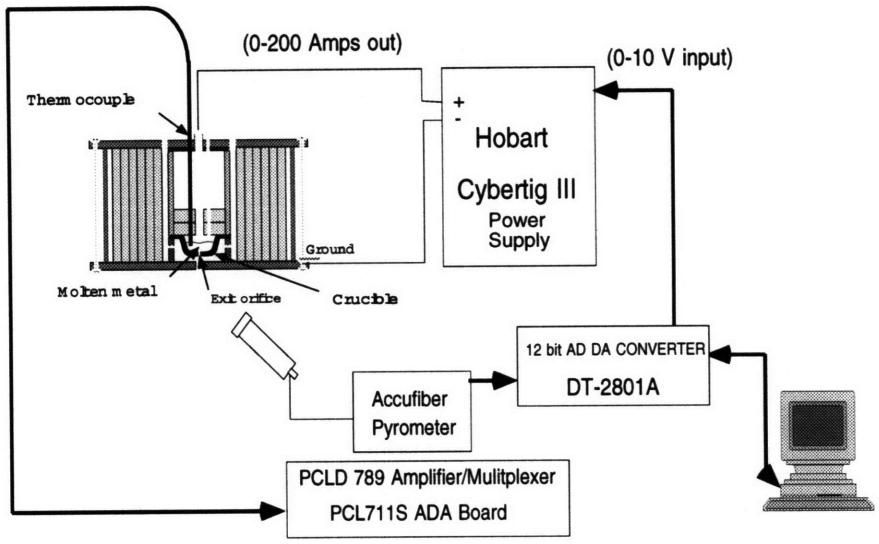

Figure 2.3 Closed Loop Temperature Control Scheme

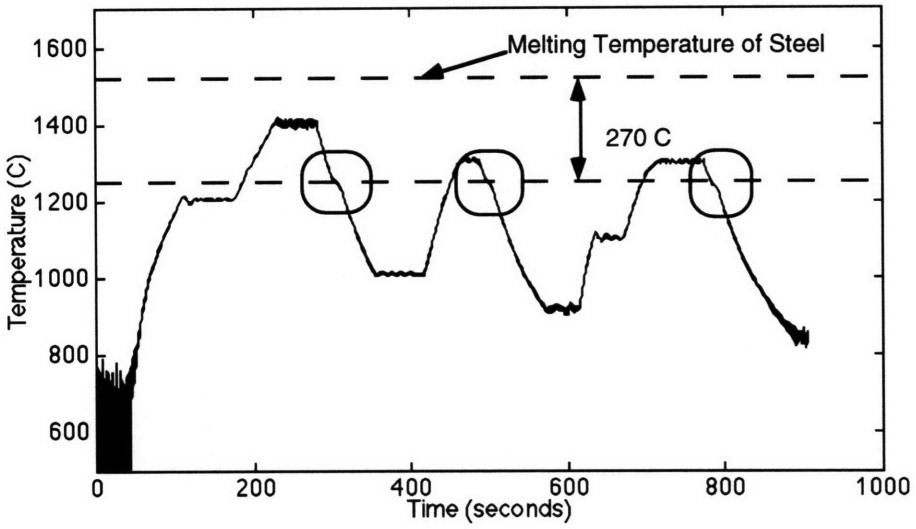

Figure 2.4 Pyrometer Response

Ratliff conducted closed loop response tests of the temperature control system. Figure 2.4 shows the response to various temperature changes. The time constant of the close loop system is approximately 75 seconds. A disadvantage of the control system is that the control current oscillates between

its saturation limits. Current oscillations change the resistance of the arc which will be used in the proposed flow controller of this research.

2.5 Arc Furnace Steel Physical Limitation

Ratliff discovered that molten steel at high temperature erodes the graphite crucible, and the graphite diffuses into the steel. The erosion presents three problems:

- the exit orifice wears excessively making the flow hard to control
- the crucible life is shortened
- the weld becomes contaminated.

Ratliff conducted an extensive search to find a suitable containment material. His main obstacle was the unavailability of documentation on materials to contain molten steel whose temperature is above 1620°C. He looked at both conductive materials, which would allow the furnace design not to be changed, and non-conductive materials, which would require a new furnace design so that the crucible was not an electrode. Ratliff also considered coating the crucibles and using inserts. Table 2.1 summarizes his findings for conductive materials, and table 2.2 summarizes his findings for non-conductive materials.

With data at high temperatures hard to find, Ratliff decided to test various materials. Cost was the deciding factor on which materials to try. A 97% pure tungsten crucible, a TiN coated graphite crucible, a graphite crucible with a BN insert and a SIC6 grade graphite crucible were tried at a furnace temperature of 1800°C and proved unsuccessful. The tungsten crucible reacted with steel as shown in Figure 2.5. The TiN coating flaked off, exposing the crucible to steel. The orifice in the BN insert enlarged. The SIC6 grade graphite crucible had as much damage as the lower grade graphite. Ratliff noted that the chance of finding a crucible material to contain steel appeared slim.

Table 2.1 Properties and Uses of Electrically Conducting, High Temperature Materials

Material	**Properties/Relevant Uses**
TiC (Titanium Carbide)	Electrode sheaths of thermocouples for measurement of temperature up to 2500 C, has high temperature strength Specific electrical resistance: 52.5 μohm/cm Thermal Expansion Coefficient: $7.74x10^{-6}$ 1/C Thermal Conductivity: .46 J/cm C sec Hardness (Rockwell C scale): 93 Melting Temperature: 3150 C
TiB_2 (Titanium Diboride)	Resists the action of molten metals, used for crucibles for precision melting. Resistant to scaling Specific electrical resistance: 14.4 μohm/cm Thermal Expansion Coefficient: $8.1x10^{-6}$ 1/C Thermal Conductivity: .264 J/cm C sec Hardness (Rockwell C scale): 86 Melting Temperature: 2980 C
ZrB_2 (Zircon Diboride)	Electrode sheaths for high temperature thermocouples for measuring temperature of molten steel, cast iron, nonferrous and rare metals, and their alloys. Resistant to scaling Specific electrical resistance: 16.6 μohm/cm Thermal Conductivity: .264 J/cm C sec Hardness (Rockwell C scale): 84 Melting Temperature: 3040 +-100C
ZrC (Zircon Carbide)	Crucibles, boats, tubes. Resists the action of molten metals Specific electrical resistance: 50 μohm/cm Thermal Expansion Coefficient: $6.73x10^{-6}$ 1/C Thermal Conductivity: .4186 J/cm C sec Hardness (Rockwell C scale): 87 Melting Temperature: 3530 C

TiN (Titanium Nitride)	Coatings on titanium and graphite components, high electrical conductivity, resistant to action of molten metals Coefficient of Thermal Expansion: $9.35x10^{-6}$/C Specific electrical resistance: 25 μohm/cm Thermal Expansion Coefficient: $9.35x10^{-6}$ 1/C Thermal Conductivity: .293 J/cm C sec Hardness (Rockwell C scale): 75 Melting Temperature: 3205 C
SiC (Silicon Carbide)	High electrical resistance, thermal shock resistance, coatings of graphite. Specific electrical resistance: $>.05x10^{6}$ μohm/cm Thermal Expansion Coefficient: $5.68x10^{-6}$ 1/C Thermal Conductivity: .4186 J/cm C sec Hardness (Rockwell C scale): 70 Melting Temperature: 2827C
W (Sintered Tungsten)	High melting temperature, Rockwell hardness of 32 (c scale)-machinable, high electrical conductivity. May creep under its own weight at elevated temperatures. Specific electrical resistance: 5.5 μohm/cm Thermal Expansion Coefficient: $7.74x10^{-6}$ 1/C Thermal Conductivity: .174 J/cm C sec Hardness (Rockwell C scale): 32 Melting Temperature: 3422 C
C (Graphite)	High electrical conductivity, reacts with oxygen, low hardness-easily machined Specific electrical resistance: 200 μohm/cm Thermal Expansion Coefficient: $.66x10^{-6}$/C Thermal Conductivity: 8.2 J/cm C sec Hardness (Rockwell C scale): very low Temperature: 3870 C

Table 2.2 Properties and Uses of Non-Electrically Conducting, High Temperature Materials

Material	**Properties/Typical Uses**
BN (Boron Nitride)	Good Refractory material, used for refractory coatings of molds and crucibles, refractory pouring spouts. Coefficient of Thermal Expansion: 7.51×10^{-6}/C Thermal Conductivity: 0.251 J/cm C sec Melting Temperature: 3000 C
ZrO_2 (Zircon Dioxide)	Thermocouple Protection Tubes Coefficient of Thermal Expansion: $.66 \times 10^{-6}$/C Thermal Expansion Coefficient: 9.9×10^{-6} 1/C Thermal Conductivity: 8.3 J/cm C sec Melting Temperature: 2537 C
MgO (Magnesium Oxide)	Thermocouple Protection Tubes Resistant to Molten Metals and Slags Coefficient of Thermal Expansion: $.66 \times 10^{-6}$/C Thermal Expansion Coefficient: 13.5×10^{-6} 1/C Thermal Conductivity: 8.3 J/cm C sec Melting Temperature: 2800 C

2.6 Molten Stream Analyses

Ratliff and Budiman both conducted analyses to determine if a steel molten stream could melt a steel base. Lee did not conduct analyses, however, he did successfully use a molten tin stream to melt a tin base. Finger penetration of 0.13 inches was achieved with a molten tin temperature of 950°C, a furnace pressure of 15 psi, and a table velocity of 5 mm/s. The weldments were not porous and the metallurgical bonds were good. Lee's success with tin encouraged steel analyses.

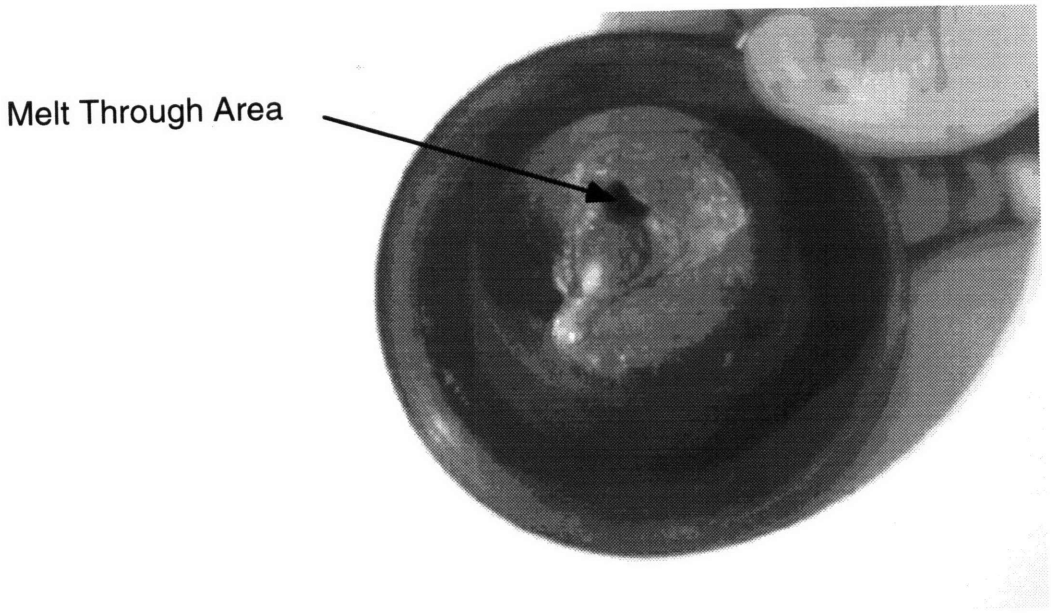

Figure 2.5 Tungsten Damage with Steel

2.6.1 First Melting Analyses

Ratliff conducted two-dimensional finite difference temperature analyses on the cross section of stream welded steel to determine if bonding would occur. The 1530°C isothermal line, the melting point of steel, was used as an indication of bonding. The molten stream used in the analysis was at a temperature of 2627°C. The analyses were conducted with various initial temperature distributions in the workpiece and workpiece geometries.

One analysis was conducted on the workpiece geometry shown in Figure 2.6. The cross-section of the workpiece was 2 cm by 0.5 cm. The cross-section of the bead was 3 mm by 3 mm. The bead is in the center of the workpiece. Ratliff divided the workpiece into 400 nodes and the stream bead into 36 nodes. The initial workpiece temperature was 27°C. The assumptions were that the workpiece properties were constant; the interface between the workpiece and the bead was a continuum; and the latent heat effects were negligible. The last

two assumptions should give a more optimistic depth of penetration than would actually occur.

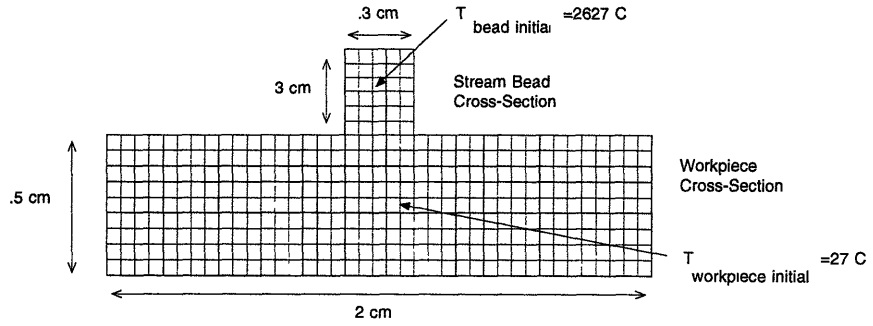

Figure 2.6 Stream Welding Model

The simulation results are shown in Figure 2.7. At 0.05 seconds the highest temperature is reached in the base metal. There was no location where the temperature exceeded 1400°C. By 0.3 seconds the highest temperature in the base metal dropped as the heat energy dispersed. Additional analyses conducted with the workpiece heated to 727°C and with the bead deposited in a groove indicated a similar conclusion, base metal melting was not likely.

Ratliff conducted a stream welding experiment to verify his analyses. Figure 2.8 shows the workpiece. Surprisingly, some base metal melting did occur. However, he was forced to use a stream that was a mixture of 25% tin and 75% steel to keep the stream flowing properly.

2.6.2 Second Melting Analyses

Budiman conducted more analyses on the capability of using a molten steel stream to melt a steel base. His analyses used a one-dimensional finite difference approximation for the workpiece assuming the width of the weld bead and the workpiece were infinite and treating the stream along the axis of the weld as a lump.

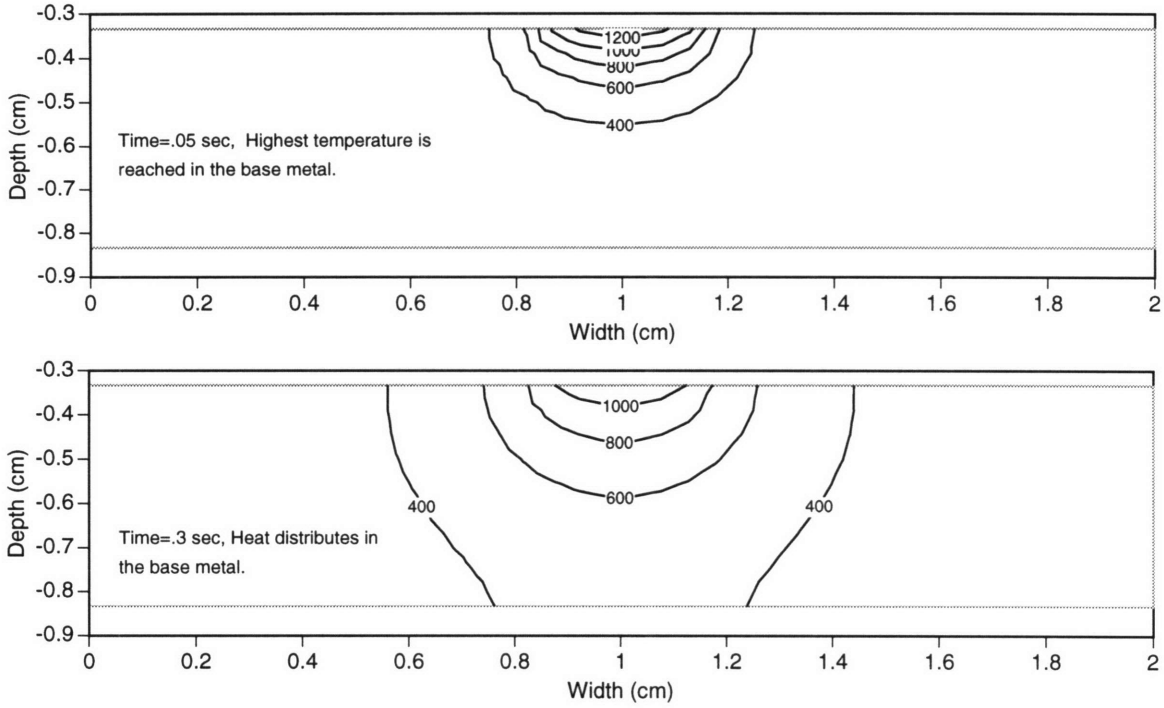

Figure 2.7 Simulated Temperature Distribution

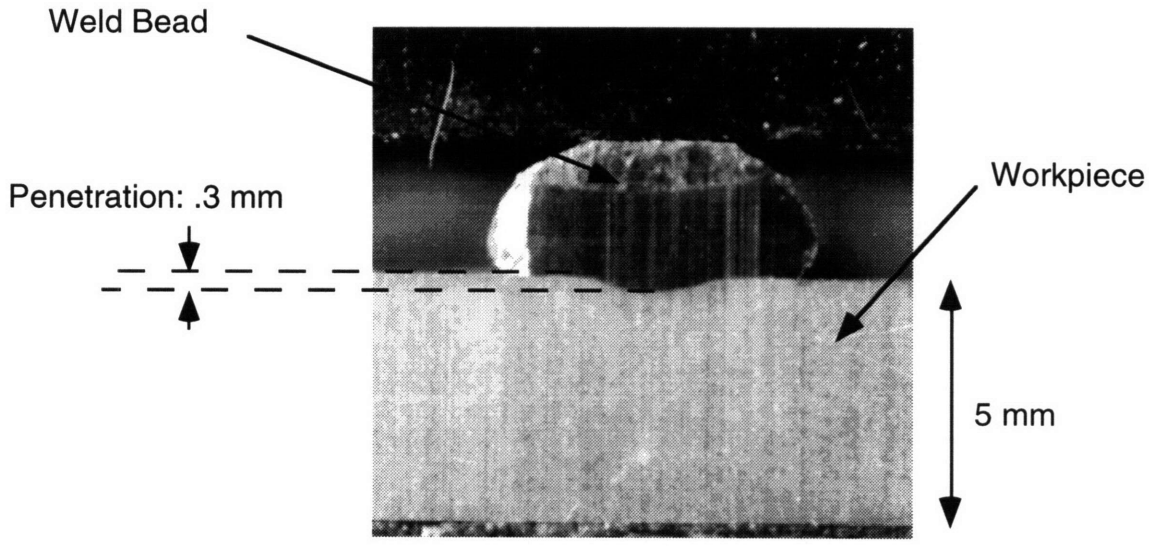

Figure 2.8 Actual Stream Welded Workpiece

The setup used in his analysis is shown in Figure 2.9. The workpiece was divided into 10 nodes. The stream bead is one node with a 3 mm height. Budiman made similar assumptions to Ratliff regarding constant metal

properties and a continuum between the bead and the workpiece. Budiman's analyses, however, should give a more optimistic depth of penetration than Ratliff's, since by assuming an infinite width the heat losses are minimized.

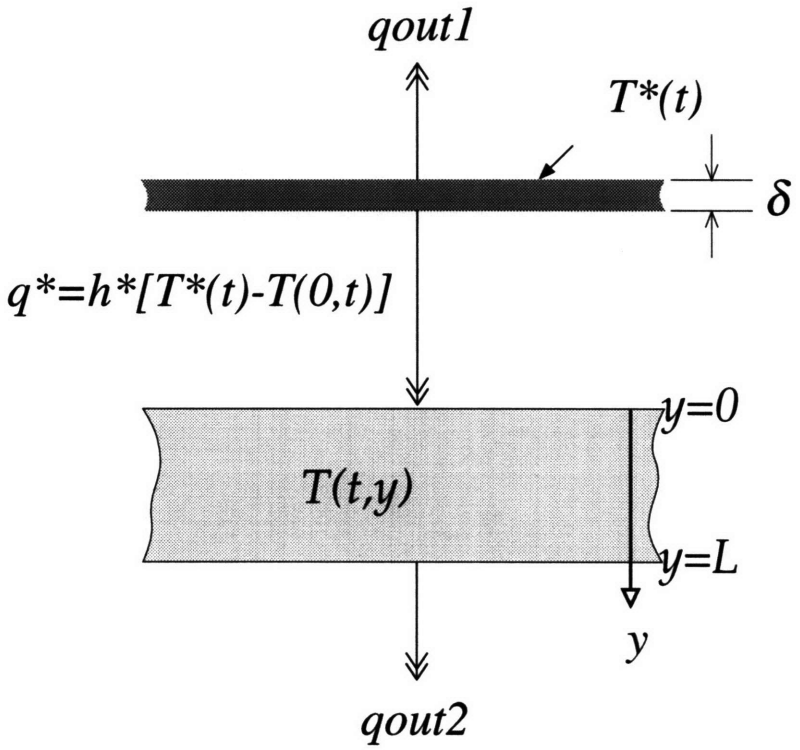

Figure 2.9 Budiman's Model

Figure 2.10 shows one result of Budiman's analyses. Initially, the stream was at 2650°C and the workpiece was at 30°C. Like Ratliff's analyses, the melting point of steel was chosen as an indication of bonding. Minimal melting resulted with only a small portion of the base reaching the melting point of steel. The surface of the base metal exceeded the melting point, but the base metal at a distance of only 0.5 mm did not. Similar results were obtained for different initial temperature distributions in the workpiece. With this approach being more optimistic than Ratliff's, it appeared that melting a steel base with a molten steel stream was not likely.

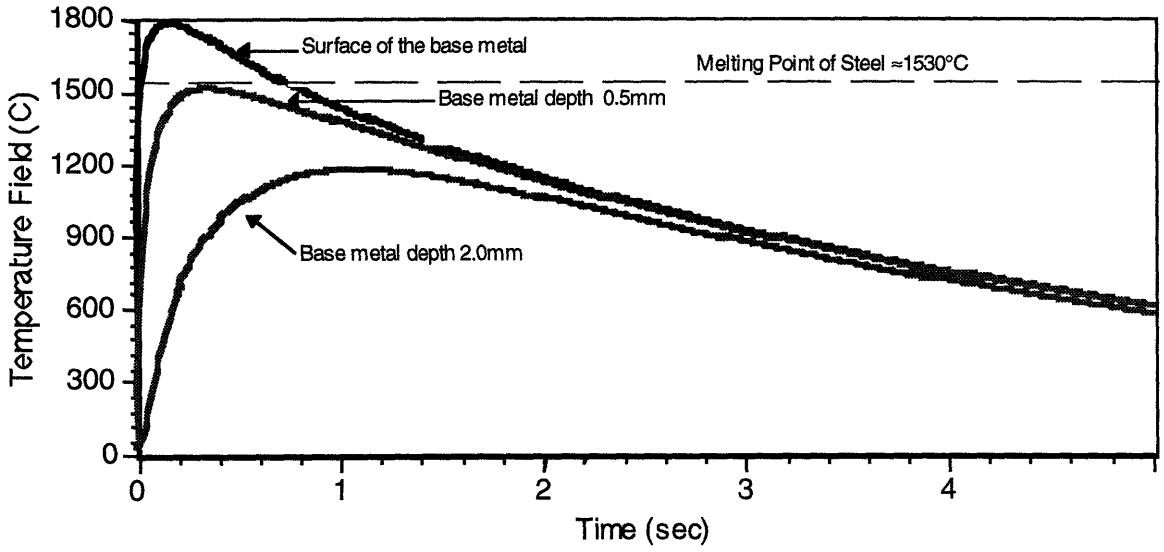

Figure 2.10 Simulation Results

2.7 Summary

Previous research developed an apparatus to control the temperature and flow of a molten stream. A physical limitation prevented the apparatus from being used with steel. In addition, analyses indicated that a molten stream of steel could not be used to melt a steel base without additional weldment heating.

Since there was an apparatus available to control a molten stream and because steel did not appear to be a good metal to use in the furnace, it was decided to continue molten metal stream control with another metal. A completed molten stream controller would make the concept available for other applications, and would provide a functioning furnace to conduct steel experiments if a material that can hold steel is ever found.

Chapter 3: Molten Stream Metal Selection

3.1 Overview

A new metal was needed for use in the proposed control scheme of this research since steel can not be used in the furnace and since a molten steel stream did not show promise of melting a steel base. The new metal should show promise of both working in the furnace and of being able to melt the base.

A comparison was conducted of the properties of various metals, and finite difference analyses were performed to determine the best choice. Aluminum, copper, tin, and zinc were the candidates. Tin was the metal chosen.

3.2 Metal Candidates

Aluminum, copper, tin, and zinc were possible metals to be used in the control scheme. They are used extensively in industry. The material properties compared were the melting point, boiling point, specific heat, thermal conductivity, diffusivity, density, electrical conductivity, and affinity for graphite. They determine the ability to be used in the furnace and to be melted by a superheated stream. The properties of the various metals are shown in table 3.1.

For a metal to have the potential to be successfully used in the arc furnace the electrical conductivity needs to be high and it must have a low affinity for graphite. The electrical conductivity of the metal determines the possibility of using the metal as an electrode. (The metal serves as the positive electrode in the furnace.) A high conductivity allows for an arc to be established between the metal and the torch. The affinity of the metal for graphite determines the potential of the metal to be contained in a graphite crucible. A low affinity reduces the chances of erosion.

Table 3.1 Properties of Various Metals

Property	Aluminum	Cooper	Tin	Zinc
Melting Point (°C)	660	1082	231.9	419.5
Boiling Point (°C)	2520	2595	2270	907
Specific Heat c_p (J/kg K) 0-100°C	900	385	222	382
Thermal Conductivity k (W/m K) 0-100°C	222	393	65	92
Diffusivity α (m^2/sec^2) 0-100°C	9.1×10^{-5}	1.1×10^{-4}	4.0×10^{-5}	3.4×10^{-5}
Density ρ (g/cm^3) 20°C	2.70	8.96	7.29	7.14
Electrical Conductivity ($\mu\Omega$ m) 20°C	.028	.0167	.155	.059

For a metal to have the potential to be successfully bonded with a stream, the diffusivity of the metal must be low. The diffusivity of the metal determines how quickly the energy from the stream propagates in the base. If the diffusivity is small, the energy propagates slowly. Consequently, the molten stream maintains its temperature for a period of time, and the base near the stream attains a temperature close to the initial stream temperature. If the diffusivity is large, the opposite occurs. Since the diffusivity is the thermal conductivity divided by the specific heat and density, the thermal conductivity of the material should be low and the specific heat and density should be large.

Tin appeared to be the best metal to use in molten stream research. It is the most likely to be able to be used in the furnace and successfully stream

bonded. Tin has the additional advantages of proven success in the furnace and availability at an economical price in bars and wire. Aluminum was tried in the furnace, but it could not be ejected from the crucible. The aluminum may have reacted with the graphite forming aluminum carbide which clogged the orifice (Lee, 1993).

3.3 Bonding Analysis

Two-dimensional finite difference analyses of stream weld cross-sections were conducted with tin and aluminum to support the conclusion that tin shows the most promise to be bonded with a stream.

Figure 3.1 shows the model used in the analyses. The work piece was 0.5 cm by 1 cm with a 0.3 cm by 0.3 cm bead. The bead was divided into 36 nodes. The base was divided onto 200 nodes. The initial temperature of the stream bead was 1000°C for tin and 1600°C for aluminum. A higher temperature was chosen for aluminum because it has a higher melting point. The work piece temperature was 27°C. Bonding was judged to occur if the base melted. The code is contained in Appendix A.

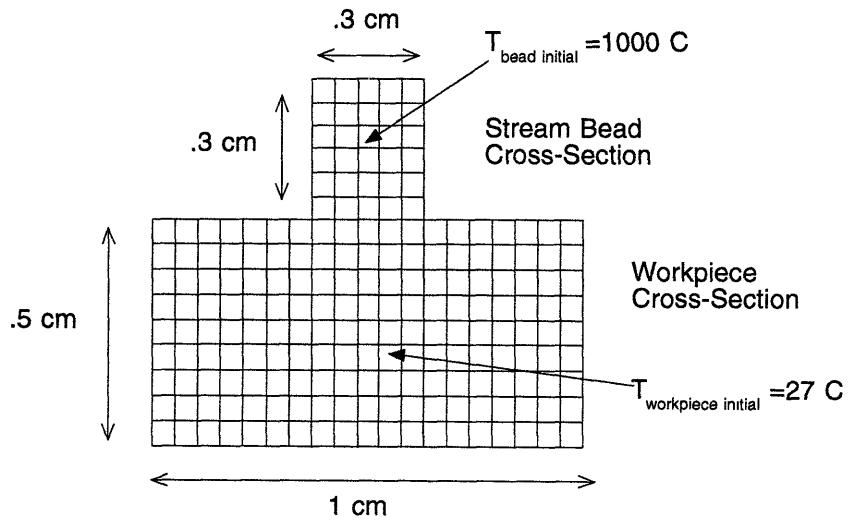

Figure 3.1 Stream Bonding Model

The results of the analyses support the previous conclusion. Bonding occurred in the tin and not in the aluminum. For tin, a large section of the base metal melts with the volume under the stream bead exceeding its melting point to a depth of 0.05 cm, Figure 3.2. This should cause bonding. For aluminum, the base metal does not melt with the surface of the base under the stream bead only reaching a temperature of 550°C well below its 660°C melting point, Figure 3.3. This will result in no bonding. The difference in the two can be accounted for by the diffusivity. Figure 3.4 shows how energy is dispersed in a tin or aluminum base. As the stream bead loses energy, its temperature drops, the temperature at a bead depth of 0.3 cm in the figure. The temperature of the base directly under the stream bead initially increases as the energy from the bead conducts into the base and then decreases as the energy is conducted throughout the base, temperatures at a bead depth of 0.0 cm and 0.05 cm in the figure. The temperature of the base away from the bead will only increase until the energy is evenly distributed throughout the bead and base resulting in a uniform temperature and then will decrease with the temperatures of the base near the bead and bead due to convective heat losses, the temperature at a bead depth of 0.5 cm in the figure. The temperature distribution during the equalization will determine if the base metal melts. Aluminum has a higher diffusivity than tin, so the energy of the stream bead is dispersed quicker throughout the base without a large temperature increase near the stream bead.

The results of the analyses are conservative. The model contains a cross section of the base and not a lengthwise section. The heat input from the stream behind and in front of the section, which helps melting, is not included.

The size of the sample used in the analysis did not affect the results. The maximum temperature of the base metal was attained before there was a significant change in the temperature at the work piece edges. This suggests the same temperature distribution would have occurred with a larger work piece.

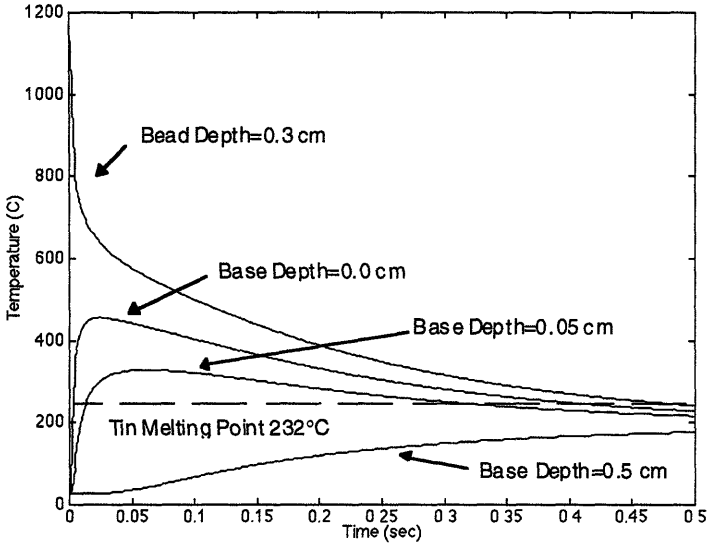

Figure 3.2 Tin Centerline Temperature, Base and Bead

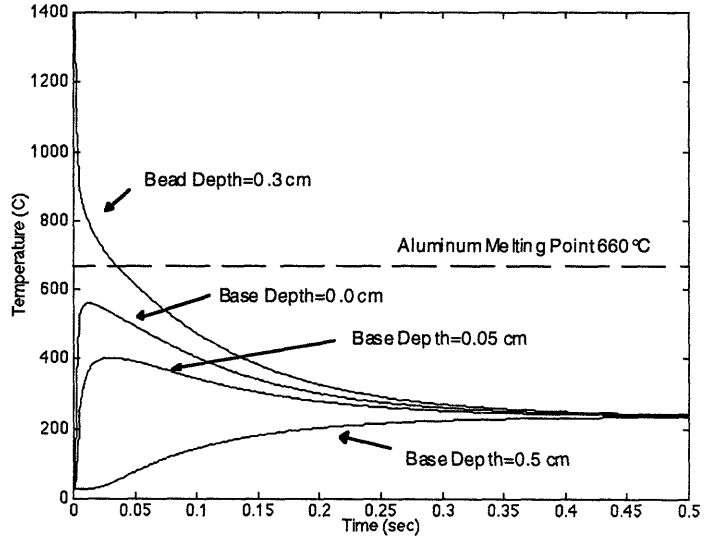

Figure 3.3 Aluminum Centerline Temperature, Base and Bead

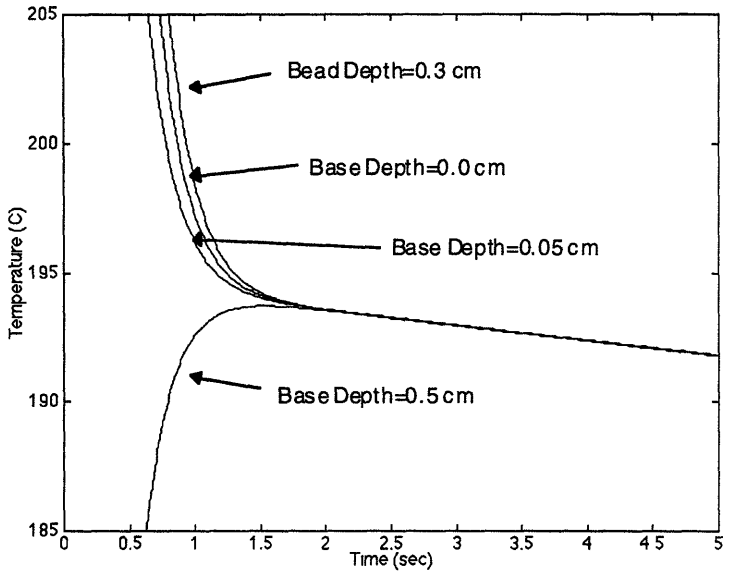

Figure 3.4 Expanded Tin Centerline Temperature, Base and Bead

3.4 Summary

Tin shows promise both for being used in the arc furnace and bonding with a stream, therefore continued molten stream research was conducted with tin. In addition to the properties listed for tin in table 3.1, the properties in table 3.2 were used throughout this research.

Table 3.2 Additional Properties of Tin

Property	Tin
Heat of Fusion (J/g)	59.5
Viscosity μ (mNsec/m^2) at 1000°C	.88
Kinematic Viscosity ν (m^2/sec) at 1000°C	1.347×10^{-7}

Chapter 4: Molten Stream Control Scheme

4.1 Overview

The proposed molten stream control scheme uses an arc furnace and two control loops, Figure 4.1. The arc furnace assembly will be used to heat, contain, and provide a means of delivering tin. Two control loops will maintain the temperature and flow of the tin. Figure 4.2 is a picture of the apparatus.

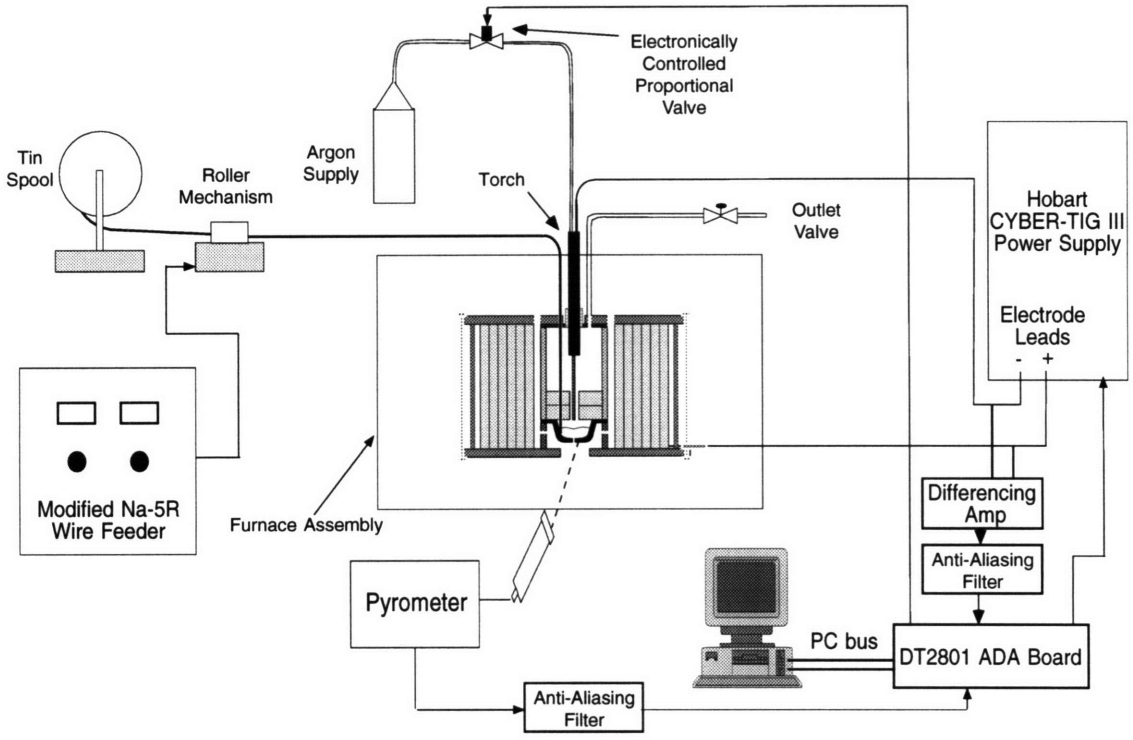

Figure 4.1 Components of the Control System

The temperature control loop controls the temperature of the graphite crucible outside wall. This temperature is an approximation to the temperature of the tin in the bottom of the crucible.

Because of the non-availability of a sensor to measure the flow rate of a molten metal flowing in an open space, the flow will be controlled indirectly by

an arc resistance regulator. The resistance regulator maintains the resistance of the electric arc by varying the pressure in the furnace and thus the flow from the furnace. The resistance is an indication of the tin level in the furnace. If the resistance is maintained constant, the flow from the furnace will equal the feed into the furnace.

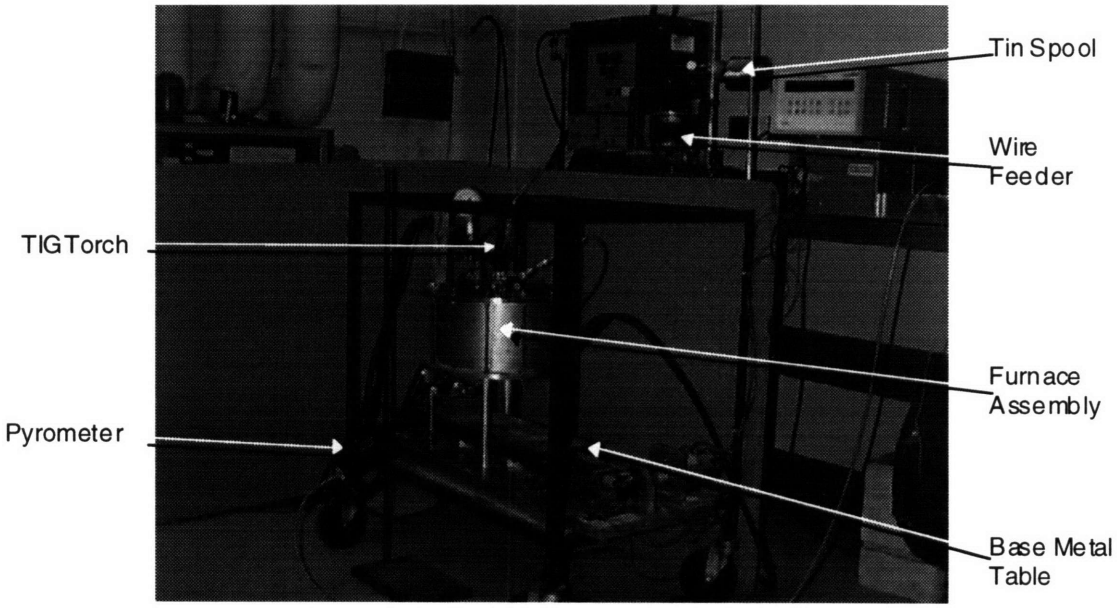

Figure 4.2 The Arc Furnace Assembly

For the proposed control scheme to work the following need to be met:

- the power supply must provide enough power to melt the tin replenishing the furnace and hold the tin at the desired temperature
- measuring the temperature of the outside of the graphite crucible with a pyrometer must give an accurate indication of the tin temperature at the bottom of the crucible
- the tin wire must melt fast enough to maintain the molten tin reservoir in the furnace
- the orifice size of the crucible must produce the desired tin flow rates with a reasonable furnace pressures.

4.2 Furnace Operating Conditions

A set of operating conditions was picked for the furnace. The conditions can vary, but the design will be based on these conditions. The operating conditions are:

- temperature: 1000°C. (This is the lowest temperature that produces a reasonable base metal melting.)
- mass of tin in the furnace: 105 grams. (This half fills the crucible used to contain the tin. The flow controller will be designed so that transients during flow rate changes do not overfill or empty the crucible.)
- diameter of tin used in wire feeder: 0.032 inch. (The maximum wire feeder feed rate is 999 in/min.)
- mass flow rate from the furnace: 1 g/sec. (This is comparable to a GMAW mass disposition rate.)

The equation to convert wire feed rate in inches per minute to mass flow rate in grams per second is:

$$m = B A \rho S$$

where:

m = the mass feed rate. (g/sec)

B = the conversion factor. (0.273 $cm^3 min/in^3 sec$)

A = the area of the tin wire. ($\pi * .016^2 = 8.04 \times 10^{-4}$ in^2)

ρ = the density of tin at 25°C. (7.29 g/cm^3)

S = the wire feed rate. (in/min)

4.3 Arc Furnace Assembly

The arc furnace heats and delivers the tin. The furnace was described in detail in Chapter 2. In short, tin is melted in the furnace by the GTAW torch and is expelled from the furnace by pressurizing the pressure chamber with argon from the GTAW torch. The pressure boundary is composed of the graphite crucible, the ceramic cylinder, and the steel lid, Figure 4.3. Modifications were done to the arc furnace to increase the integrity of the pressure boundary which was leaking in three places; between the ceramic cylinder and the steel lid; around the Swagelok union NPT fitting; and around the torch clamp.

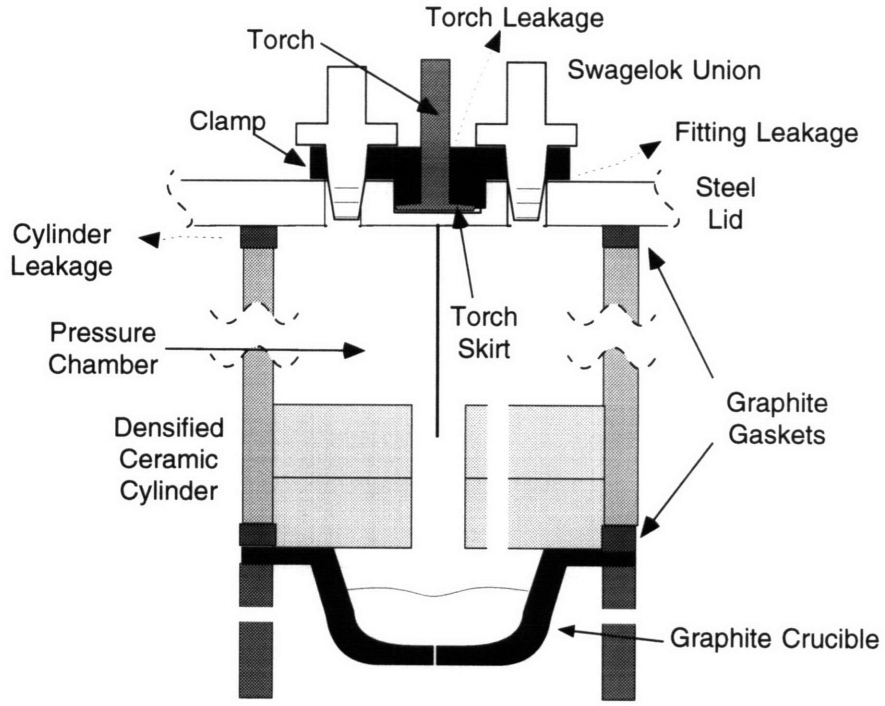

Figure 4.3 Previously Existing Torch Clamp Arrangement

Argon was leaking from between the ceramic cylinder and the steel lid because the steel lid rested on the steel outer cylinder of the furnace instead of the ceramic cylinder. An additional graphite gasket was placed between the crucible and its support to increase the height of the ceramic cylinder.

Argon was leaking around the Swagelok fittings and the torch clamp because the NPT fittings were used both to secure the torch and to make a pressure tight connections for external equipment, such as the wire feeder, to be attached. Both can not be done with the same fitting. Either the torch will be securely fastened or the NPT fitting will make a good seal. To correct this, the Swagelok union was replaced with a Swagelok bulkhead union and a lower clamp section was added, Figure 4.4. The bulkhead union has an extra nut in addition to the NPT fitting. The extra nut can be used to secure the upper and lower clamp sections which allows the NPT fitting to be securely connected, forming a pressure tight seal.

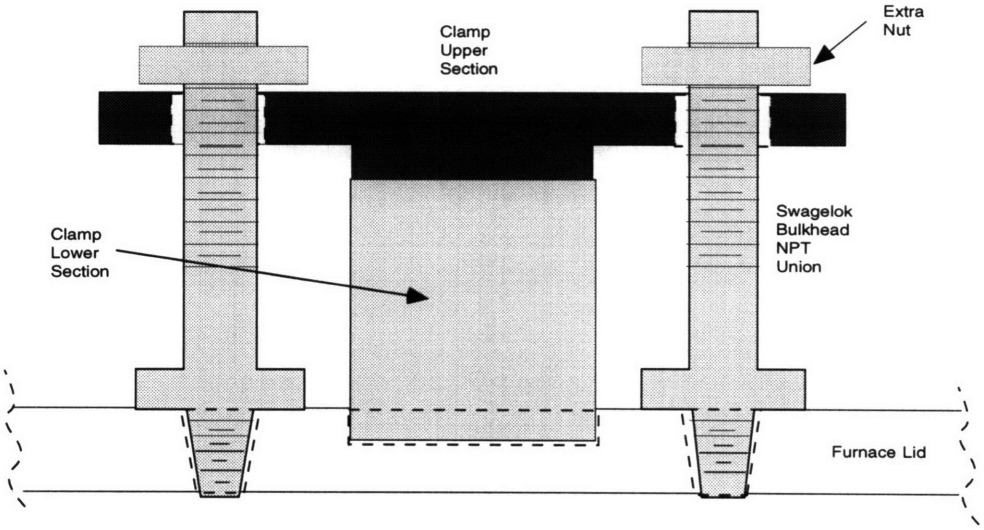

Figure 4.4 New Torch Clamp

4.4 Temperature Control Loop

The temperature control loop components control the temperature of the outside of the graphite crucible. The error between the desired tin stream temperature and the temperature of the crucible is used to drive the GTAW power supply, Figure 4.5. In order for the loop to effectively control the temperature of the molten tin stream, the power supply must be capable of maintaining the graphite crucible at the desired temperature and the

temperature of the graphite crucible must be close to the temperature of the tin in the bottom of the crucible.

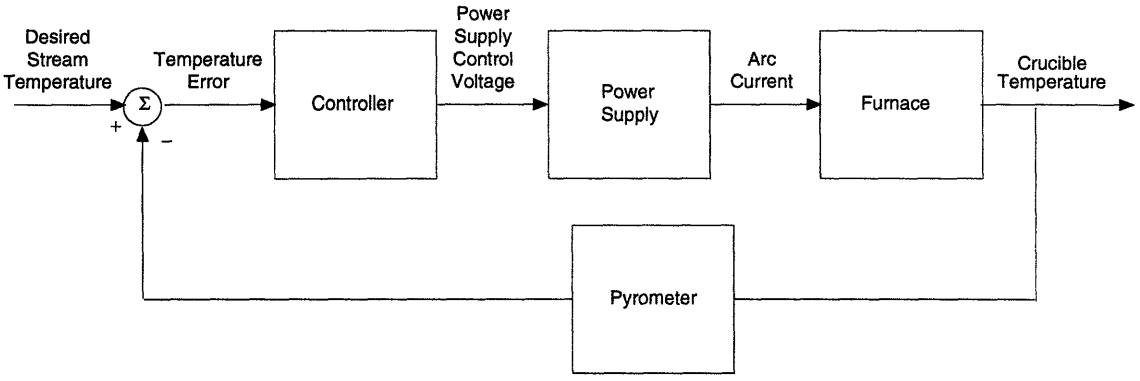

Figure 4.5 Simplified Temperature Control Loop

4.4.1 Temperature Control Components

The temperature control loop will consist of an Accufiber pyrometer, model 100C; a Hobart TIG power supply, CYBER-TIG III; a Data Translation Data Acquisition and Control (DAQC) Card, DT2801-A; a 386 based personal computer; and an anti-aliasing filter.

The pyrometer will be used as the temperature sensor. Its useful temperature range is 900 to 2000°C. Below 900°C the output is very noisy. The pyrometer's bandwidth is 25 Hz, and its output is 0 to 10V varying linearly over the temperature range.

The GTAW power supply will vary the temperature of the tin. It is a constant current supply with the current linearly varying between 0 and 200A for a 0 to 10V input. Its 100% duty cycle is 150A at 16V, equating to a power of 2.4 kW. The bandwidth of the supply is 1000 rad/sec.

The DAQC card will perform A/D and D/A conversions. The card can handle 8 differential analog inputs and 2 analog outputs. The resolution is 12 bits. The A/D conversion and acquisition time is 25 μsec, and the D/A settling time is 30 μsec. The card will convert the 0 to 10V pyrometer signal to a 12 bit

digital signal for the computer to process and will convert the 12 bit digital signal from the computer into a 0 to 10V analog signal to control the power supply.

The 386 computer will be used to implement the control algorithm. The input to the control algorithm will be the digitized pyrometer signal. The output of the algorithm will be the digital power supply control signal. The sampling period of the computer will be 0.5 sec. This will allow the computer time to perform all needed calculations while allowing the controller to have sufficient bandwidth so that the worst temperature disturbances, a change in feed rate, can be rejected.

The anti-aliasing filter will condition the signal from the pyrometer before it is sampled by the DAQC card. It is a first order active filter, Figure 4.6, that rejects any frequency greater that half the sampling rate. The sampling rate is approximately 13 rad/sec. The cutoff frequency of the filter is approximately 3 rad/sec to insure attenuation of frequencies greater than 6.5 rad/sec despite the poor roll off characteristics of a first order filter.

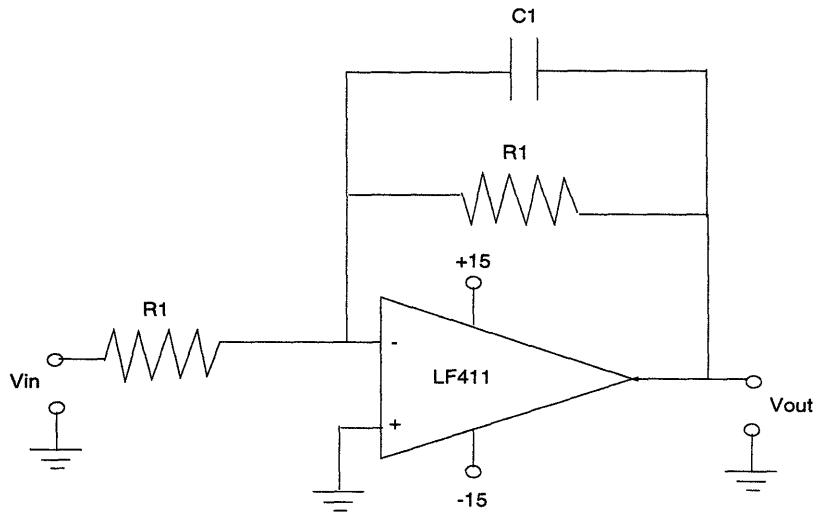

R1=60kΩ

C1=5μF

Figure 4.6 Anti-Aliasing Filter

4.4.2 Temperature Control Power Capability

The power supply must be able to provide enough power to maintain the graphite crucible at the desired temperature. This power will compensate for the heat losses from the furnace and will provide the energy to melt the feed wire and raise its temperature to 1000°C. As previously mentioned, the maximum sustainable operating power from the GTAW power supply is 2.4 kW. The steady state power requirements were analyzed to give an indication of the power supply adequacy.

Equilibrium Power Requirements

The power to keep the furnace at various temperatures without flow was determined empirically for tin masses in the furnace of 71, 106, and 136.5 grams. Solving for the power to compensate for heat losses would be very difficult analytically. There are a variety of geometric shapes, and heat transfer occurs by conduction, convection, and radiation. 106 grams was chosen as one of the masses because it will, approximately, be the equilibrium mass of tin in the furnace. 30 grams on either sides of 106 grams were chosen to allow for variations in the tin mass caused by the flow controller.

The results of the experiments are shown in Figure 4.7. The solid lines are first order polynomial curve fits. The symbols are the experimental data. The results show that the lower the temperature and the less the tin mass, the smaller the power consumption. Ideally, the furnace should be operated at low temperatures with a minimum amount of tin in the furnace, but the need for bonding and the need to have a volume of tin to expel limit their lower value. The amount of mass in the furnace probably affects the heat loss because the tin's area to volume ratio changes.

Wire Melting Power

The power to melt the wire fed into the furnace and raise its temperature to 1000°C was calculated analytically.

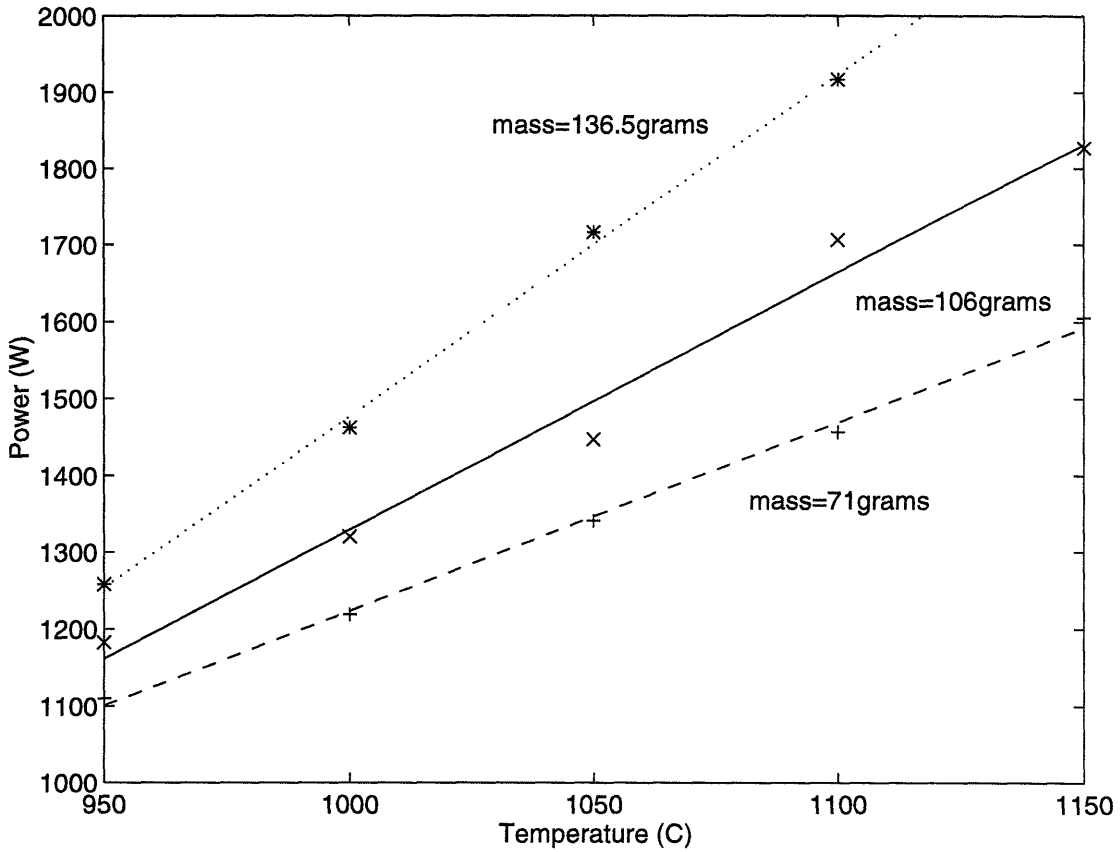

Figure 4.7 Power Required to Compensate for Heat Losses

The equation for the maximum power assuming a constant specific heat is:

$$\text{power} = m_{max}\,(h_f + c_p \Delta T)$$

where:

m_{max} = the maximum wire mass feed rate. (1.6×10^{-3} kg/sec.)

h_f = the heat of fusion. (59.5 J/g)

c_p = the specific heat of tin at 25°C. (222 J/kg K)

ΔT = the temperature increase. (975°K)

The maximum power is:

$$\text{power} = 1.6 \times 10^{-3}(59.5 \times 10^{3} + 222 \times 975) = 442\text{W}$$

The power requirement to melt and raise the temperature of the wire to 1000°C is small.

An experiment was conducted to verify the analysis. The furnace temperature was raised to a temperature of 1000°C. A 0.48 g/sec feed and flow rate was initiated. The change in power required to maintain 1000°C was 135 W. The analytical result was 132 W.

Total Power Requirements

The maximum total power, power to maintain the tin temperature because of heat losses and power to melt the tin fed into the furnace, required from the power supply to maintain the graphite crucible temperature at 1000°C with the largest feed/flow is approximately 1770 W. The power supply can provide this, but the efficiency will be poor. Over half of the power to the furnace, 1330 W, is lost by conduction and convection.

4.4.3 Temperature Measurement Errors

A pyrometer reading of the graphite crucible outside wall temperature must agree closely with the temperature of the tin at the bottom of the crucible. The temperature of the outside of the crucible is what is controlled. In order for the temperature controller to work effectively, the temperature of the outside of the crucible must not lag far behind the temperature of the tin during transients and the temperature should not differ significantly from the tin temperature at steady state. Analyses were conducted to determine the transient time lag and the steady state temperature difference.

Temperature Time Lag

An indication of the temperature time lag associated with the graphite during transients was obtained by simplifying the thermal diffusion equation. The one dimensional thermal diffusion equation assuming no heat generation in the graphite and constant thermal conductivity is:

$$\frac{\partial T}{\partial t} = \alpha \frac{\partial^2 T}{\partial z^2}$$

where:

α = the diffusivity of graphite at 1000°C. (1.07×10^{-4} m^2/sec)

T = the temperature of the graphite in on dimension. (°C)

t = the time. (sec)

z = the distance in the one dimension. (m)

Approximating the partial derivatives:

$$\frac{\Delta T}{\Delta t} = \alpha \frac{\Delta T}{\Delta z^2}$$

Dividing by ΔT and rearranging the equation:

$$\Delta t = \frac{\Delta z^2}{\alpha}$$

Substituting the thickness of the graphite crucible, 6.35×10^{-3}m, and the diffusivity of graphite:

$$\Delta t = \frac{(6.35 \times 10^{-3})^2}{1.07 \times 10^{-4}} = 0.38 \text{sec}$$

The temperature time lag associated with crucible during transients is small. It will take approximately 0.38 seconds for a temperature change to be completed on the outside of the crucible from a temperature change on the inside of the crucible. A time lag of 0.38 seconds is short compared to the open loop time constant of the furnace, which is 50 seconds.

Steady State Temperature Difference

An indication of the steady state temperature difference between the tin and the outside of the crucible was obtained by simplifying the one dimensional Fourier's Law. The equation for Fourier's Law assuming no heat generation in the crucible and constant thermal conductivity is:

$$q = \frac{Power_{in}}{Area} = k\frac{dT}{dz}$$

where:

q = the heat flux. (W/m^2)

k = the thermal conductivity of graphite at 1000°C. (448 W/m K)

T = the temperature of the graphite in on dimension. (°C)

z = the distance in the one dimension. (m)

Assuming all the power of the furnace is conducted through the bottom of the crucible:

$$q = \frac{Power_{in}}{Area_{cruciblebatom}} = k\frac{dT}{dz}$$

Approximating the derivatives and rearranging:

$$q = \frac{Power_{in}}{Area_{cruciblebottom}} = k\frac{\Delta T}{\Delta z} \Rightarrow \Delta T = \frac{\Delta z \bullet Power_{in}}{k \bullet Area_{cruciblebottom}}$$

Substituting the maximum sustainable power, 2.4 kW, the area of the bottom of the crucible, 0.007 m^2, the thickness of the crucible, 6.35×10^{-3} m, and the thermal conductivity of graphite:

$$\Delta T = \frac{(6.35 \times 10^{-3})2400}{448 \times 0.007} \approx 5°$$

The temperature difference across the crucible is small at steady state. When the maximum sustainable power is supplied to the furnace there will only be a 5°C temperature difference. A 5°C difference is not noticeable when the temperature measured is 1000°C.

This estimate is conservative. All the power from the furnace will not be conducted through the bottom of the crucible, so the temperature difference should be less.

4.5 Flow Control Loop

The flow control loop components control the resistance of the electric arc which depends on the arc length and the arc current, Figure 4.8. When the furnace is at a constant temperature, the current will be steady making the resistance a function of only the arc length. If the resistance is kept constant, the tin level will not change, and the tin mass feed rate, which is set at the desired tin flow rate, will equal the tin mass flow rate. The controller, Figure 4.9, uses the difference between the desired resistance and the actual resistance to drive the proportional control valve. The valve varies the pressure and thus the flow from the furnace so that the resistance stays constant. In order for the loop to be able to control the flow of the molten tin stream, the tin wire fed into the furnace must melt quick enough to maintain a molten tin supply, and the pressure for different flows from the orifice must be reasonable.

4.5.1 Flow Control Components

The flow control loop will consist of a modified Lincoln Wire Feeder, model NA-5R; an Omega Electronically Controlled Proportional Valve, PV104-10V; a differential amplifier; a Data Translation Data Acquisition and Control (DAQC) Card, DT2801-A; a 386 based personal computer; and an anti-aliasing filter.

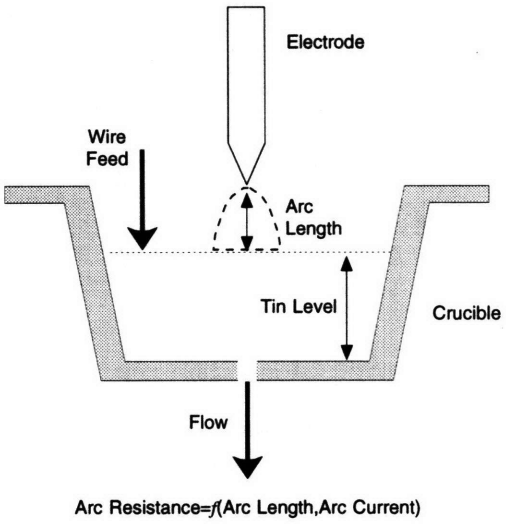

Figure 4.8 Arc Resistance

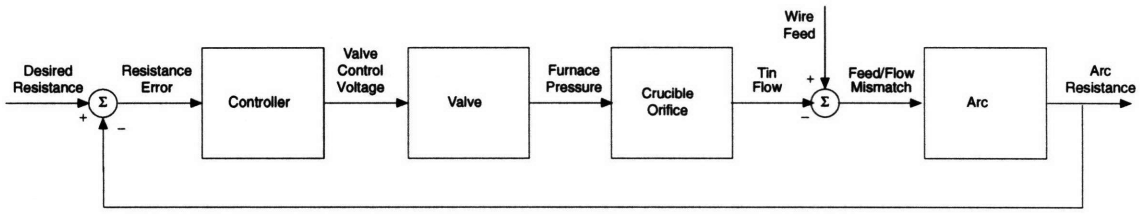

Figure 4.9 Simplified Flow Control Loop

The wire feeder with some modifications will be used to replenish the tin in the furnace. The modifications enabled tin with its low strength and stiffness to be unwound from its spool and to be pushed into the furnace. Figure 4.10 shows the modified wire feeder. To increase the chance of unwinding the tin from the spool without the tin failing, the tension on the wire was reduced by replacing the large steel spool with a small 5 lbs spool and by placing the spool so that the wire had a straight path to the roller mechanism. To increase the chance of pushing the wire into the furnace, a short attachment with an opening only slightly larger than the wire diameter was made to connect the roller mechanism to the furnace, Figure 4.11. The attachment was made with 1/8 in. outer diameter cooper tubing. The close tolerance between the attachment and

the wire is small enough to prevent the wire from bending, thus minimizing the chance of jamming, but large enough so that there is not a significant force on the wire. The close tolerance has the added benefit of reducing the pressure losses from the furnace.

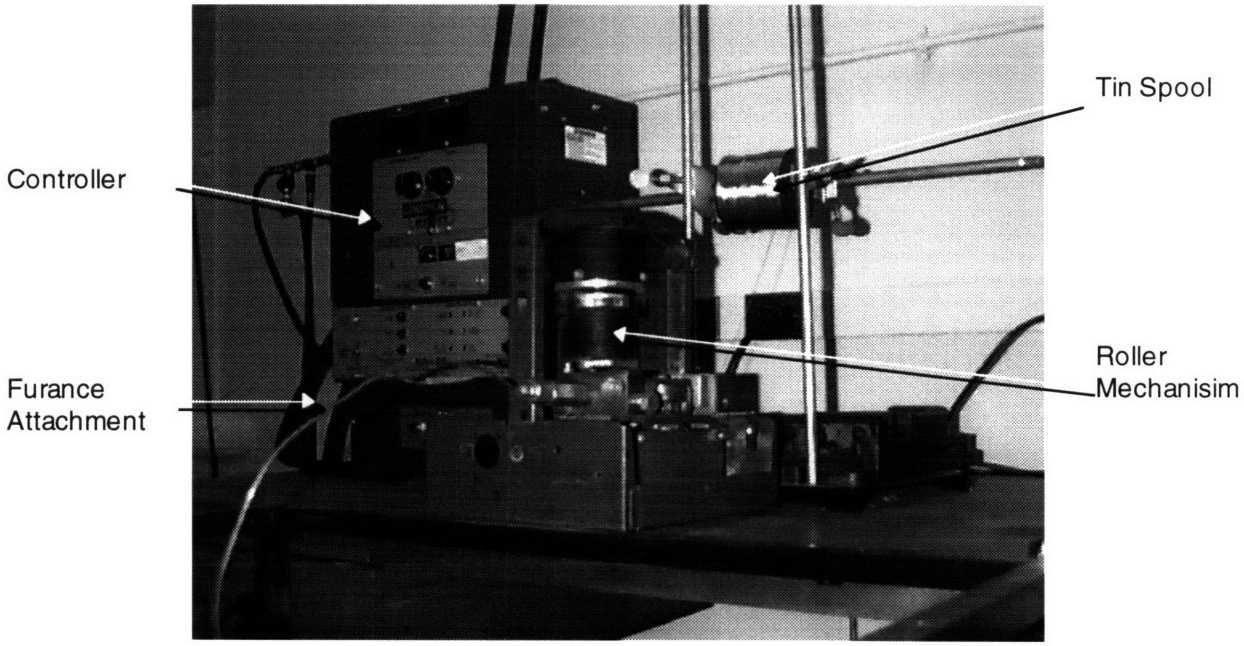

Figure 4.10 Tin Wire Feeder Mechanism

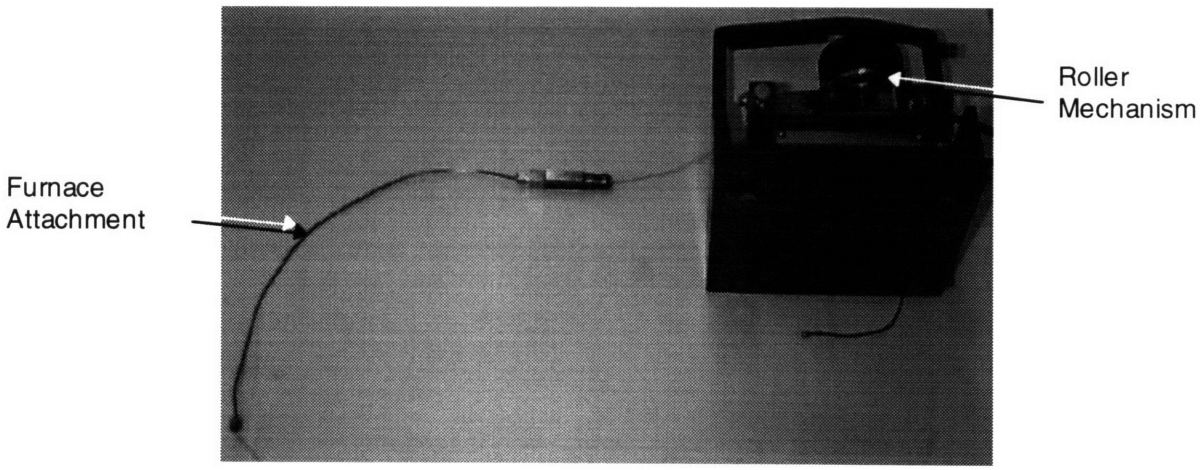

Figure 4.11 Close Up of the Wire Feed Attachment

The proportional control valve will be used to vary the pressure in the pressure chamber. It has a 5/64 inch orifice which results in a $4.5X10^4$ sccm at 10 psi across the fully open valve. The maximum allowable pressure across the valve is 40 psi. The control input to the valve, 0 to 10V, linearly varies the flow through the valve from 0 to 100%. The bandwidth of the valve is 10 Hz.

Three different pressure configurations for the proportional control valve were tried. Configuration 1, Figure 4.12, had the proportional control valve at the output and a set flow going into the pressure chamber through the torch. By varying the flow from the pressure chamber the pressure in the chamber was altered. The configuration suffered from two problems. The hot argon overheated the valve and the fumes from the furnace clogged the valve. Configuration 2 had the proportional control valve in the argon flow line to the torch and the outlet valve from the pressure chamber open, Figure 4.13. A pressure difference of 20 psi was placed across the valve. This configuration seemed to control the pressure in the furnace and resulted in tin flow from the furnace. It has the disadvantage, though, of altering the argon flow to the torch which could vary the power output from the torch. Configuration 3 added an additional input line to the pressure chamber in addition to the torch input, Figure 4.14. This new line has the proportional control valve. The argon flow to the torch was kept constant and the flow in the additional input line was altered to change the pressure in the chamber. This configuration seemed to control the pressure in the chamber, but the tin flow from the furnace did not appear as steady as with configuration 2. This configuration also added to the complexity of the system. For these reasons configuration 2 will be used as the pressurization scheme.

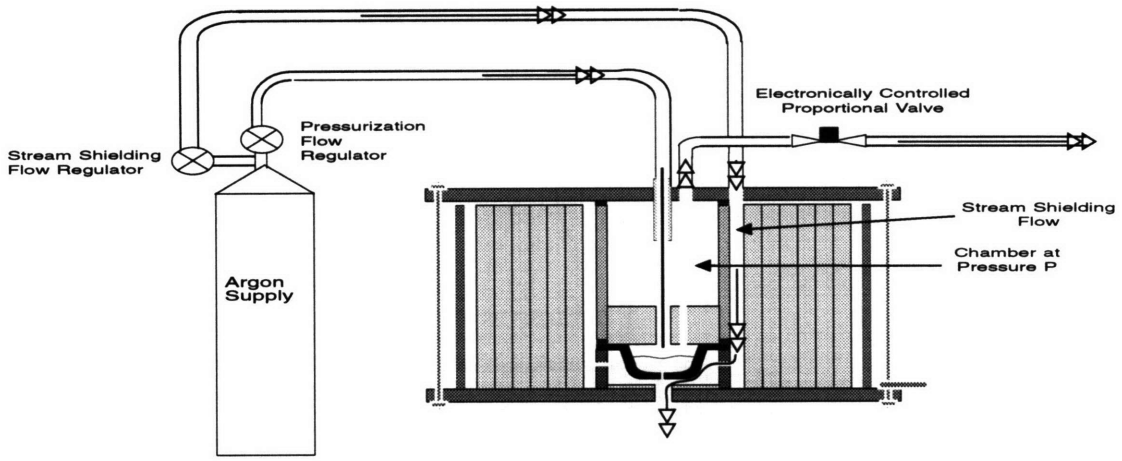

Figure 4.12 Pressure Configuration 1

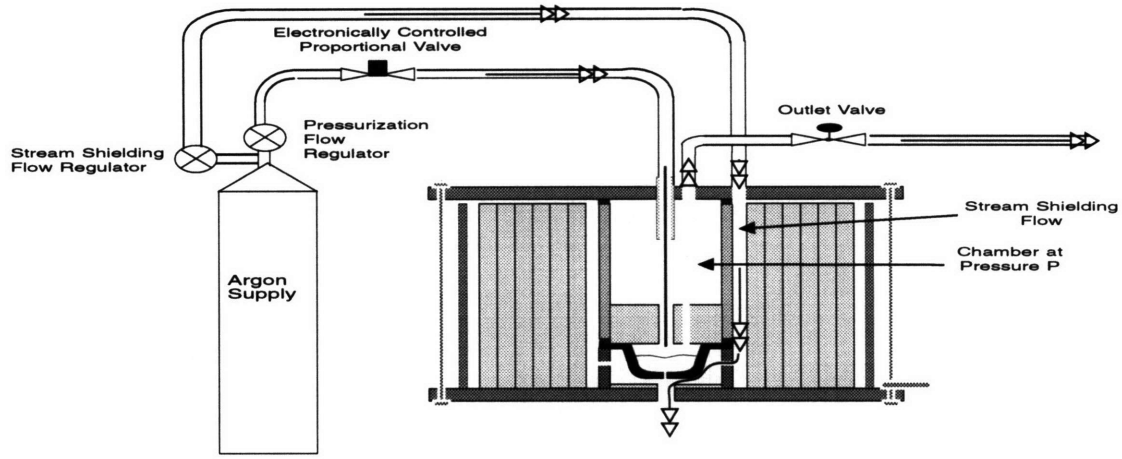

Figure 4.13 Pressure Configuration 2

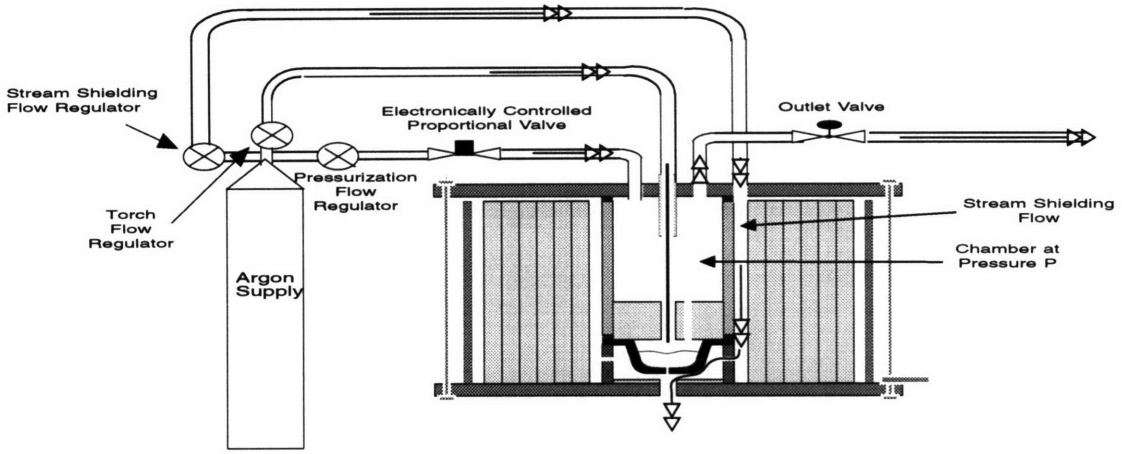

Figure 4.14 Pressure Configuration 3

The differential amplifier will condition the arc voltage signal so that it is in the range of the DAQC card. The gain of the filter is 0.24. This will allow the power supply voltage to be 40V, well above the expected voltages, while keeping the input to the DAQC less than 10V. Figure 4.15 shows the differential amplifier circuit.

The DAQC card will be the same card described in the temperature control section. Here, it will convert the attenuated analog arc voltage signal into a digital signal and will convert the digital proportional control valve signal from the computer into an analog signal.

The 386 computer with a 0.5 sec sampling period will again be used to implement the control algorithm. The input to the control algorithm will be the digital arc voltage signal. The output of the algorithm will be the digital proportional control valve signal. The output signal will adjust the valve position so that the pressure in the pressure chamber produces the correct tin flow. The sampling period length was chosen for the same reasons as the temperature controller. It will allow the computer time to perform all needed calculations while allowing the controller to have sufficient bandwidth so that the worst feed change disturbance will not overfill or empty the crucible.

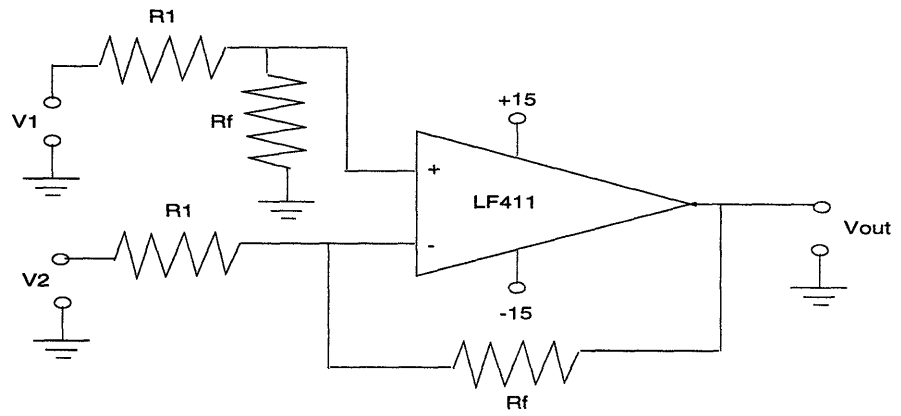

R1=61.5kΩ

Rf=14.8kΩ

V1=Positive Electrode Voltage

V2=Negative Electrode Voltage

Figure 4.15 Differential Amplifier

The anti-aliasing filter will be identical to the temperature loop filter. The same cutoff frequency will be used because the same sampling period will be used for both control loops.

Arc Resistance as a Measure of Tin Level

Two measurements, the arc voltage and the arc resistance, were looked at to determine which gave a better indication of tin level in the crucible. The resistance of the arc was determined to be the best. Figures 4.16 and 4.17 show the arc resistance and voltage variation with arc length. The solid line is a first order polynomial curve fit. The experimental data is shown with x's. The slope of the resistance curve is much steeper which gives a better indication of tin mass change.

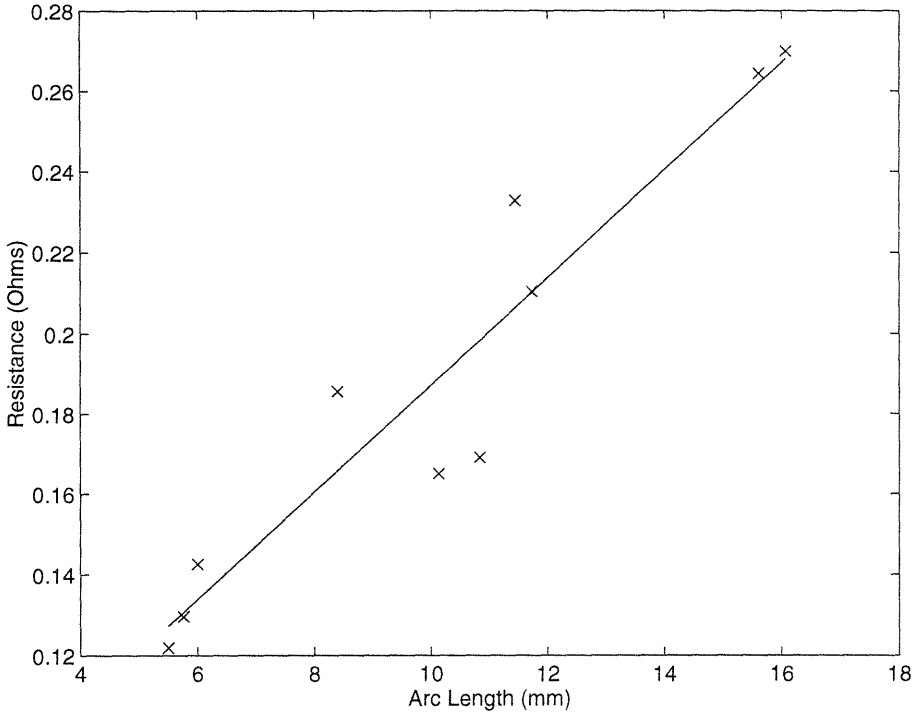

Figure 4.16 Resistance vs Arc Length

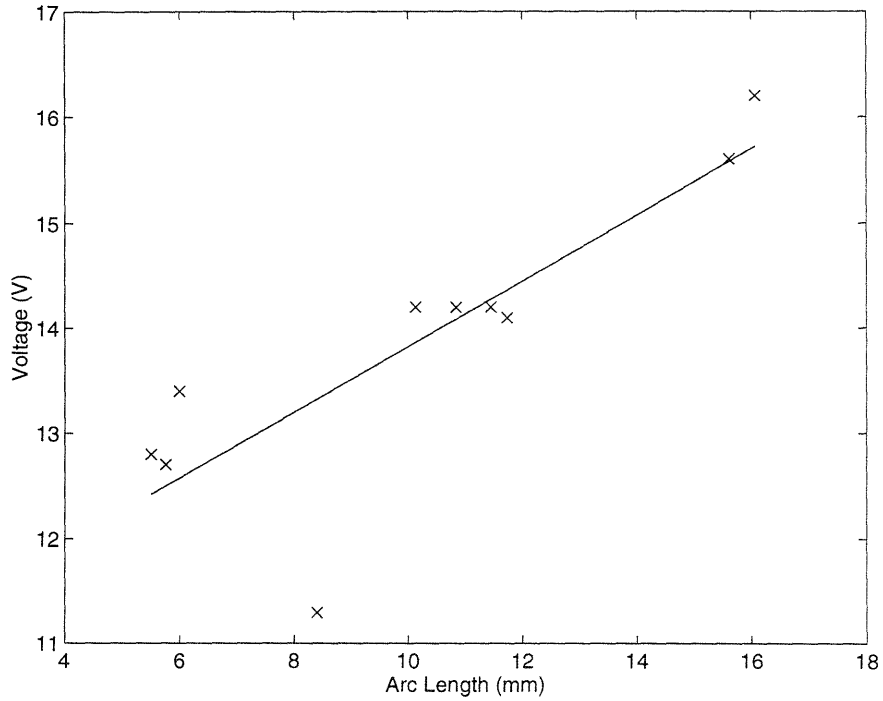

Figure 4.17 Voltage vs Arc Length

4.5.2 Tin Wire Melting Rate

To keep a molten tin reservoir for the flow control system to expel, the tin wire fed into the furnace must melt before it reaches the bottom of the graphite crucible. An analysis was conducted to verify the tin will melt.

The analysis compared the time for the center of the wire to reach the melting point, 232°C, to the time it takes the wire to travel the distance of the molten pool height, 0.55 in, at 999 in/min, the maximum wire feed rate. The melting time must be less than the travel time. Figure 4.18 shows the molten pool and wire setup. The analysis assumed the heat transfer will occur only when the wire is in the 1000°C molten tin pool; the wall temperature of the wire will instantaneously jump to the temperature of the molten pool; and the wire is of infinite length.

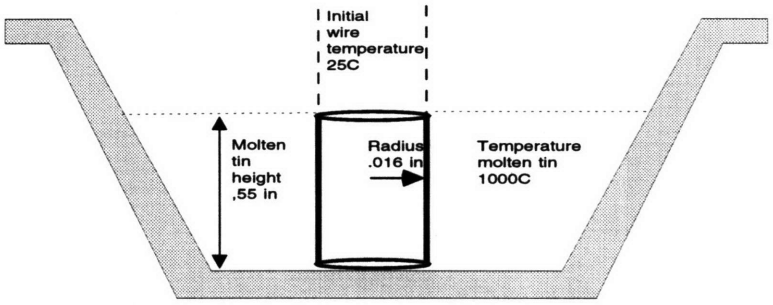

Figure 4.18 Molten Pool and Wire Setup

To calculate the time for the center of the wire to reach its melting point, the heat diffusion equation in cylindrical coordinates was solved. The equation assuming no heat generation with appropriate boundary conditions is:

$$\rho c_p \frac{\partial T}{\partial t} = \frac{1}{r}\frac{\partial}{\partial r}(k\frac{\partial T}{\partial r})$$

$$T(r,0) = T_{ambient} = 25°C$$

$$T(r_o,t) = T_{moltenbath} = 1000°C$$

$$\left.\frac{\partial T}{\partial r}\right|_{r=0} = 0$$

where:

r = the radial distance from the center. (in)

r_o = the radius of the wire. (0.016in)

k = the thermal conductivity of tin at 25°C. (65 W/m K)

T = the temperature of the tin in the radial direction. (°C)

c_p = the specific heat of tin at 25°C. (222 J/kg K)

t = the time. (sec)

The solution to this problem is (Incropera and DeWitt, 1981):

$$\Theta^* = \sum_{n=1}^{\infty} C_n \exp(-\zeta_n^2 Fo) J_0(\zeta_n r^*)$$

where:

$$C_n = \frac{2}{\zeta_n} \frac{J_1(\zeta_n)}{J_0^2(\zeta_n) + J_1^2(\zeta_n)}$$

$$\Theta^* = \frac{T_{desired} - T_{moltenbath}}{T_{wireinitial} - T_{moltenbath}}$$

$$Fo = \frac{4\alpha t}{r_o^2}$$

$$r^* = \frac{r}{r_o}$$

$$Bi = \frac{h \bullet r_o}{2k}$$

J_1 & J_2 = the Bessel Functions of the first kind.

h = the heat transfer coefficient. (0 W/m^2 K) The wire surface temperature instantaneously jumps to the molten pool temperature.

ζ_n = the positive roots of the transcendental equation:

$$\zeta_n \frac{J_1(\zeta_n)}{J_0(\zeta_n)} = Bi$$

$T_{desired}$ = the desired wire centerline temperature. (232°C)

$T_{moltenbath}$ = the tin bath temperature. (1000°C)

$T_{wireinitial}$ = the initial wire temperature. (25°C)

Using the graphs in Incropera and DeWitt (1981) for an infinite rod, Fo can be found for a wire centerline temperature of 232°C. Fo is 0.1. The time for the centerline temperature to reach tin's melting point is:

$$Fo = \frac{4\alpha t}{r_o^2} = \frac{4(4\times10^{-5})t}{(.016\times.0254)^2} = 0.1 \Rightarrow t = 1\times10^{-4}\,\text{sec}$$

The wire melts quickly once it enters the time pool. 1×10^{-4} seconds is negligible.

The result of the calculation may be a optimistic. The outside of the wire will not instantaneously jump to the molten bath temperature. However, the wire preheat is, also, neglected. The wire is preheated in the furnace before it enters the molten bath.

The time for the wire to travel the height of the pool, when the feed rate is a maximum, was calculated from:

$$\text{time of wire travel} = \frac{\text{height of molten pool}}{\text{wire feed rate}} = \frac{.55\text{in}}{999\text{in/min}\times\frac{1}{60}\text{min/sec}} = 3.3\times10^{-2}\text{sec}$$

The travel time is 3.3×10^{-2} seconds.

The analysis indicates that the tin wire fed into the furnace will always melt before the wire travels to the bottom of the crucible. The wire melts in 1×10^{-4} seconds, while it takes the wire 3.3×10^{-2} seconds to travel the molten pool height at its maximum feed rate.

4.5.3 Furnace Pressure to Flow Relationship

For the flow control system to deliver the desired flow, the pressure required to produce the flow must be reasonable. Large pressures will over stress the system. Small pressures will make the flow difficult to control. An analysis was conducted to determine the pressures required for different steady state flows.

To calculate the pressure to flow relationship, the Navier-Stokes equation was solved. This equation assumes laminar viscous flow. The results were adjusted to account for turbulent flow. Figure 4.19 shows the dimensions of the exit orifice.

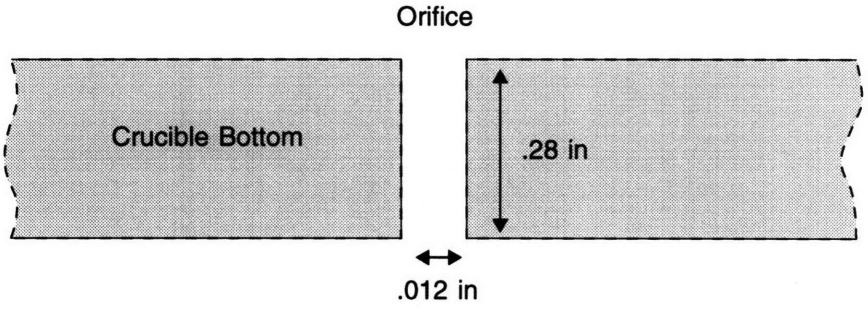

Figure 4.19 Exit Orifice Dimensions

The Navier-Stokes equation to be solved was:

$$\frac{D\mathbf{V}}{Dt} = -\frac{1}{\rho}\nabla p + g + \upsilon\nabla^2\mathbf{V}, \text{ if } \nabla\cdot\mathbf{V} = 0\,;\ \mu = \text{constant}$$

where:

$\mathbf{V}$ = the velocity. (m/sec)

p = the pressure. (N/m^2)

g = the gravitational acceleration. (9.8 m/sec^2)

υ = the kinematic viscosity of tin at 1000°C. (1.347×10^{-7} m^2/sec)

ρ = the density of tin at 1000°C. (6529 kg/m^3)

μ = the viscosity of tin at 1000°C. (0.88 mNsec/m^2)

t = the time. (sec)

For steady flow through a circular pipe, where the height change between the ends is small, the equation in circular coordinates with appropriate boundary conditions is:

$$\frac{d^2V_z}{dr^2}+\frac{1}{r}\left(\frac{dV_z}{dr}\right)=\frac{1}{r}\frac{d}{dr}\left(r\frac{dV_z}{dr}\right)=\frac{1}{\mu}\frac{d(p)}{dz}$$

$$\left.\frac{dV_z}{dr}\right|_{r=0}=0$$

$$V_z|_{r_O}=0$$

where:

r = the radial distance from the center. (m)

r_o = the radius of the orifice. (1.5×10^{-4} m)

V_z = the tin velocity in the z direction. (m/sec)

z = the distance in the z direction. (m)

The solution to this problem is (Fay, 1994):

$$-\frac{dp}{dz}=\frac{128\mu Q}{\pi D^4}$$

where:

Q = the volumetric flow rate. (m^3/sec)

D = the diameter of the orifice. (3×10^{-4}m)

Adjusting for turbulent flow and assuming the orifice is straight with length L and a constant diameter, the equation becomes:

$$p_{in} - p_{out} = f\frac{8\rho Q^2 L}{\pi^2 D^5}$$

Where f is empirically derived Darcy friction factor. To calculate numerical values to this solution, the Darcy factor must be obtained by using the Reynolds number.

The Reynolds number, R_e, is defined as:

$$R_e = \frac{4\rho Q}{\mu\pi D}$$

The Reynolds number for the maximum flow rate was found by substituting the maximum volumetric flow rate, $2.45\text{x}10^{-7}$ m^3/sec, the density of tin at 1000°C, the diameter of the orifice, and the viscosity of tin at 1000°C into the Reynolds number expression:

$$R_e = \frac{4\rho Q}{\mu\pi D} = \frac{1}{\pi}\left(\frac{4\times 6529\times 2.45\times 10^{-7}}{3\times 10^{-4}\times 0.88\times 10^{-3}}\right) = 7715$$

For the maximum flow, the Reynolds number indicates turbulent flow, a Reynolds greater than 2300. Most reasonable flow rates will also be turbulent.

With the Reynolds number, the Darcy friction factor can be calculated using the graph in Fay (1994). The Darcy friction factor is 0.04. Wall roughness is not needed to use the graph. For Reynolds numbers less than $8\text{x}10^4$ but greater than 2.3×10^3 regardless of the wall roughness, the Darcy friction factor is approximately the same.

Finally, the pressure for obtaining the maximum flow rate was found by substituting the Darcy friction factor, the density of tin at 1000°C, the maximum volumetric flow rate, the diameter of the orifice, and the length of the orifice,

7.62×10^{-3} m, into the adjusted solution to the Navier-Stokes equation. The pressure is:

$$p_{in} - p_{out} = .04\left(\frac{8 \times 6529(2.45 \times 10^{-7})^2}{\pi^2 (3 \times 10^{-4})^4}\right)\frac{7.62 \times 10^{-3}}{3 \times 10^{-4}} = 3945Pa = 5.78psi$$

This pressure is reasonable. Figure 4.20 shows the pressure, calculated in a similar manner as the maximum flow rate pressure, for various mass flow rates from the furnace

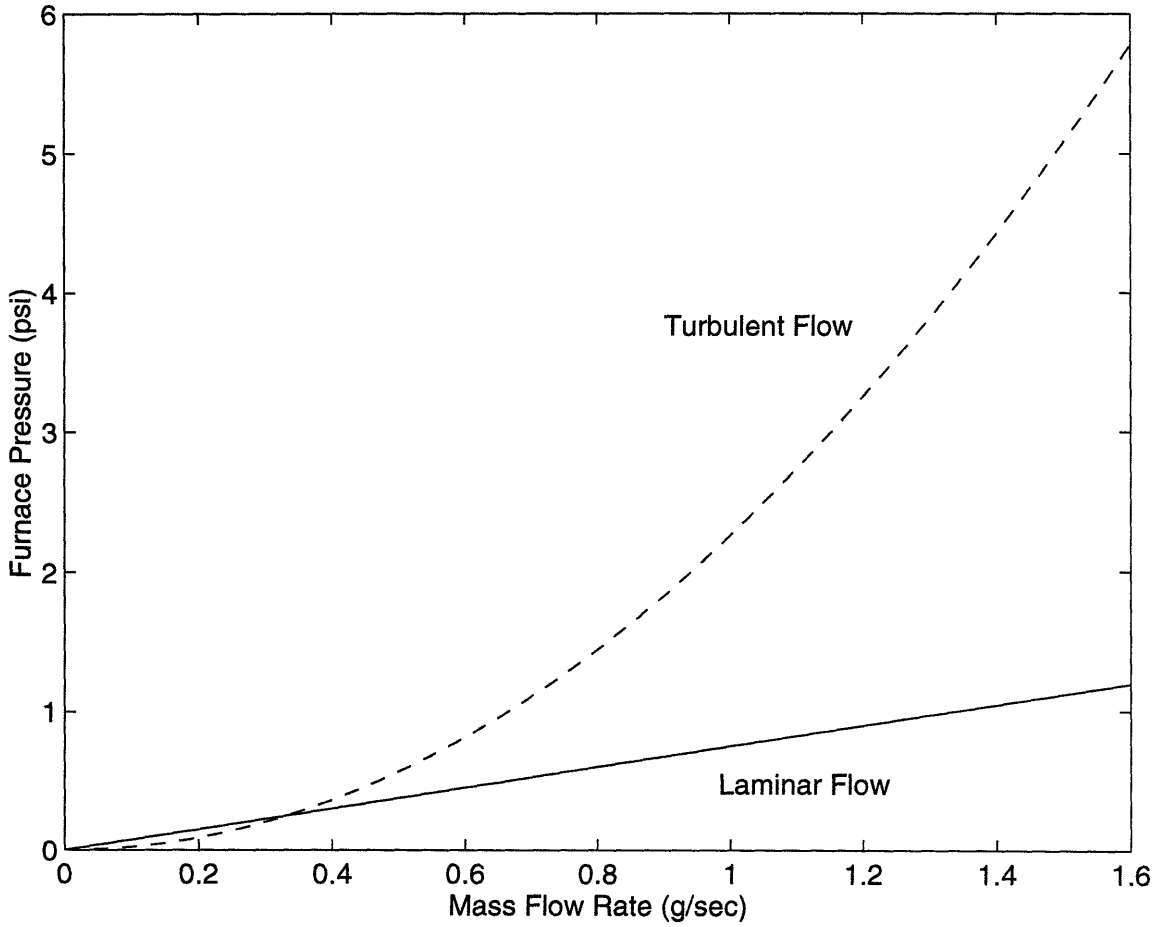

Figure 4.20 Mass Flow Rate vs Furnace Pressure

An experiment was conducted to verify the analysis. The furnace was heated to a temperature of 1000°C and then pressurized to 5.75 psi. The actual

mass flow rate obtained was 1.36 g/sec. The analysis indicated the flow rate should be 1.6 g/sec. The values agree closely.

The analysis of the pressures required in the furnace to obtain the desired tin flow rates from the furnace shows the pressures are reasonable, but small. For flow rates below 1 g/sec, the pressure is very small. The flow controller may have trouble maintaining those pressures, and the orifice may clog more easily.

4.6 Summary

The control scheme consists of a furnace and two control loops. Analysis of the arc furnace components indicates, the control scheme should be able to produce streams with different temperatures and flow rates. The temperature controller development is described in the next chapter. The flow controller development is described in chapter 6.

Chapter 5: Temperature Controller

5.1 Overview

A temperature controller is required for the arc furnace to maintain the temperature of the molten stream when the desired value is constant and change the temperature in a minimum amount of time when the desired value changes. The controller must do these in the face of uncertainties, disturbances and noise. The temperature of the furnace is important because it determines the energy available to melt the base metal. Since the molten stream temperature can not be measured, the temperature of the graphite crucible is controlled instead. As shown in Chapter 4, the graphite crucible temperature is a good approximation of the stream temperature.

The sequence followed in developing the controller was:

- formulate the performance requirements
- obtain the system model
- design the controller
- simulate the system to verify performance and determine the magnitude of the control signals
- implement the controller
- adjust the controller to account for actuator saturation and other effects.

An analog design approach, Bode diagrams, was used to develop the temperature controller. An analog design approach can be used for digital controllers, if the sampling rate is 10 times the desired closed loop bandwidth (Franklin, et al., 1986).

5.2 Performance Requirements

The performance requirements for the temperature control system are:

- a zero steady state error
- a damping ratio of 0.7
- a closed loop bandwidth of 0.35 rad/sec.

They are based on the desire for the temperature system to reject worst case disturbances, follow the desired stream temperature, and be insensitive to noise. A zero steady state error insures that the output temperature will eventually equal the reference temperature after a step change. A damping ratio of 0.7 limits the temperature response oscillations. A closed loop bandwidth of 0.35 rad/sec will allow the output temperature to track reference temperatures of less than 0.35 rad/sec, to reject disturbances at the system input of less than 0.35 rad/sec, and to be insensitive to sensor noise greater than 0.35 rad/sec. Figure 5.1 shows a simplified block diagram of the closed loop system indicating the location of disturbances and noise.

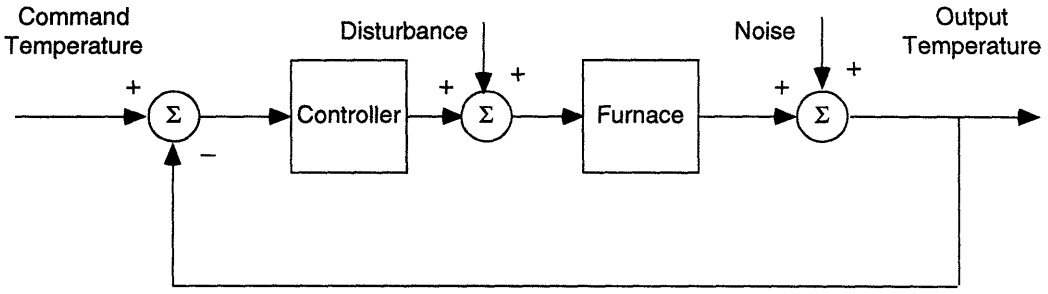

Figure 5.1 Simplified Block Diagram of the Temperature Control Loop

The damping ratio and the closed loop bandwidth were derived on the assumption that the closed loop system was second order without zeros (a simple second order system). Since the temperature system is more

complicated, the system was simulated, after the controller was designed, to verify the performance was adequate. In a simple second order closed loop system, a 0.7 damping ratio results in a time response without oscillations. Determining the closed loop bandwidth was more involved and is described in the next section.

As will be shown, the desired performance of the temperature control system can not be meet due to physical limitations. The attainable performance is adequate, though.

Determination of the Closed Loop Bandwidth

Factors considered when determining the closed loop bandwidth were:

- the time for a temperature change to occur
- the effect of a disturbance on the temperature
- the power required
- the effect of noise on the temperature.

The effect of a disturbance on the temperature is the most important factor, and it served as the basis for choosing the bandwidth. A change in the wire feed rate, which is a disturbance to the temperature system, is the most likely change to the system. Once the bandwidth was obtained, the time for a temperature change and the effect of noise on the temperature were checked to see if they were adequate. The power requirement was checked in simulation.

The worst possible wire feed rate change is from 0 to 1.6 g/sec or 1.6 to 0 g/sec. The change results in a power mismatch of 440 W, from Chapter 4, and a

temperature variation of 20°C/sec[1]. A rise time of 5 seconds for the closed loop system, which equates to a bandwidth of 0.35 rad/sec[2], will prevent the temperature from varying by more than 100°C. The reason for choosing 100°C as the maximum temperature change will be discussed in the next section.

The time for a temperature change with a closed loop bandwidth of 0.35 rad/sec is 5 seconds, provided there is power. This is adequate. If the furnace has a travel speed of 1 in/sec, a temperature change could be conducted within 5 inches of travel along the base metal.

The effect of measurement noise on the temperature will not be significant. The frequency content of the noise was determined by conducting a Fast Fourier transform on the measured temperature output of the furnace in open loop when the temperature should have been constant. Figure 5.2 shows the time domain output signal upon which the Fast Fourier transform was conducted. Figure 5.3 is the transform. The content of the signal is largely zero frequency. This corresponds to the temperature for the supplied power. Figure 5.4 is an expanded version of the frequency spectrum. There is no particular

---

[1] The power mismatch was used to calculate the rate of temperature change of the tin. Assuming the volume of tin in the crucible stays constant at 105 grams, i.e. the feed rate into the furnace equals the flow rate from the furnace, the temperature drop per second of the tin in the furnace was calculated from:

$$°C/s = p/(c_p m_{tin})$$

where:

p = the power mismatch. (440 W)

c_p = the specific heat of tin at 25°C. (222 J/kgK)

m_{tin} = the tin mass. (0.105 kg)

For the maximum feed rate, this equates to a temperature drop of:

$$440/(222 \times 0.105) \approx 20°C/sec$$

[2] The rise time for a simple second order system is roughly the same for different damping ratios (Franklin, et al., 1986). The average is $1.8/\omega_n$ where ω_n is the natural frequency of the system. The natural frequency for a simple second order system is approximately the bandwidth of the system. For a rise time of 5 seconds, the closed loop bandwidth is 0.35 rad/sec.

frequency which it would be desirable to have the temperature system insensitive.

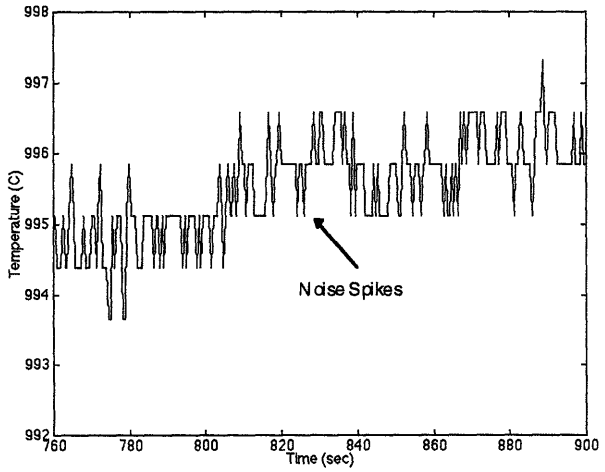

Figure 5.2 Temperature Measurement

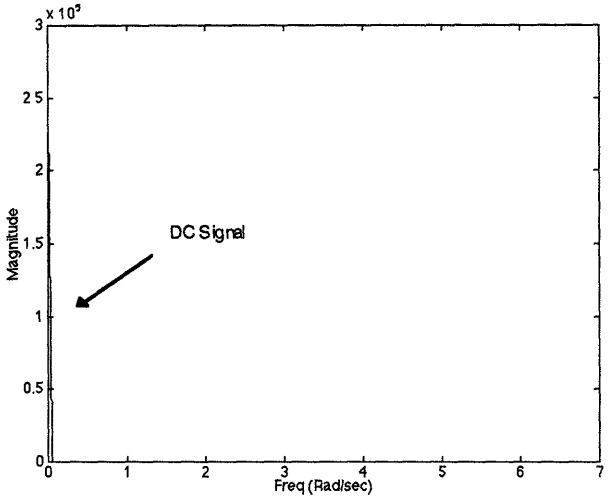

Figure 5.3 Frequency Spectrum of the Temperature Measurement

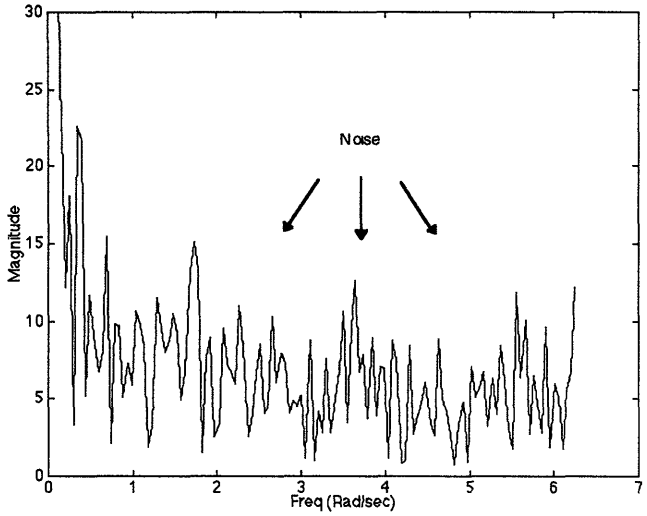

Figure 5.4 Expanded Frequency Spectrum

Effect of a 100°C Temperature Change

A 100°C maximum temperature variation for the system was chosen because it changes the heat content of the molten stream by less than 8% and the viscosity by less than 5%. The effect of the temperature change on the heat content and viscosity was calculated from the specific heat of tin and the viscosity of tin as a function of temperature.

The heat content available to melt the base metal per a kilogram of tin, assuming the specific heat does not vary with temperature, is:

$$\text{energy/mass} = c_p T$$

where

c_p = the specific heat of tin. (222 J/kg°K)

T = the tin temperature. (°K)

At 1000°C the energy is:

$$\text{energy/mass} = 222 \times 1273 = 283 \ {}^{kJ}/_{kg}$$

A 100°C change in temperature results in an energy change of:

$$\text{energy/mass} = 222 \times 100 = 22.2 \ {}^{kJ}/_{kg}$$

The change is approximately 8%.

The viscosity of the tin is given by:

$$\mu = \mu_o \exp^{(E/RT)}$$

where

μ = the viscosity. (mNsec/m^2)

μ_0 = the tin viscosity as the temperature goes to ∞. (.5382 mNsec/m^2)

E = the tin conversion factor. (5.19 kJ/mol)

R = the universal gas constant. (8.3144 J/mol°K)

T = the tin temperature. (°K)

At 1000°C the viscosity is:

$$\mu = .5382 \exp^{(5.19 \times 10^3 / (8.3144 \times 1273))} = .88 \text{ mNsec/m}^2$$

At 900°C the viscosity is:

$$\mu = .5382 \exp^{(5.19 \times 10^3 / (8.3144 \times 1173))} = .90 \text{ mNsec/m}^2$$

The change is approximately 5%.

5.3 System Model

A system model is needed so that a controller can be designed to give a combined controller/system response which meets the performance requirements. When frequency analysis techniques are used, the open loop Bode diagram of the system without the controller is required. As described in chapter 4, the temperature control system consists of a pyrometer, a GTAW power supply, a DAQC which includes an A/D and D/A converter, a computer to implement the control, and an anti-aliasing filter. Figure 5.5 is a block diagram representation of the system.

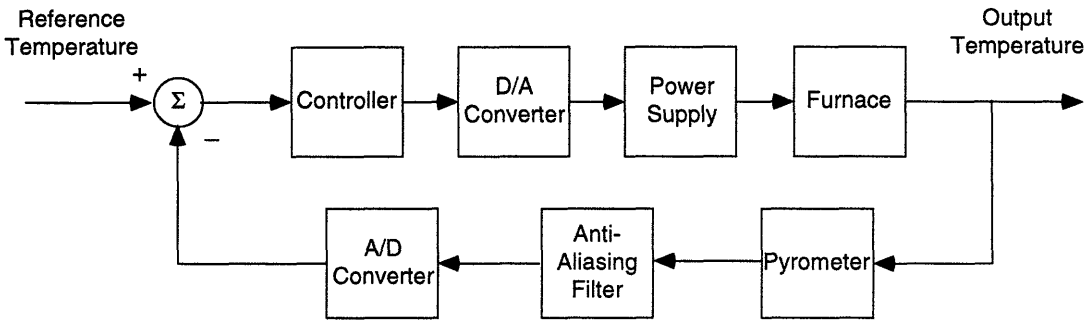

Figure 5.5 Block Diagram of the Temperature Control Loop

In developing the open loop Bode diagram of the system, components which do not greatly affect the dynamic response of the system were neglected. The D/A and A/D converter, the anti-aliasing filter, the pyrometer, and the power supply dynamics were ignored. The dynamics of the A/D and D/A converter can be ignored if the sampling rate is 10 times the desired closed loop bandwidth, (Franklin, et al., 1986). The sampling rate of the system is 12.5 rad/sec and the desired closed loop bandwidth is 0.57 rad/sec. The dynamics of the anti-aliasing filter can be ignored if its bandwidth is sufficiently higher than the desired closed loop bandwidth, (Franklin, et al., 1986). The bandwidth of the anti-aliasing filter is 3 rad/sec. The pyrometer and the power supply were neglected because their bandwidths are much higher than the bandwidth of the furnace. The frequencies which those components attenuate have already

been greatly attenuated by the furnace. The bandwidth of the pyrometer is 157 rad/sec and the bandwidth of the power supply is 1×10^3 rad/sec. Figure 5.6 shows the open loop block diagram of the temperature control system with the neglected components crossed out. The only component that needs to be modeled is the furnace.

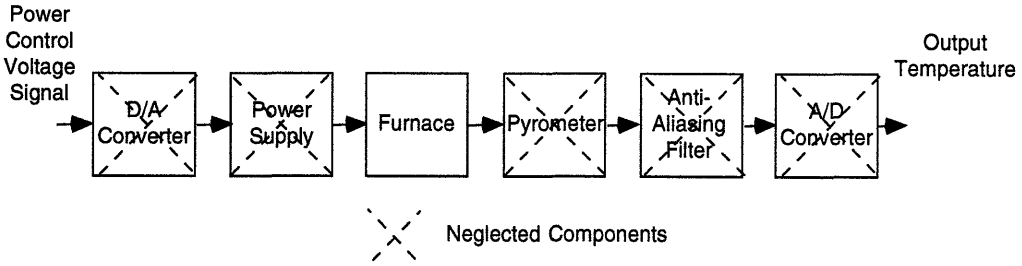

Figure 5.6 Block Diagram of the Open Loop Temperature System

An open loop step response was used to determine the dynamics of the furnace. The furnace was assumed to be first order with a time delay. The equation for a first order system with a delay is:

$$\frac{k_p}{ts+1}\exp(-sT)$$

where

k_p = the steady state gain.

t = the time constant.

T = the time delay.

Figure 5.7 shows the open loop temperature response of the furnace to a 160W power change. There was 114 g of tin in the furnace and the temperature of the furnace was 995°C. k_p is :

$$\frac{\Delta\text{Temperature}}{\Delta\text{Power}}$$

The temperature change was approximately 45°C. The exact value was difficult to determine because the GTAW power supply would trip before the temperature leveled off. The power change was approximately 160W. k_p is, therefore, 0.28. τ is the time for the temperature to reach 2/3 of its change. From Figure 5.7, τ is 66 seconds.

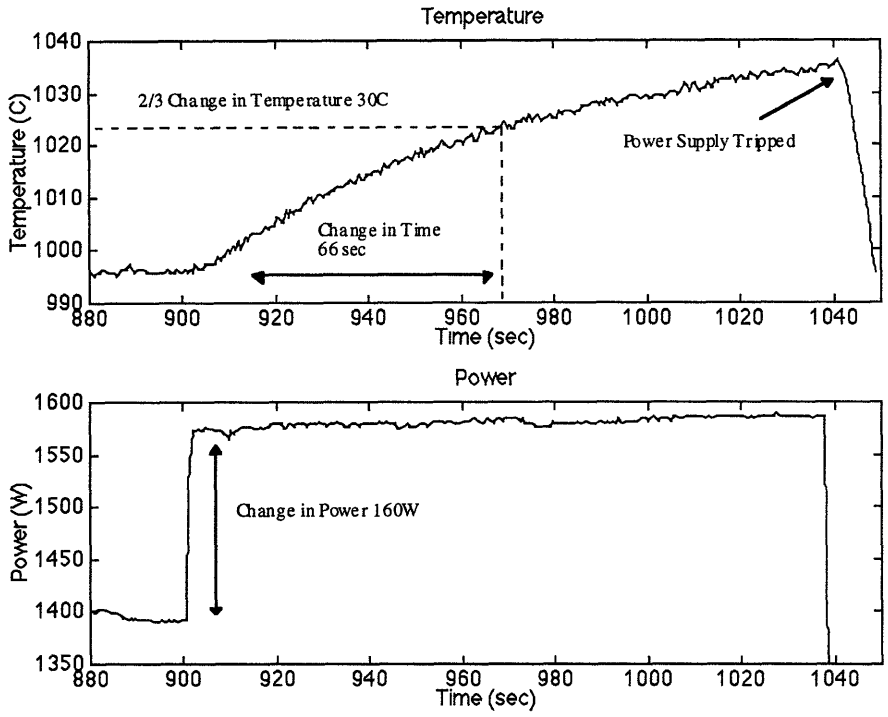

Figure 5.7 Open Loop Temperature Response of the Furnace

T is the time between when the input is changed to a system and when the system first starts to respond. From Figure 5.8, the expanded open loop temperature response of the furnace, T is approximately 4 seconds. The furnace model is, therefore:

$$\frac{0.28}{66s+1}\exp(-4s)$$

The Bode diagram of the furnace and thus the open loop Bode diagram without the controller is shown in Figure 5.9. The furnace attenuates all frequencies with frequencies greater then 0.015 rad/sec being greatly attenuated. The furnace also exhibits large phase lags for most frequencies because of the time delay. The Bode diagram reflects the slow response of the system.

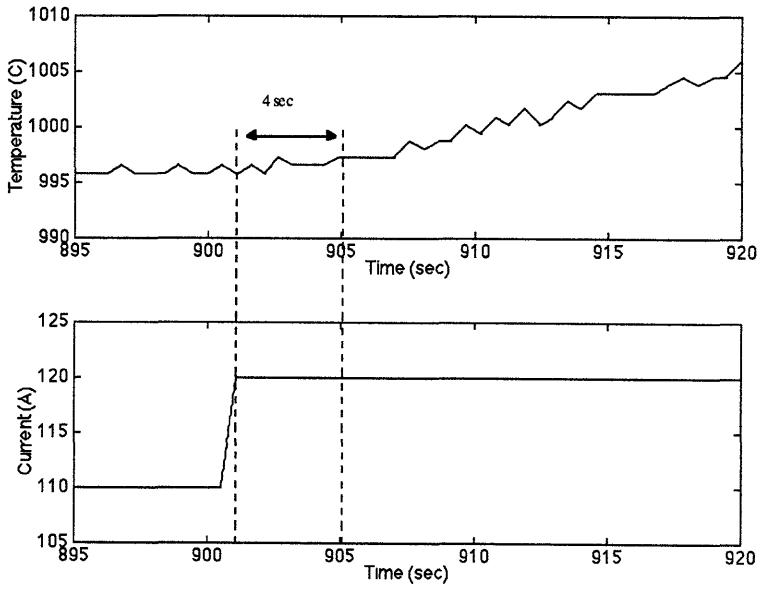

Figure 5.8 Expanded Open Loop Temperature Response of the Furnace

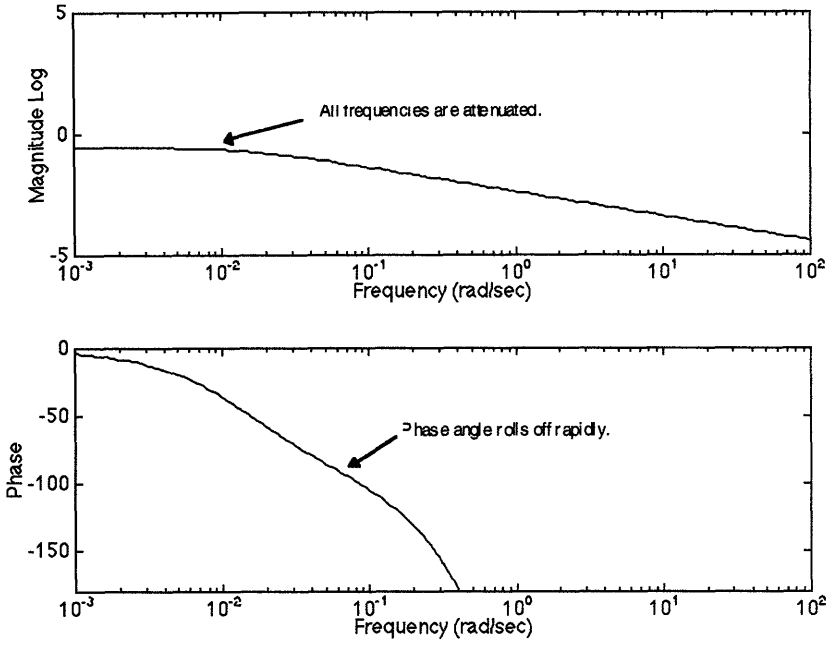

Figure 5.9 Bode Diagram of the Furnace

The cause for the large time delay was investigated because it created problems when designing the controller. It limits the maximum bandwidth possible for the closed loop system. The delay was determined to be caused by the tin mass in the crucible. It takes time for the tin at the bottom of the crucible to be affected by a temperature change of the tin at the top of the crucible. This problem can not be corrected. A volume of molten tin is required so that a molten supply is available at the desired temperature of the stream. If the volume of tin in the crucible is reduced, the flow from the furnace may be interrupted and the tin stream may be composed of newly melted tin which has not had time to reach the correct temperature. An analysis, similar to the one conducted for graphite in Chapter 4, indicates there is a large time delay associated with the tin. The one dimensional simplified thermal diffusion equation is:

$$\frac{\Delta T}{\Delta t} = \alpha \frac{\Delta T}{\Delta z^2}$$

where:

α = the diffusivity of tin at 1000°C. (2.06×10^{-5} m^2/sec)

T = the temperature of the tin in one dimension. (°C)

t = the time. (sec)

z = the distance in the one dimension. (m)

Solving for the time:

$$\Delta t = \frac{\Delta z^2}{\alpha}$$

Substituting the thickness of 105 g of tin, $14.1\text{x}10^{-3}$m, and the diffusivity of tin:

$$\Delta t = \frac{(14.1\times10^{-3})^2}{2.06\times10^{-5}} = 9.6\,\text{sec}$$

This time delay is large. The actual time delay, 4 seconds, is less because convection is probably occurring in the tin as well as conduction.

5.4 Controller Design

The performance requirements determine the required shape of the open loop Bode diagram for the controller and the system. The frequency where the open loop magnitude Bode plot crosses zero, the crossover frequency, is approximately the bandwidth of the closed loop system. The magnitude of the Bode plot at zero frequency determines the steady state error. An infinite magnitude is required for a zero steady state error. The difference in the phase and -180° at the crossover frequency divided by 100 is approximately the damping ratio of the system, provided the phase is less than -180°. The controller is used to alter the open loop Bode diagram to achieve the needed characteristics.

A PI controller was picked as the compensator for the system. A PI controller is of the following form:

$$\frac{k_p(s+a_p)}{s}$$

where

k_p = the proportional gain.

a_p = the zero. (integral gain/proportional gain)

The integrator, pole at zero, gives an infinite magnitude at zero. The zero of the controller alters the phase of the open loop Bode plot. The proportional gain adjusts the magnitude. The desired performance specification requires that the crossover frequency be greater than 0.35 rad/sec with a phase less than -110°. Figures 5.10 to 5.12 show the Bode plots for zero locations at 0.5, 0.05, 0.005. The phase can never be made less than -110° over that range with a zero steady state error. A zero less than 0.005 will make the phase less than -110° but the steady state error is no longer zero. The zero almost cancels the integrator pole. A good zero location is 0.05. The crossover frequency could be as large as 0.1 rad/sec with a damping ratio still of 0.5. A higher crossover frequency was not chosen because it would result in response oscillations and could lead to instability if plant parameters vary. A proportional gain of 25 was used to get a crossover frequency of 0.1 rad/sec.

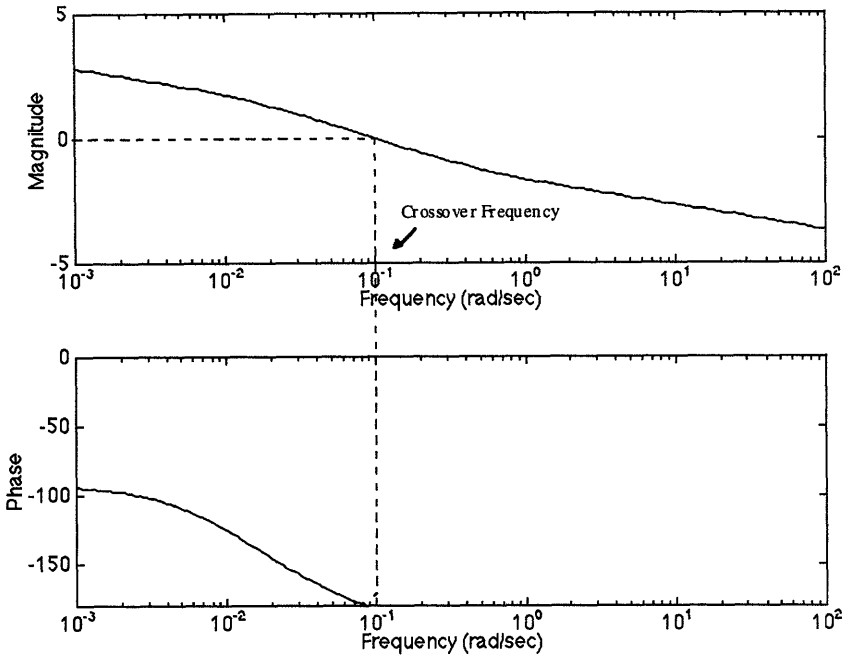

Figure 5.10 Bode Plot of the System with Controller 5(s+.5)/s

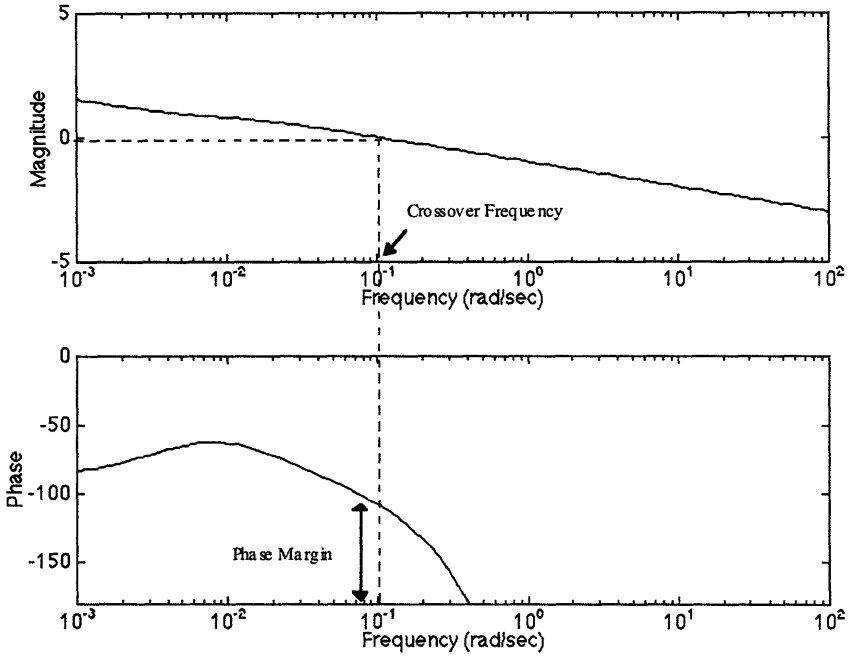

Figure 5.11 Bode Plot of the System with Controller 25(s+.005)/s

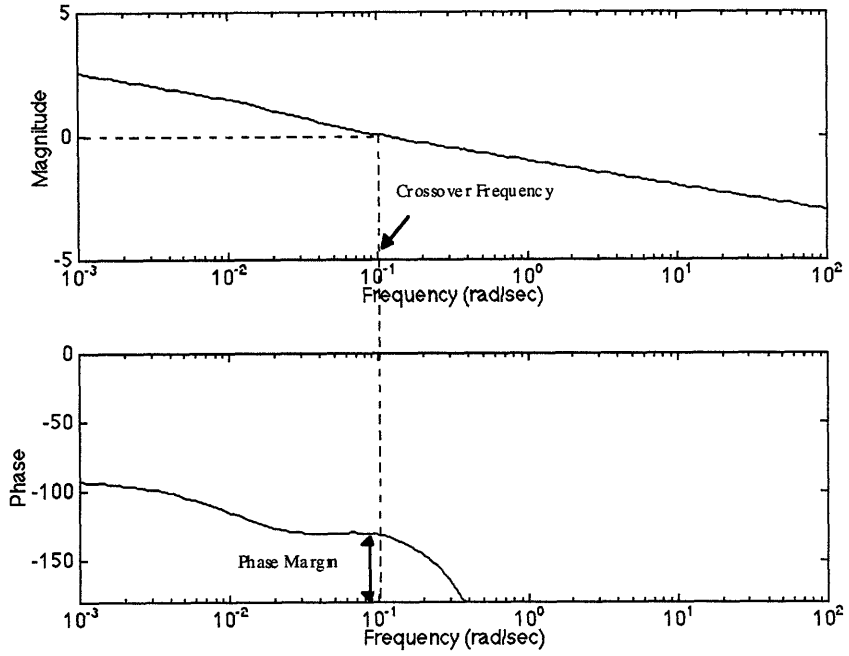

Figure 5.12 Bode Plot of the System with Controller 25(s+.05)/s

The designed controller is:

$$\frac{25(s+0.05)}{s}$$

Appendix B contains the code for its digital implementation. The controller will result in a closed loop system that has zero steady state error, has a damping ratio of 0.5, and has a bandwidth of 0.1 rad/sec. It rejects disturbances up to 0.1 rad/sec, follows commands up to 0.1 rad/sec, and is not affected by noise greater than 0.1 rad/sec. Using the same analysis as in section 5.2, the maximum wire feed change that can be rejected in 0.46 g/sec, and the time to change temperature is now 18 seconds.

A more complicated controller would not significantly increase performance. Higher order controllers may increase the phase margin slightly, but noise would also be amplified. The time delay of the furnace, which can be thought of as a non-minimum phase zero, degrades any controller that can be

used. Non-minimum phase plants can result in systems that have low phase and gain margins (Stein, 1985).

5.5 Simulations

Figure 5.13 shows the simulation block diagram that was used to see if the designed controller will give the expected performance and to check to see if the power supply can provide the required power. Only the relevant temperature control components that were used in the design were included. Those components were the furnace and the controller.

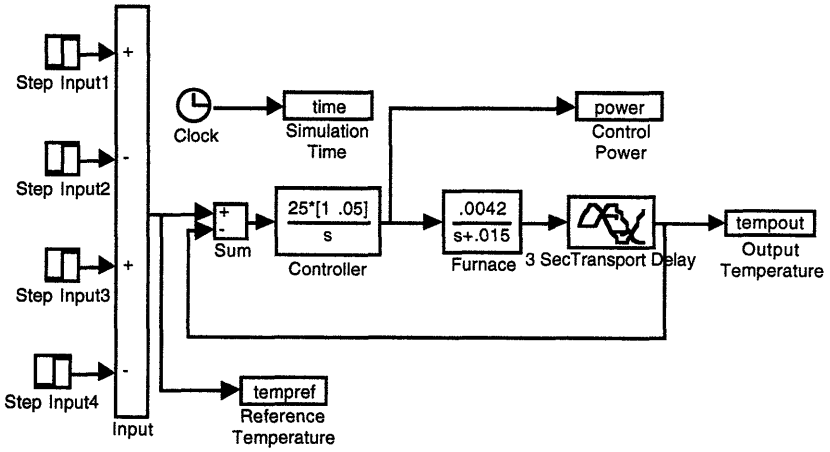

Figure 5.13 Temperature Simulation Block Diagram

Simulations show the expected response, Figure 5.14. The steady state error is zero. There is overshoot because of the 0.5 damping ratio but no oscillations. The rise time is approximately 18 seconds. The time delay is also evident. Fortunately, the power required by the controller is reasonable. The power supply can provide the power. The 100% duty cycle power limit of the GTAW power supply is 2.4 kW and the short term limit is 3.2 kW.

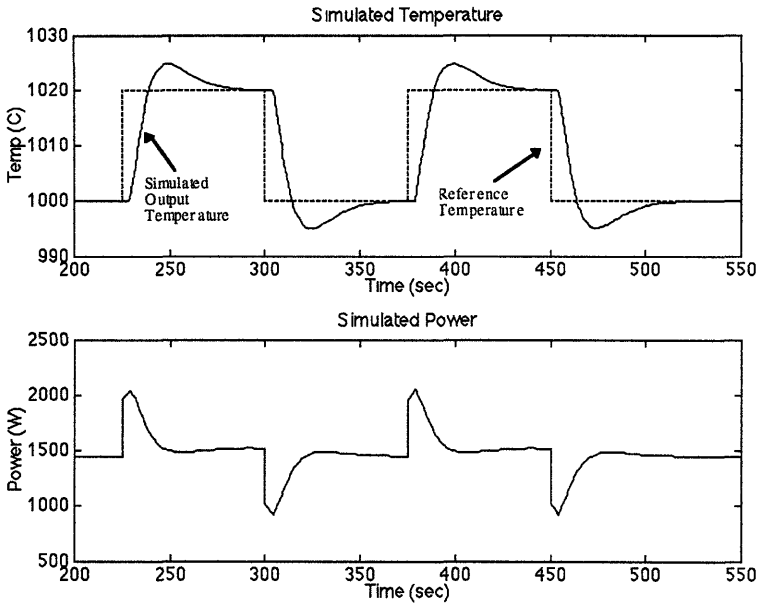

Figure 5.14 Simulated System Response with Controller 25(s+.05)/s

5.6 System Response

Using the controller, the system response was obtained with 114 grams of tin in the furnace. This was the mass of tin used for the controller design. The same reference temperatures as in the simulation were used. Figure 5.15 shows the response. Figure 5.16 shows a comparison between the simulation and actual response. The simulation is the dotted line. The actual response is the solid line. They are almost exact. The reference temperature is the dashed line. This verifies that the assumptions used in developing the system model were valid and that the controller designed based on the model is a good controller for the actual system.

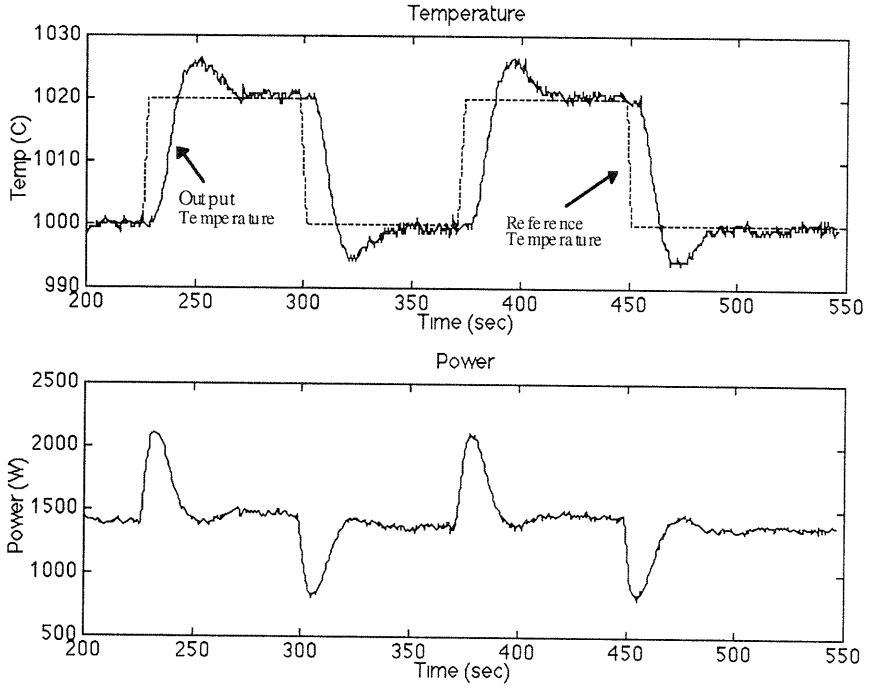

Figure 5.15 System Response with Controller 25(s+.05)/s

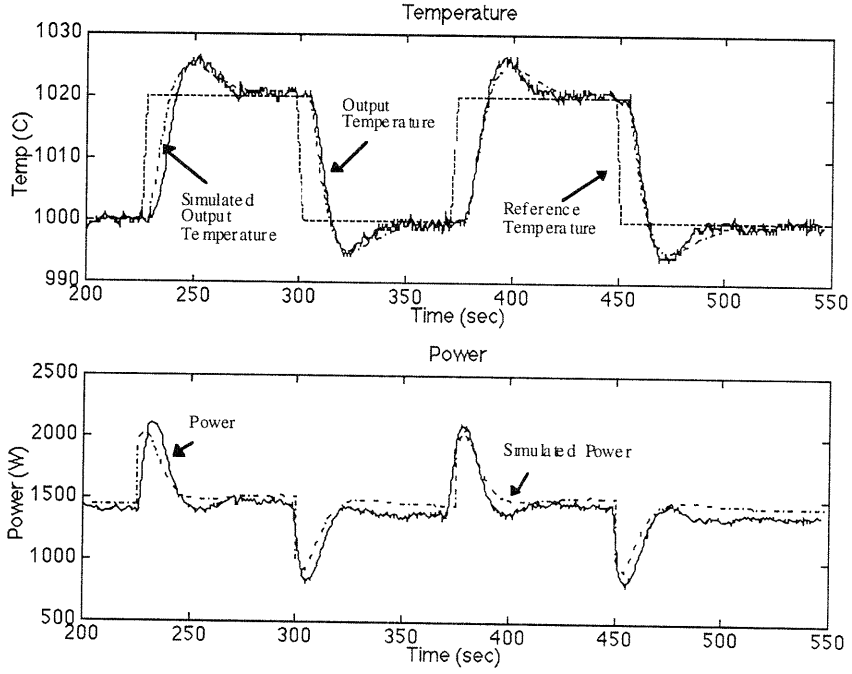

Figure 5.16 Comparison of Simulated and Actual System Response

5.7 Controller Adjustments

The temperature exhibits large oscillations during initial startup. The oscillations are a result of an erroneously large integral value. The controller causes the GTAW power supply to saturate because more power is demanded of the power supply than it can provide. The saturation results in a slower response and thus a larger controller integral value than would occur if saturation did not occur. To correct the integral value an anti-windup feature was added. The anti-windup feature subtracts a scaled integral of the error, when the actuator is saturated, from the integral value. By proper selection of the scaling factor, large overshoots can be prevented. See appendix B for the code. Figure 5.17 shows the temperature response during start up when the scaling factor was 10. There are no oscillations. The response begins when the temperature is at 750°C, the lower range of the pyrometer.

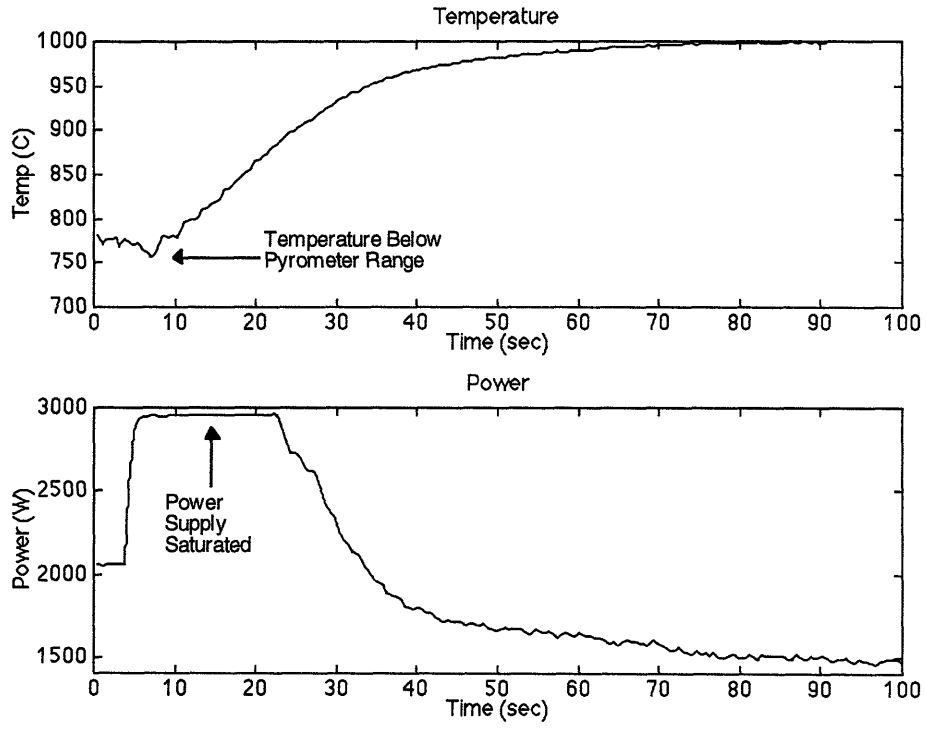

Figure 5.17 Temperature Response During Start Up

5.8 Summary

A PI controller was developed for the temperature control system which gives the best expected response considering the physical limitation, the large temperature delay. The system performs temperature changes in 18 seconds. It rejects disturbances from the wire feeder for step changes in the feed rate of 0.46 g/sec. The steady state error is zero. Temperature oscillations during temperature changes and when rejecting disturbances are small. The controller will be adequate for maintaining the stream at the desired temperature value.

Chapter 6: Flow Controller

6.1 Overview

Similar to the temperature, a controller is required for the flow of molten tin from the arc furnace. The flow determines the geometry of the bonded region and, given the heat content of the stream, determines the energy deposited on the base. As described in Chapter 4, an arc resistance regulator is used to control the flow. When the resistance is constant, the level of tin in the crucible is constant, and the flow from the furnace equals the feed into the furnace. The controller development sequence was the same as in Chapter 5.

The flow control system was implemented, but it could only be operated for short periods of time. The GTAW torch tungsten electrode melts and resolidifies in the crucible orifice which increases the pressure required to sustain a specified flow. Eventually for reasonable pressures, there will not be any flow. Hoping to eliminate the tungsten build up in the orifice, different modifications, that still used a tungsten electrode, were tried without success. It appears a new heating source, such as resistive or inductive heaters that do not use tungsten electrodes, a more powerful GTAW power supply which can maintain the furnace temperature with the flow rates from a larger orifice, or a shorter furnace which will allow the electrode to be more effectively cooled by the torch is needed.

6.2 Performance Requirements

The performance requirements for the resistance regulator are:

- a zero steady state error
- a damping ratio of 0.7
- a closed loop bandwidth of 0.04 rad/sec.

The zero steady state error specification was derived from the desire to have a constant mass of tin in the crucible. A constant mass is important because the temperature controller design was based on 114 grams of tin in the crucible. The damping ratio and closed loop bandwidth were derived using similar reasoning to that used in Chapter 5. The only differences are in the derivation of the closed loop bandwidth where there is no need to track a reference resistance here and there is a different reason for rejecting disturbances. Now a change in the feed rate into the furnace is rejected so that the crucible will not overfill or empty. This derivation will be shown in the next section. As with the temperature controller, simulations were conducted after the controller was designed because the resistance regulator is more complicated than the simple second order system that served as the basis for the performance requirements. Figure 6.1 shows the block diagram of the closed loop system with the disturbance and noise locations.

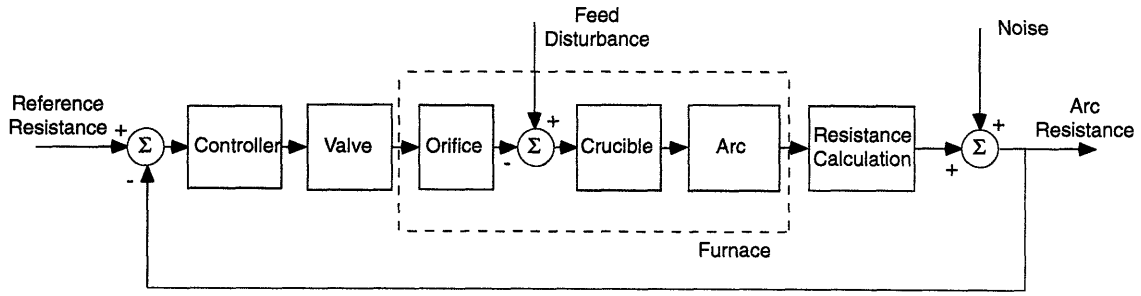

Figure 6.1 Simplified Block Diagram of the Resistance Regulator

Determination of the Closed Loop Bandwidth

Factors that were considered when determining the closed loop bandwidth were:

- the effect of a disturbance on the level of tin in the crucible
- the valve position for the pressure required to produce the tin flow
- the effect of noise on the tin flow.

The effect of a disturbance on the level of tin was the basis for the bandwidth. A change in the wire feed rate disturbance is the most likely change to the system. The effect of the noise on the flow was checked after the bandwidth was obtained to see if it was adequate. The valve position requirement was checked in simulation.

The worst case change in feed is a change from 0 to 1.6 g/sec or 1.6 to 0 g/sec. The rise time for the closed loop system was chosen so as to prevent the crucible from emptying or overfilling due to the resulting feed/flow mismatch. Figure 6.2 shows the operating level of tin in the crucible and the volume available for the tin to fill or empty. The volume, 10.9 cm^3, equates to 71 grams of tin at 1000°C. Tin's density at 1000°C is 6.529 g/cm^3. With a 1.6 g/sec feed/flow mismatch, a rise time of 44 seconds will prevent the volume from being filled or emptied. The rise time equates to a bandwidth of 0.04 rad/sec[1].

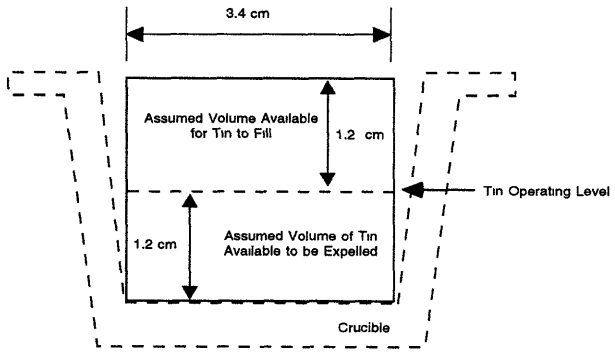

Figure 6.2 Volume Approximation

[1] As stated in Chapter 5 the rise time for a simple second order system is approximately $1.8/\omega_n$ where ω_n is the natural frequency of the system (Franklin, et al., 1986). The natural frequency for a simple second order system is approximately the bandwidth of the system.

The effect of measurement noise on the flow will not be significant. Similar to the temperature, there is no particular noise frequency in the calculated resistance to be rejected. Figure 6.3 shows the time domain open loop resistance signal upon which a Fast Fourier transform frequency analysis was conducted. Figure 6.4 is the frequency transform. The content of the signal is largely zero frequency. Figure 6.5, the expanded frequency spectrum, shows there are no notable frequencies.

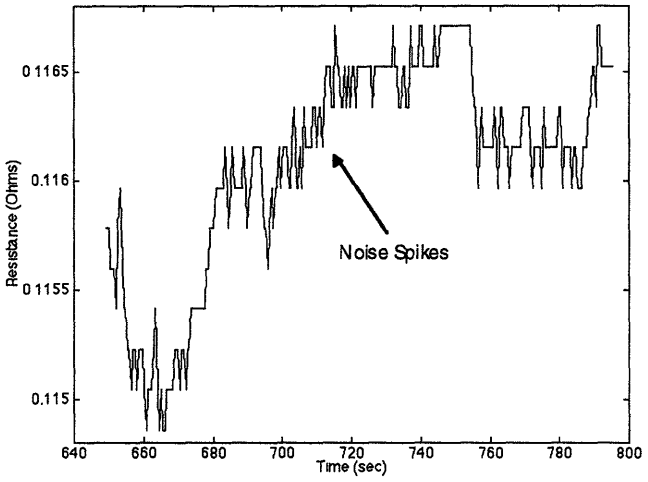

Figure 6.3 Open Loop Calculated Resistance Signal

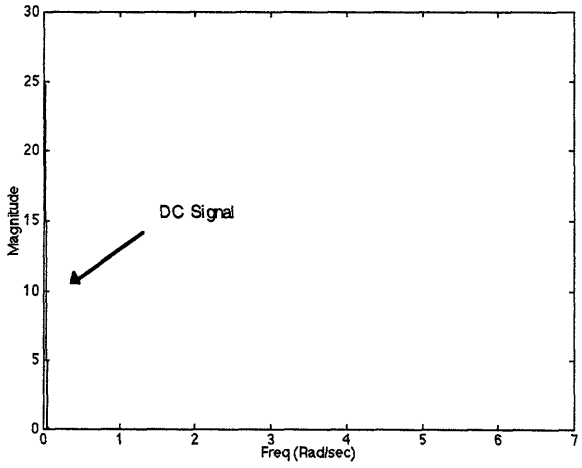

Figure 6.4 Frequency Spectrum of the Resistance Signal

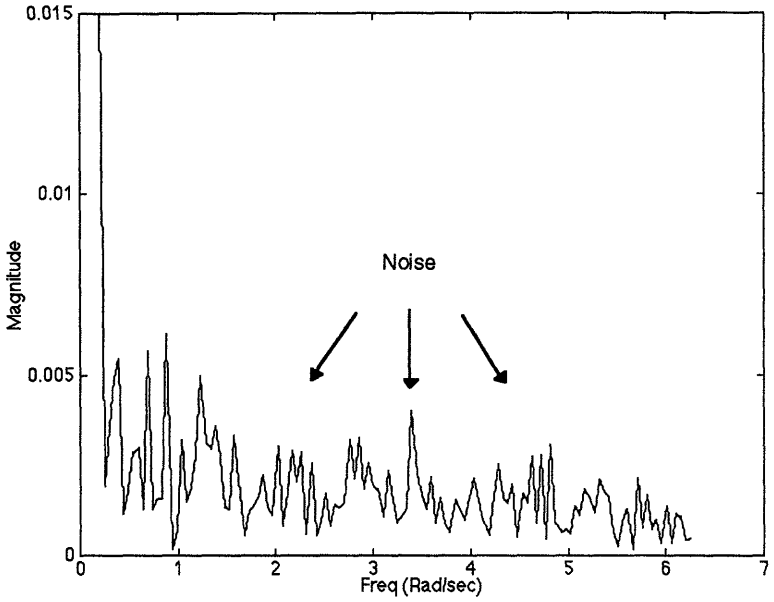

Figure 6.5 Expanded Frequency Spectrum of the Resistance Signal

6.3 System Model

The components of the flow controller resistance regulator to be modeled are the proportional control valve, the furnace, the differential amplifier, the anti-aliasing filter, the resistance calculation, and the DAQC card. A block diagram of the resistance regulator is shown in Figure 6.6. The resistance regulator is more complicated than the temperature system. Two elements, the furnace and the resistance calculation, are nonlinear and multi-input. To obtain the open loop Bode diagram without the controller some of the elements are neglected. The elements that are not neglected need to be modeled as linear and single input-output. Linear single input-output models for the elements are required to use the Bode diagram design technique. The linearization will be done by experimentally determining the models about an operating point, by linearizing empirical data, or by linearizing an analytic expression about an operating point.

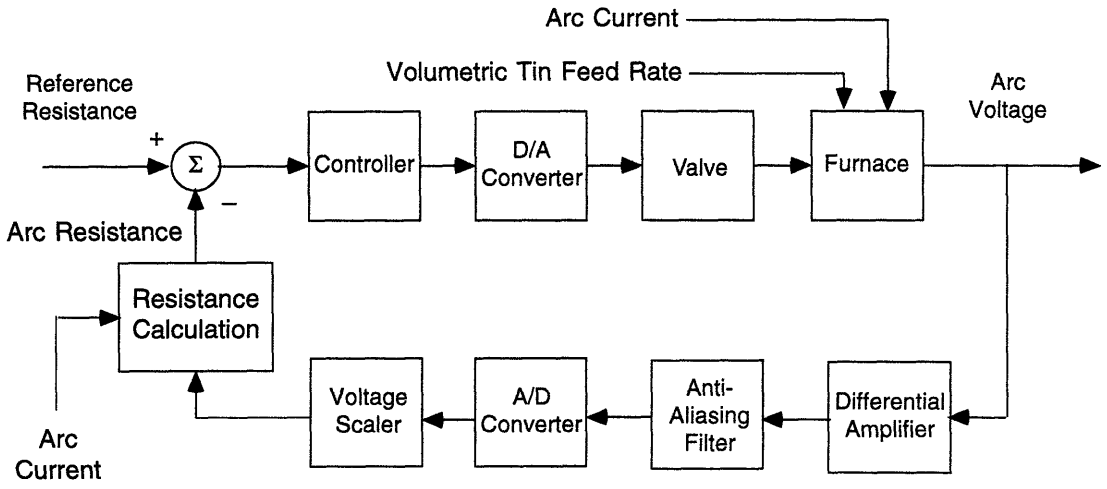

Figure 6.6 Block Diagram of the Resistance Regulator Loop

The D/A converter, A/D converter, anti-aliasing filter, differential amplifier, and voltage scaler are not included when determining the open loop Bode diagram. The D/A converter, A/D converter, and anti-aliasing filter are neglected, as in Chapter 5, because the system closed loop bandwidth will be much smaller than the sampling rate and the anti-aliasing filter bandwidth. The differential amplifier and the voltage scaler are neglected because they are essentially non-dynamic. The differential amplifier's bandwidth is 3 Mhz. The voltage scaler is an algebraic operation. The differential amplifier, merely, scales the arc voltage so it is within the A/D converters range. The voltage scaler converts the scaled signal back to its original value. Figure 6.7 shows the open loop resistance system with the neglected components crossed out.

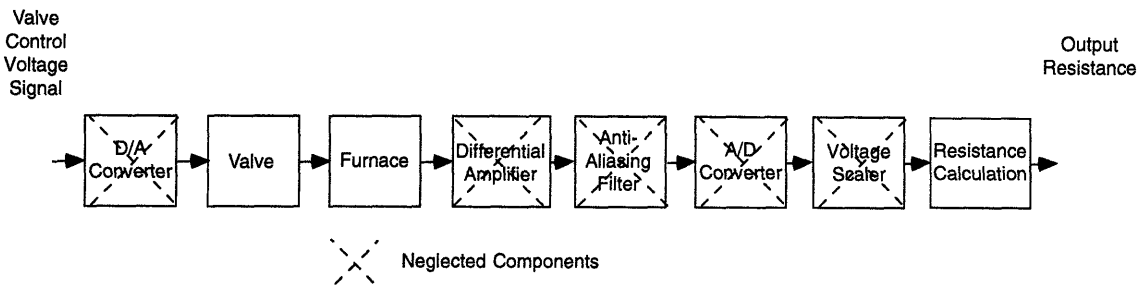

Figure 6.7 Block Diagram of the Open Loop Resistance System

The model for the valve is first order. The valve varies the argon flow to the furnace in proportion to the applied control voltage. An argon pressure of 20 psi is applied to the inlet of the valve. The argon flow changes the pressure in the furnace until the argon leakage flow from the furnace equals the argon flow into the furnace. The model was obtained by performing a 0.3 V step response about the anticipated operating point of the furnace. The valve operating point is 5.65 V which results in a 2.25 psi furnace pressure. This pressure causes a 1 g/sec tin flow from the furnace. A first order model is:

$$\frac{k_p}{ts+1}\exp(-sT)$$

where

k_p = the steady state gain. (Δ Pressure Total/ Δ Voltage Total)

t = the time constant. (Time for pressure to reach 2/3 of Δ Pressure Total)

T = the time delay. (Time after voltage change pressure changes)

Figure 6.8 shows the open loop voltage-pressure response of the valve. From the plot, k_p is 3.3, and t is 1.5 seconds. An expanded version of the response, Figure 6.9, shows there is no time delay (T equals 0). The model for the valve is, therefore:

$$\frac{3.3}{1.5s+1}\exp(-0s) = \frac{3.3}{1.5s+1}$$

A block diagram of the valve is shown in Figure 6.10.

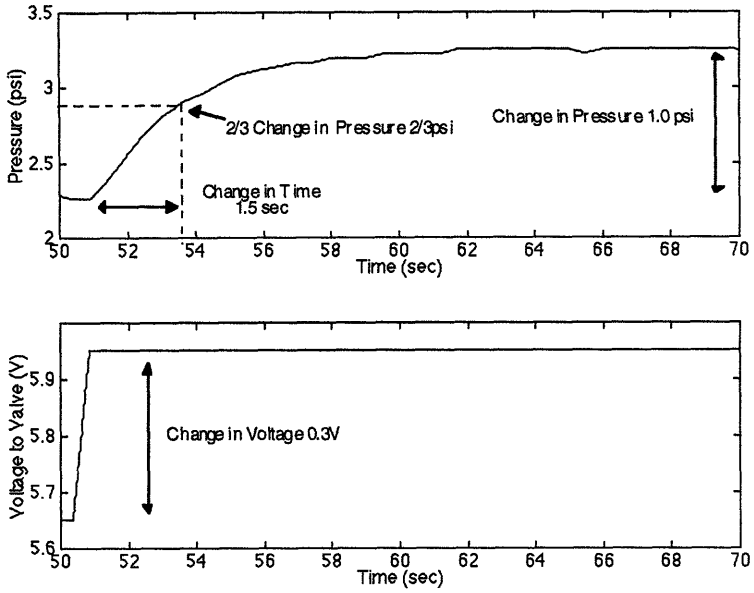

Figure 6.8 Valve Voltage-Pressure Response

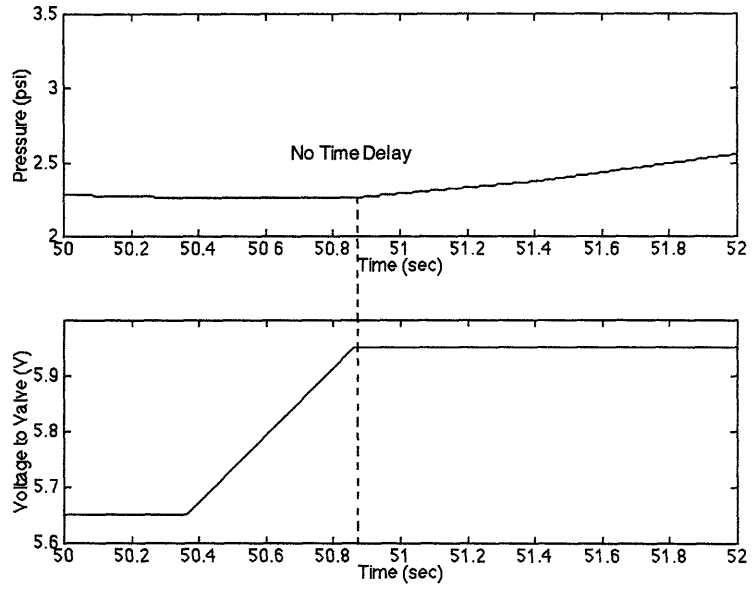

Figure 6.9 Expanded Valve Voltage-Pressure Response

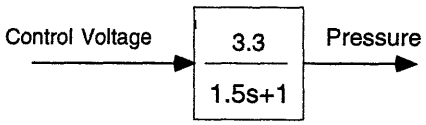

Figure 6.10 Valve Model

The furnace model is composed of three parts, a model for the orifice, a model for the crucible, and a model for the arc, Figure 6.11. There are three inputs to the furnace, the pressure in the furnace, the tin feed, and the arc current. The orifice converts the pressure of the furnace into a tin flow. The crucible converts tin feed and flow into a level. The arc converts a level and arc current into an arc voltage. The linear single input-output model for each part was obtained in different ways. The model for the orifice was obtained by taking a linear approximation of the analytical model of the orifice pressure to flow relationship about the operating point. The model for the crucible was obtained analytically. The model for the arc was obtained by taking a linear curve fit of empirical data for arc voltage vs tin height.

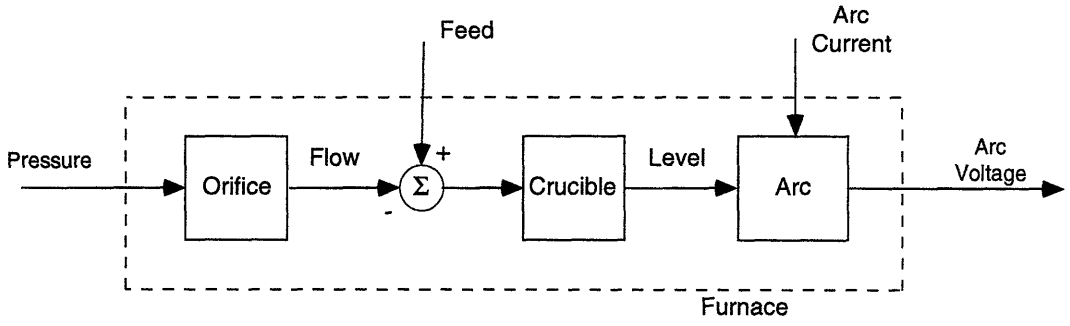

Figure 6.11 Furnace Block Diagram

The model for the orifice is a gain. The orifice pressure to tin flow relationship of the furnace was analytically obtained in Chapter 4. The result is repeated in Figure 6.12. The curve was linearized about the 2.25 psi and 1 g/sec operating point. The gain, the change in flow rate divided by the change in furnace pressure, is 0.235g/sec/psi. Converting this to a volumetric flow rate with tin density at 1000°C 6.529 g/cm^3, the gain is 36.4 mm^3/sec/psi.

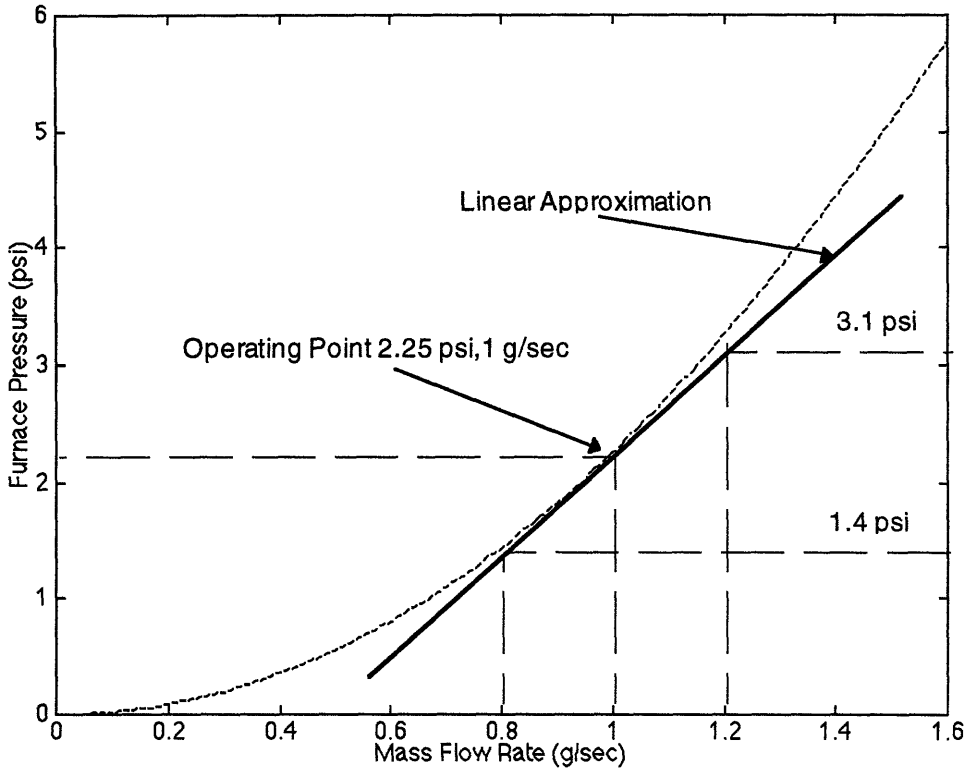

Figure 6.12 Pressure to Tin Flow Relationship

The model for the crucible is an integrator. The feed into the crucible and flow from the crucible integrate to determine the tin level. Figure 6.2 showed the dimensions of the crucible. Assuming the inside of the crucible is a cylinder, the level is given by:

$$\pi r^2 \frac{dl}{dt} = \text{flow in} - \text{flow out}.$$

where:

l = the tin level in the crucible. (mm)

r = the radius of the crucible. (17 mm)

Taking the Laplace transform and rearranging, the crucible model becomes:

$$\frac{l}{\text{(flow in - flow out)}} = \frac{1.1\times10^{-3}}{s}$$

The model for the arc voltage is a gain. The arc voltage is obtained by deriving a linear approximation from empirical data of arc voltage vs tin height in the crucible with a GTAW electrode length of 126 mm. The electrode is always measured to be 126 mm long. The arc current is allowed to vary to keep the tin temperature at 1000°C, the operating temperature for the furnace. The empirical data, shown with x's, and the linear approximation are shown in Figure 6.13. The gain, the ratio of the change in voltage to change in tin level, is -0.33 V/mm.

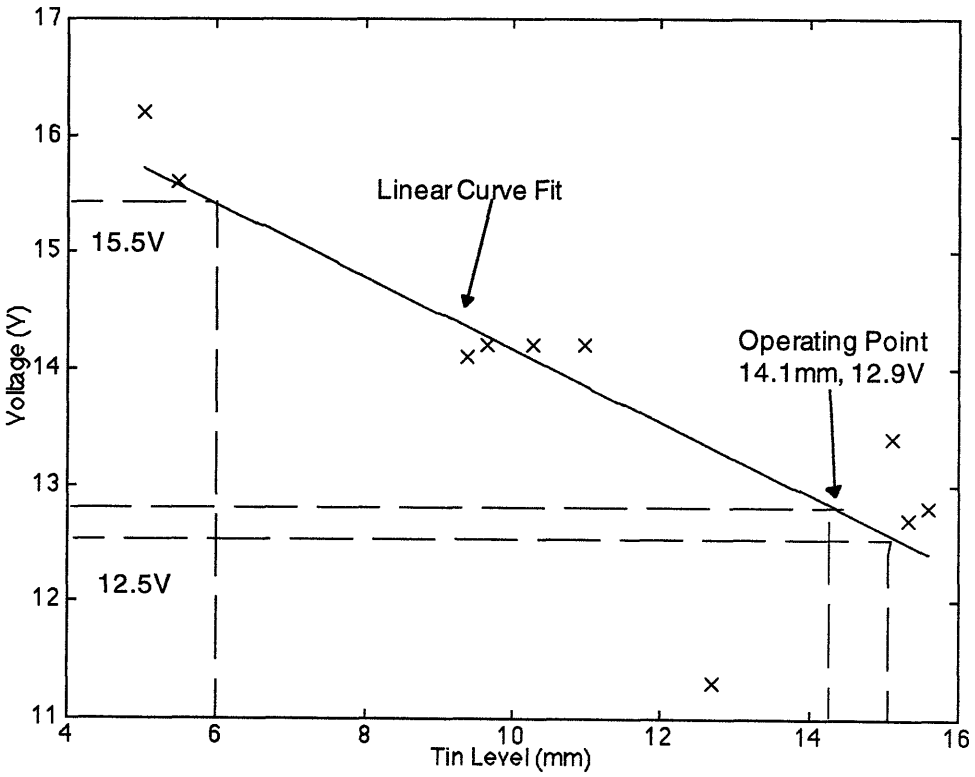

Figure 6.13 Approximation of Arc Voltage vs Tin Level

The furnace model is a combination of the orifice, the crucible, and the arc models. A block diagram of the furnace is shown in Figure 6.14.

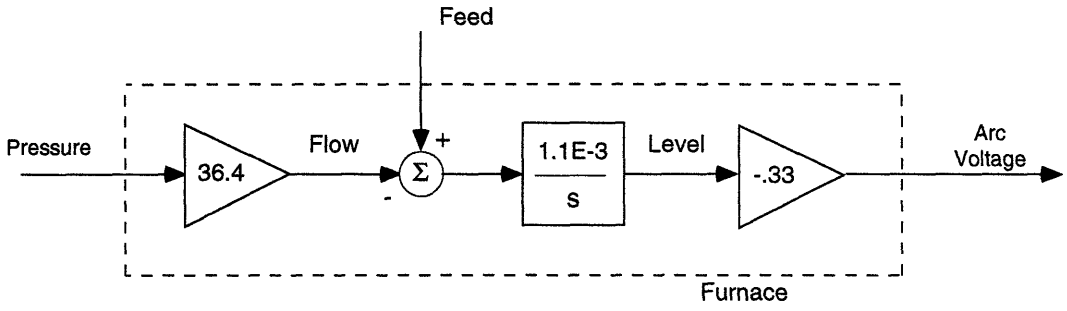

Figure 6.14 Furnace Block Diagram

The model for the resistance calculation is a gain. In reality the computer will divide the measured arc voltage by the commanded arc current. For modeling purposes, the arc current is assumed to be a constant. The constant is the operating arc current of 110A. The gain becomes 1/110 or 9.1×10^{-3}. Figure 6.15 is a block diagram of the resistance calculation.

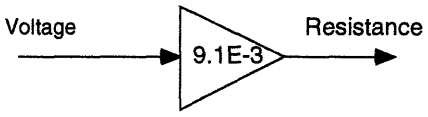

Figure 6.15 Resistance Calculation Block Diagram

The models of the resistance system components, which were not neglected, are combined to obtain the open loop Bode diagram without the controller. The Bode diagram is shown in Figure 6.16. All frequencies are attenuated. The phase margin is always less than -180°. If the system was closed with only a proportional controller, the system would never go unstable. An integrator is needed, though, in the controller to give a zero steady state error to a feed disturbance.

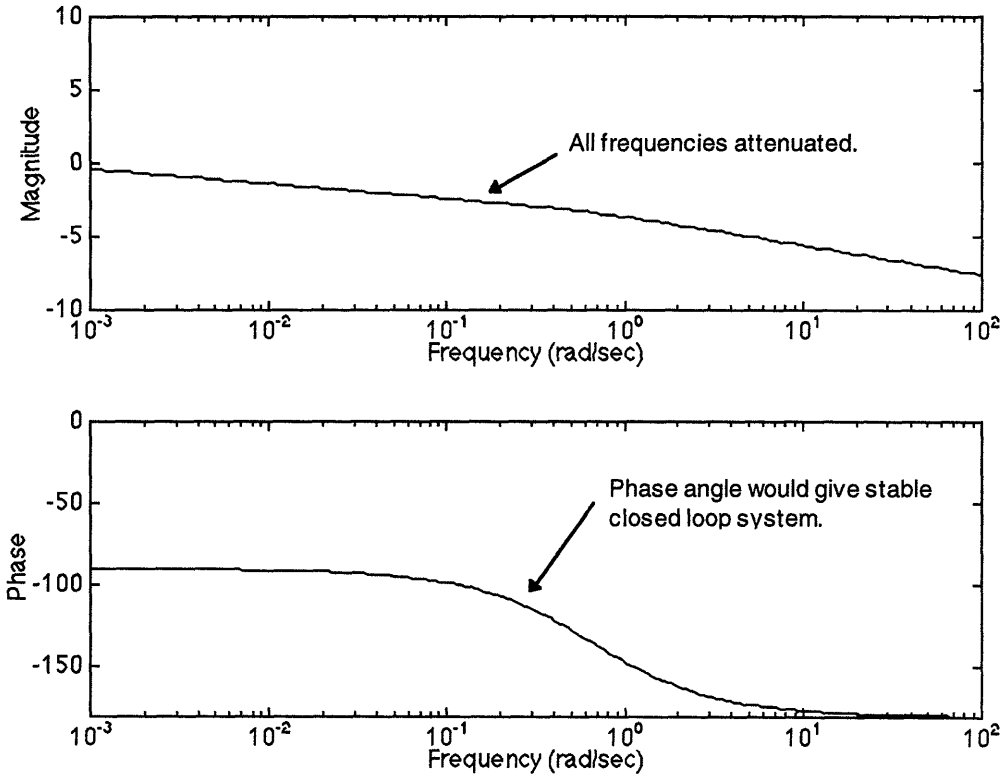

Figure 6.16 Resistance Open Loop Bode Diagram without Controller

6.4 Controller Design

The designed controller needs to modify the open loop Bode diagram of the resistance regulator without the controller. An infinite magnitude is required at zero frequency. The crossover frequency needs to be greater than 0.04 rad/sec with a phase less than -110°.

A PI controller was, again, picked to compensate the system. As a reminder the form of a PI controller is:

$$\frac{k_p(s+a_p)}{s}$$

where

k_p = the proportional gain.

a_p = the zero. (integral gain/proportional gain)

The same methodology was used to get k_p and a_p as was used with the temperature controller. As happened when designing the temperature controller, both the damping ratio and zero steady state requirements could not be met. The smaller the zero the larger the damping ratio at the desired crossover frequency but also the larger the steady state error. A zero at 0.03 rad/sec was chosen. A gain of 200 was selected to get a crossover frequency of 0.1 rad/sec. The crossover frequency is larger than the needed 0.04 rad/sec to obtain a larger damping ratio. The phase has a peak here. The larger crossover frequency should be acceptable as long as the increased demand from the controller does not cause the valve to saturate and as long as the noise level of the resistance calculation is not increased. Since the noise had no notable frequency peaks, the later should not happen to a great degree. The former will be evaluated in simulations. Figure 6.17 shows the open loop Bode diagram with controller.

The designed controller is:

$$\frac{200(s+0.03)}{s}$$

The code for its digital implementation is contained in Appendix B. The controller should result in good performance. There should be zero steady state error, a damping ratio of 0.6, and a bandwidth of 0.1 rad/sec. The bandwidth should result in a flow rise time of 18 seconds to a change in the feed rate.

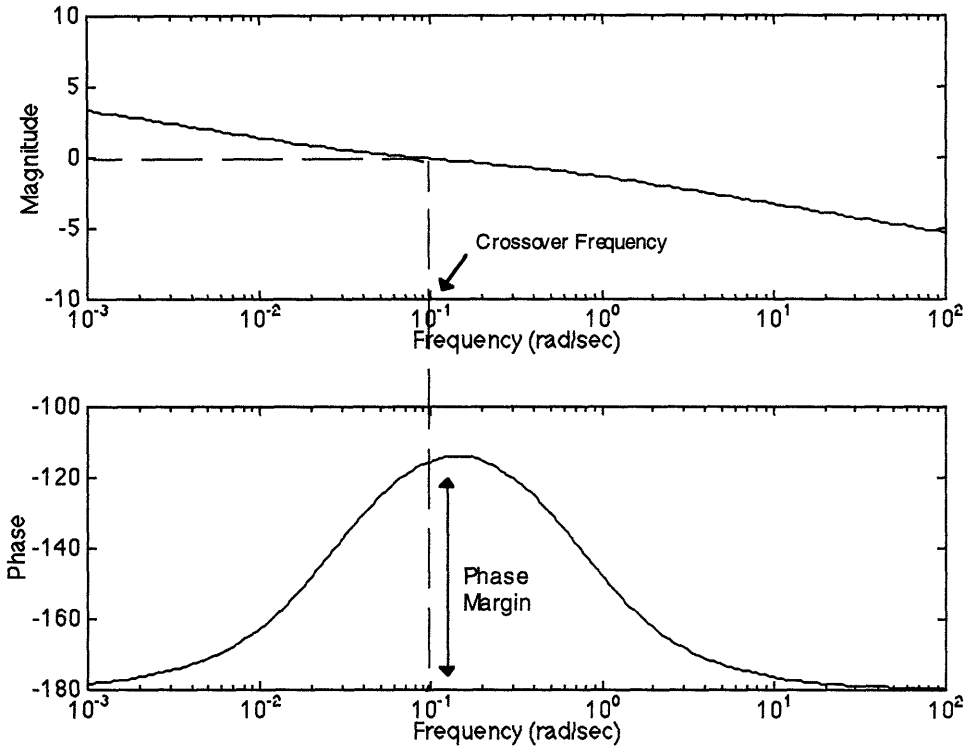

Figure 6.17 Open Loop Bode Plot with Controller

6.5 Simulations

Figure 6.18 shows the simulation block diagram that was used to determine if the designed controller will give the expected performance and to check to see if the control voltage to the valve would saturate the valve, a control voltage of less than 0 V or greater than 10 V. The components used in the design were included in the simulation.

The simulation response to a step change in wire feed rate from 1 to 1.25 g/sec is shown in Figures 6.19A and 6.19B. The flow response is exactly as expected with a flow rise time of 18 seconds, a slight overshoot but no oscillations, and a zero steady state error between the feed and flow. The valve does not saturate with the control voltage to the valve never exceeding 6 V.

The simulation also shows that the tin level change is small. The resistance varies by 1/1000 Ω. This correlates to approximately only a millimeter change in level.

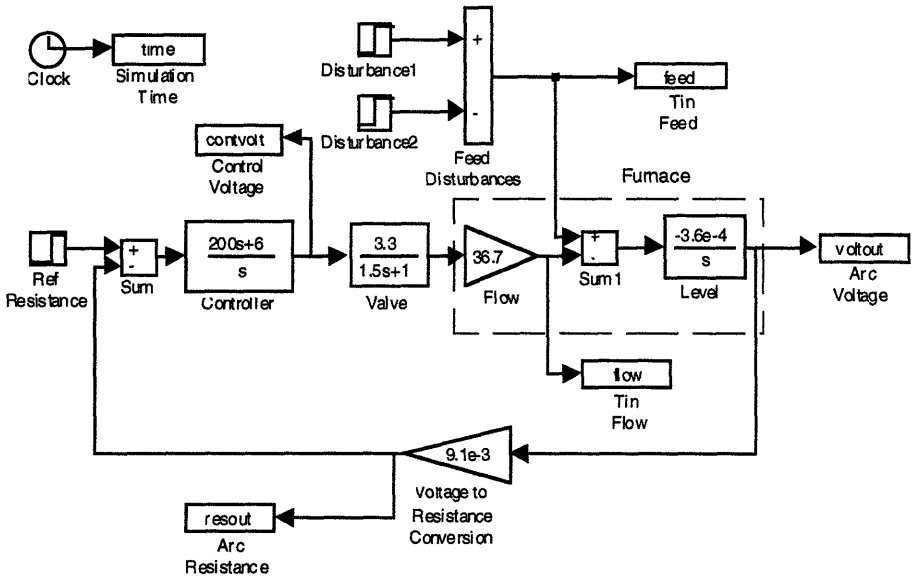

Figure 6.18 Resistance Loop Simulation Block Diagram

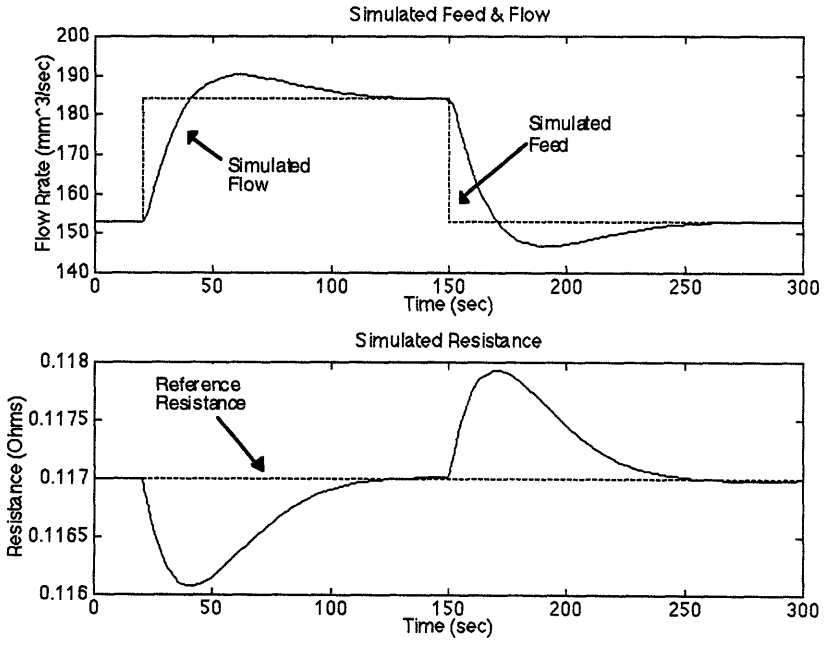

Figure 6.19A Simulated Resistive System Response

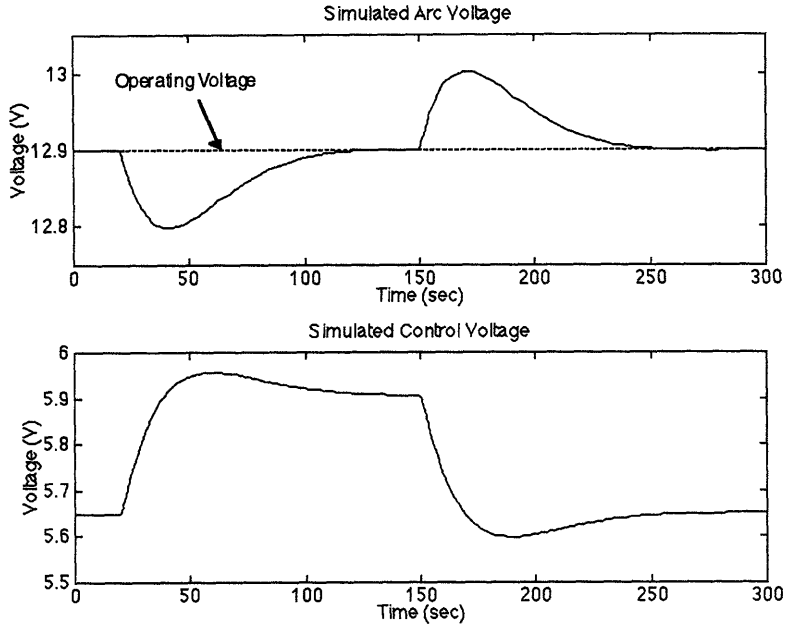

Figure 6.19B Simulated Resistive System Response

6.6 System Response

The flow closed loop response for a step change in wire feed rate from 1 to 1.25 g/sec at 450 seconds is shown in Figure 6.20 along with the simulated response for comparison. As expected, the arc resistance slowly decreases, and the valve control voltage slowly increases so that the pressure in the furnace produces the new flow rate. The first 30 seconds of the response matches the simulated response closely with a time constant of 20 seconds vice 18 seconds, a maximum change in resistance of 0.006Ω vice 0.001Ω, and a maximum change in control voltage of 1V vice 0.3V. The difference in the time constant is negligible. The differences in the magnitudes can be accounted for by build up on the orifice wall. The build up increases the pressure required to achieve a flow rate which results in a larger control voltage to attain the higher pressure and a larger change in resistance to produce the larger control voltage. The flow closed loop response shows that the model used to derive

the flow control system was accurate and the scheme to control the flow will work.

The flow closed loop response for extended periods of time becomes erratic, Figure 6.21. This response to a step change in wire feed rate from 1 to 1.25 g/sec at 450 seconds is typical of responses seen in other runs. Although the response is erratic, it can be explained. The flow is well behaved for the first 40 seconds. After 40 seconds the arc resistance suddenly starts to decrease without a change in feed rate. This indicates that the orifice is starting to clog which limits the flow from the furnace. The control system compensates for the decreased resistance by increasing the valve control voltage and thus the pressure in the furnace in an attempt to increase the flow rate. At 60 seconds the pressure is the furnace is large enough to clear the orifice some and to reestablish flow. Now the pressure is too large for the feed rate which results in a larger than needed flow rate and oscillations while the flow controller stabilizes the system. The power supplied to the furnace to control the temperature and the furnace temperature oscillate with the varying resistance. The power supplied to the furnace is the product of the arc current and the arc voltage. The furnace temperature is a function of the power. For example, when the resistance suddenly increases at 510 seconds, after the flow is reestablished, the power to the furnace increases and thus the temperature of the furnace increases. The long term behavior of the flow control system shows that the cause of the orifice blockage needs to be found and eliminated.

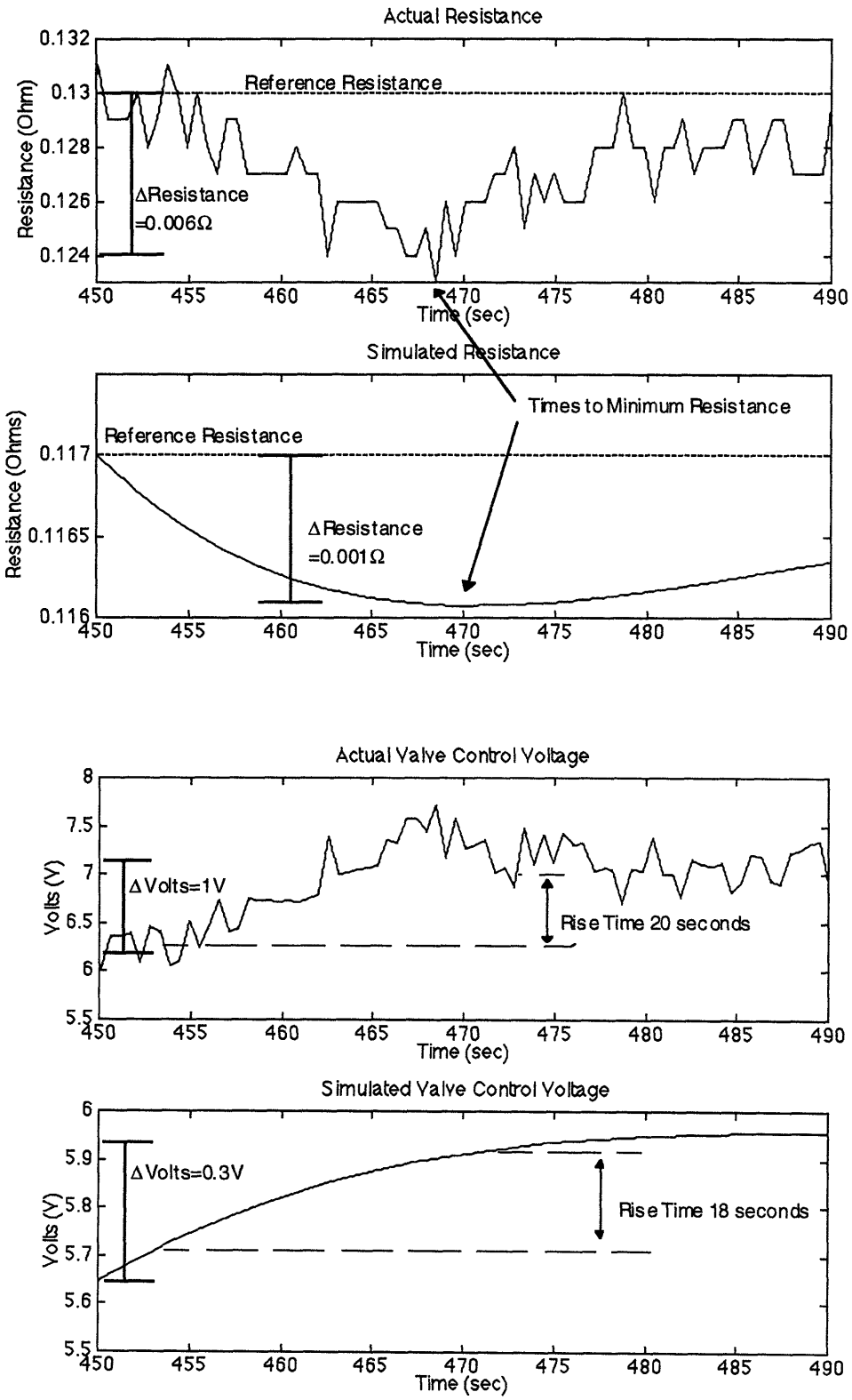

Figure 6.20 Actual and Simulated Flow Control Response

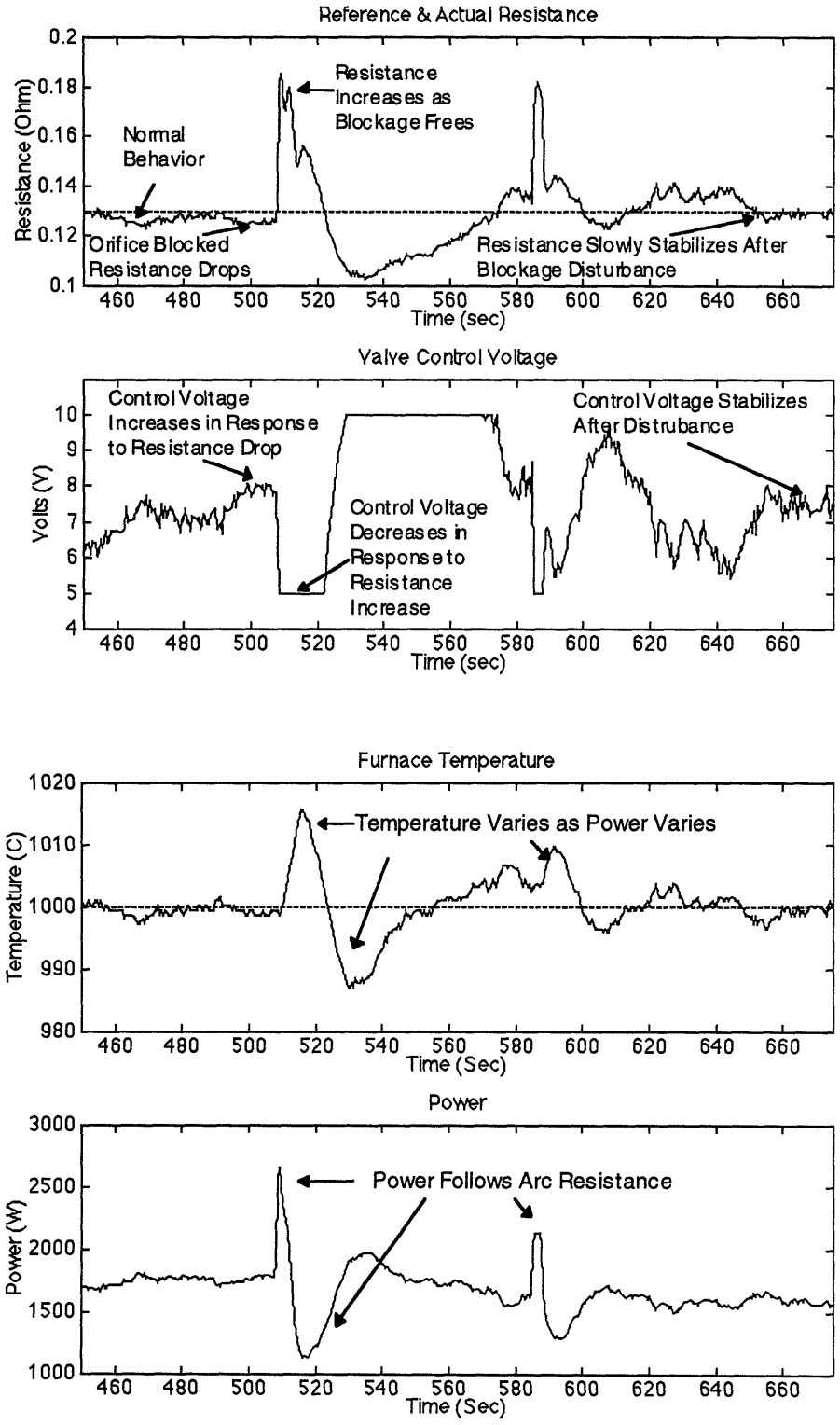

Figure 6.21 Flow Control Response for an Extended Time

6.7 Investigation of the Orifice Blockage

The long term behavior of the flow control system showed a consistent tin flow for a constant pressure could not be maintained. Typically, higher furnace pressures were required throughout a run to produce the same tin flow, and eventually the highest desired pressure in the furnace, 15 psi, could not produce a flow. Since the actual mechanism that causes the blocking could not be observed, two indirect approaches were tried to determine the cause: flow experiments and scanning electron microscope analyses of blocked orifices. The experiments involved expelling tin from the furnace under different conditions. The scanning electron microscope analysis involved examining blocked orifices under high magnification and conducting energy dispersive spectroscopy and wavelength dispersive spectroscopy to determine the materials in the orifice.

The experiments conducted to determine the cause of the orifice blockage consisted of partially expelling a tin shot placed in the furnace, totally expelling a tin shot placed in the furnace, and expelling tin when the wire feeder was replenishing the tin. If impurities that float to the top of the tin in the crucible cause the blockage then partial emptying of the crucible should result in no blockage. If impurities from the wire fed into the furnace cause the blockage, then both partially and totally expelling a tin shot should result in no blockage. Blockage was observed in all of the three cases. The frequency of blockage was the least when a tin shot was only partially expelled and the most when the wire feeder replenished the furnace. The results are inconclusive and could have many interpretations. A possible conclusion is that impurities on the top of the tin in the crucible and impurities added when wire is fed into the furnace do not affect the blockage, but since the experiments when wire is feed into the furnace last longer, there is a higher probability of orifice blockage. Another conclusion is that impurities that float to the top of the tin in the crucible and impurities from the wire fed into the furnace both aid in blockage, so a higher frequency is observed when wire is fed into the furnace.

Scanning electron microscope analyses conducted to determine the cause of the orifice blocking consisted of examining two blocked orifices visually under high magnification and chemically through spectroscopy. No foreign particles were observed in the orifices. Besides tin, only tungsten was present. Some of the tungsten combined with the graphite forming tungsten carbide. The other tungsten just appeared to solidify. Figure 6.22 shows the light tungsten carbide build up noticed in some areas. The lighter material along the orifice wall is the tungsten carbide. Figure 6.23 shows more significant tungsten carbide build up noticed in only a few areas. The smoother material that protrudes into the orifice is the tungsten carbide. In one of the samples the tungsten carbide appeared to block the orifice, Figure 6.24. The tungsten carbide blockage is below tin which solidified in the orifice. Energy dispersive spectroscopy and wavelength dispersive spectroscopy were conducted to determine the composition of the material building up on the orifice wall. Energy dispersive spectroscopy is used to detect heavy elements such as tin and tungsten. Wavelength spectroscopy is used to detect light elements such as carbon and oxygen. Figure 6.25 shows the energy dispersive spectrum of x-rays emitted when tin is bombarded with electrons. There are two peaks in the spectrum which are associated with tin. Figure 6.26 shows the energy spectrum of the build up when it is bombarded with electrons. The tin peaks are much smaller, and there are two peaks associated with tungsten. Wavelength density spectroscopy detected the carbon in the build up.

The solidifying tungsten and the tungsten carbide build up observed with the scanning electron microscope must change the pressure to flow relationship of the orifice which results in the observed closed loop flow behavior. The tungsten decreases the size of the orifice which increases the resistance to flow and increases the pressure required to achieve a set flow. This phenomenon takes time to occur because it takes time at high temperature for the tungsten electrode to melt. Running the wire feeder increases the time of operation of the furnace and possibly increases the electrode contamination with the feed wire

touching the electrode occasionally resulting in more consistent blockages. A contaminated electrode melts quicker.

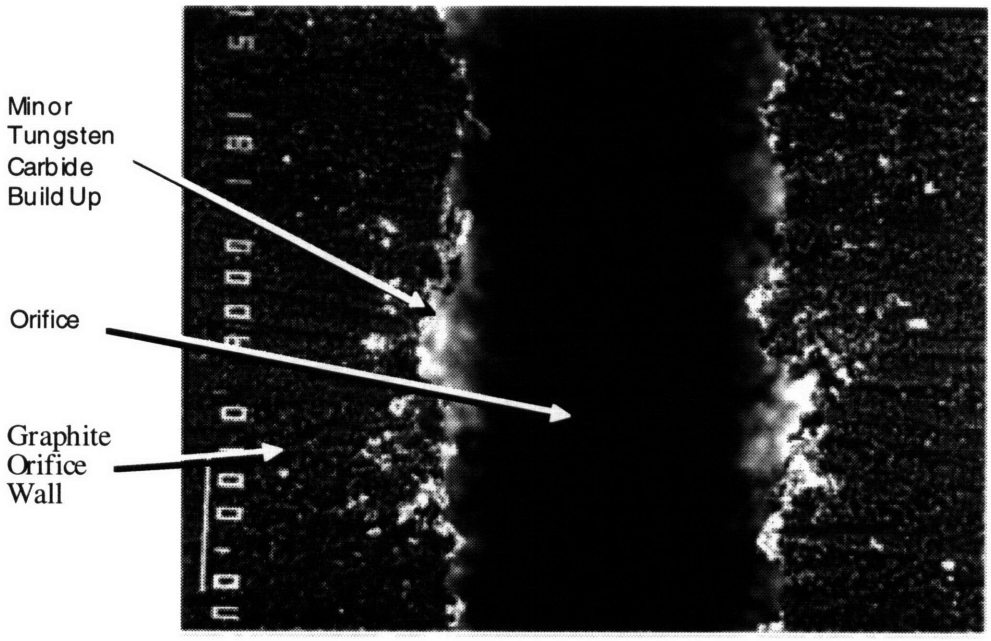

Figure 6.22 Orifice with Minor Tungsten Carbide Build Up

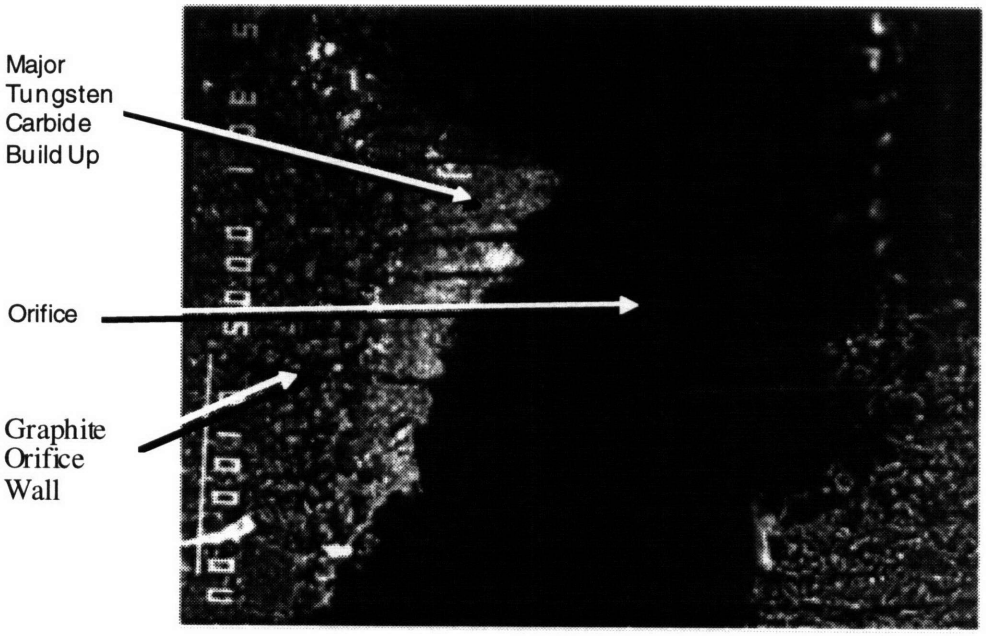

Figure 6.23 Orifice with Major Tungsten Carbide Build Up

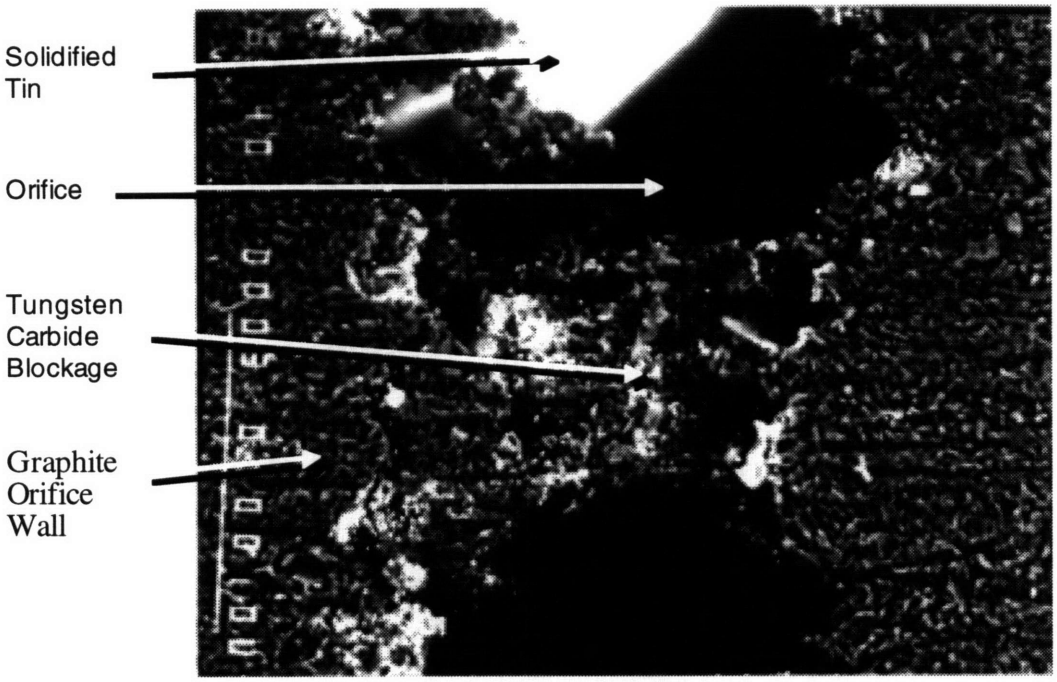

Figure 6.24 Orifice with Tungsten Carbide Blockage

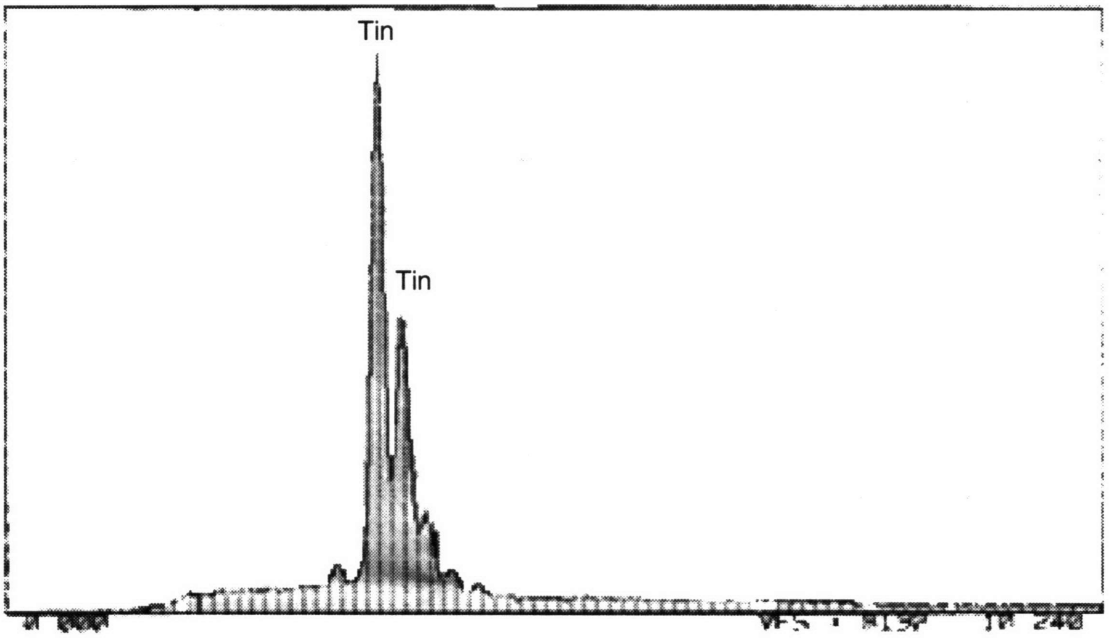

Figure 6.25 Energy Density Spectrum of Tin

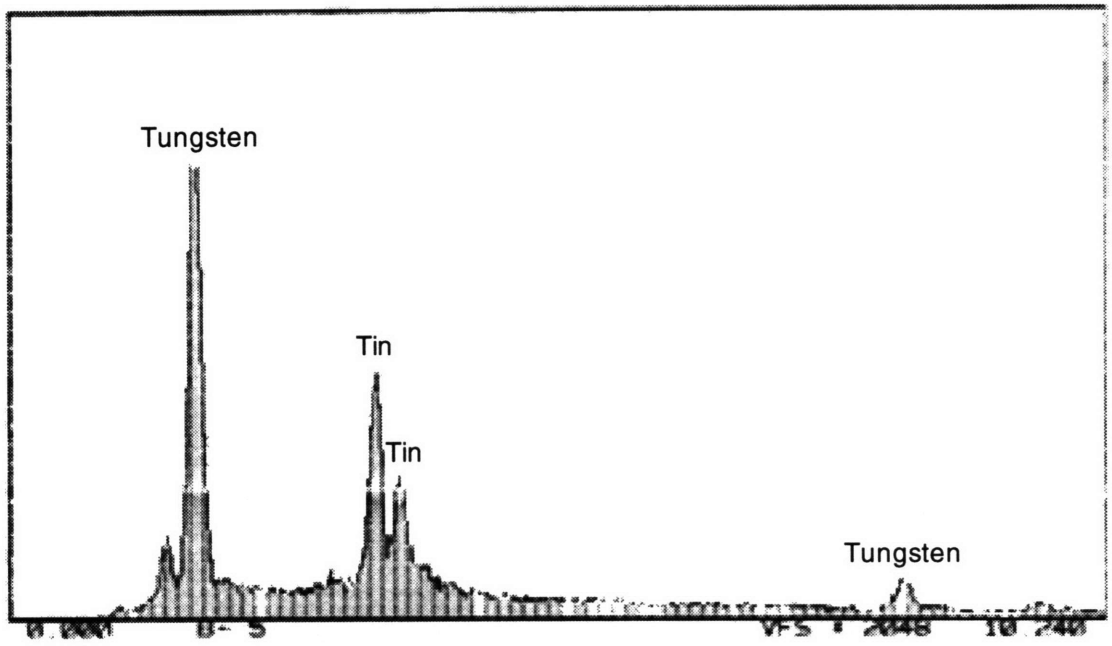

Figure 6.26 Energy Density Spectrum of Orifice Build UP

6.8 Possible Modifications to Reduce the Orifice Blockage

Three modifications to the furnace were investigated with hopes of reducing the orifice blockage. They were to increase the orifice size, use a larger diameter electrode with zirconium, and replace the graphite orifice with a non-graphite insert. None were successful.

Graphite crucibles with different size orifices were tried in the furnace to determine the size that would increase the time before the tungsten had a noticeable effect on the pressure/flow relationship. The orifice size was found to be 0.034 inches. An analysis similar to Chapter 4 was conducted to determine the furnace pressures for flows whose temperature could be maintained by the GTAW power supply. The maximum tin feed/flow rate the power supply can handle is 3.82 g/sec. With a hole size of only 0.027 inches 0.5 psi will result in the maximum feed/flow. With a 0.034 inch diameter orifice hole, the pressure would be too small to get a flow that the power supply could handle.

A 5/32 inch diameter zirconium tungsten electrode was tried in the furnace in an attempt to reduce the amount of electrode melting and thus the amount of build up in the orifice. Previously 1/8 inch diameter 2% thorated tungsten electrodes were used in the furnace. The larger diameter electrode melts slower because there is less resistive heating, and the zirconium makes the electrode more heat resistant. The electrode increased the time before the tin flow stopped, but the pressure to keep the flow constant before the flow stopped increased almost as quickly as with the original electrodes.

A crucible with a 0.012 inch orifice boron nitride insert was tried in the furnace. Without graphite in the orifice, the tungsten should not form a tungsten carbide build up, however, the orifice still became blocked with the solidifying tungsten.

The initial modifications to the furnace showed that the tungsten from the melting electrode is a significant orifice blockage problem which is not easily prevented. Tungsten is used in almost all GTAW electrodes and it reacts with many materials. The tungsten electrode which is the most resistant to melting was tried in the furnace, but it melted. A different material was tried for the orifice, but the tungsten still affected its performance. It appears as if only major modifications may prevent the blockage. Three possible major modifications are: using a different heating source such as resistive or inductive heaters, using a GTAW power source with a higher power output so that a larger orifice can be used, and decreasing the height of the furnace so that the electrode is shorter and more effectively cooled by the torch.

6.9 Summary

Performance of the closed loop flow control system shows that a resistance closed loop system can control the tin flow from the furnace. Step changes in the tin flow can be conducted in 20 second with a small amount of overshoot. The current furnace set up can not be used to implement the flow control system for extended periods of time. The viscosity of tin requires the orifice size in the crucible to be small so that the GTAW power supply can

maintain the tin flow temperature. The small orifice becomes blocked with solidifying tungsten and tungsten carbide. Possible furnace modifications to eliminate the blockage are: to heat the tin with a non-tungsten source, to increase the capacity of the GTAW power supply so that the furnace temperature can be maintained for the flow rate from a larger orifice, and to decrease the height of the furnace so that the electrode is cooled more effectively.

Chapter 7: Conclusion

This research investigated a way to independently control the temperature and flow rate of a molten metal stream. Tin was the metal used because it showed the potential of both being contained in a graphite crucible and being bonded by a molten stream. The control scheme modified a previously designed arc furnace to hold the tin. A temperature loop controlled the temperature of the tin, and an arc resistance regulator indirectly controlled the flow of tin. The control scheme was designed, simulated, and implemented. However, persistent blockage of the outlet prevented the flow control loop from being operated for extended periods of time.

The temperature control loop used a PI controller. The bandwidth of the system was 0.1 rad/sec with a damping ratio of 0.5 and a zero steady state error. The bandwidth results in a step command temperature change that occurs in 18 seconds without oscillations and a disturbance response to a step tin feed rate change of 0.46 g/sec into the system that limits the temperature change to less than 100°C. The bandwidth of the furnace can not be increased because there is a large time delay between when power is input into the furnace and the resulting tin temperature change at bottom of the crucible. It takes time for the energy to diffuse. The time delay is shown by the large negative phase on the Bode diagram of the open loop system. If the bandwidth is increased, the system will become unstable as the controller tries to change the temperature quicker than the power input can change the tin temperature at the bottom of the crucible.

A novel control approach was proposed to control the flow rate from the furnace because there is not a sensor available to measure the mass flow rate of a molten stream flowing in an open space. The approach involves varying the pressure in the furnace which in turn varies the tin flow from the furnace to keep the arc resistance, which is a function of the tin level, constant. At

equilibrium, the arc resistance is constant; the crucible tin level is constant; and tin flow into the furnace equals the flow out of the furnace.

A PI controller regulated the resistance. The bandwidth of the resistance loop was 0.1 rad/sec with a damping ratio of 0.6 and a zero steady state error. With the bandwidth, a step command flow change can be conducted in 18 seconds without oscillations and without a large transient tin level change.

A physical limitation prevented the flow scheme from being implemented for extended periods of time. The viscosity of tin at high temperatures is low which necessitates a small orifice size in the crucible so that the tin stream temperature can be maintained with the GTAW power supply. However, small amounts of tungsten from the tungsten electrode solidify in the small orifice, which leads to blockage. If this approach is to be implemented either, a larger GTAW power supply that can maintain the tin temperature at the larger flow rates from a wider diameter orifice, a shorter furnace so the electrode can be more effectively cooled by the torch, or a new heat supply, such as inductive or resistive heaters that does not use tungsten electrodes, is needed.

Controlling the temperature and flow rate of a molten stream was initially attempted in previous research to enable process control in welding. Current welding techniques (GMAW) do not allow the process outputs to be varied independently. The apparatus used in this research can not be used for that application because a crucible material is not available that can hold molten steel at high temperatures, and previous research analysis showed there is not enough energy stored in the steel stream to melt the base metal. A different approach is needed to vary the welding outputs which does not use a crucible to hold molten steel and which has an additional heat source to melt the base metal.

This apparatus may be used for process control in applications that bond metals. A disadvantage of this setup is its efficiency. A significant portion of the power supplied to the furnace is used to maintain the temperature of the metal and is not used to melt the base metal, resulting in a low efficiency.

Appendix A: Finite Difference Code

```
% Stream Model 3 mm x 3 mm bead
% 2 Dimensional Finite Difference Temperature Distribution
% Boundary Conditions: Convective heat transfer at all edge nodes
% Initial Conditions: Top center nodes at 1400K while rest of nodes at
% room temp
% Formulation of the parameter matrices A,B,C,D
% Ken Amoruso 1-14-96

function[a,b,c,d,input,time,u0]=fdiftin(m,n);

e=6;
f=6;
ef=e*f;

r=7290;
cp = 222;
kc = 65;
t0 = 300;
ts = 300;
h= 10;
mn=m*n;
mnef=ef+mn;
dx = .0005;
q1=n/2;
q2=n/2+1;
a=zeros(mnef,mnef);
%
%puddle matrix
%interior nodes
for i=1:ef
      a(i,i) = -4*kc/(r*cp*dx^2);
      if (i-1)>=1,
            a(i,i-1)=1*kc/(r*cp*dx^2);
      end;
      if (i+1)<= ef,
            a(i,i+1)=1*kc/(r*cp*dx^2);
      end;
      if (i-f)>=1,
            a(i,i-f)=1*kc/(r*cp*dx^2) ;
      end;
      if (i+f)<= ef,
            a(i,i+f)=1*kc/(r*cp*dx^2);
      end;
end;
%
%puddle matrix
%left edge column
for k=1:e
      i=(k-1)*f +1; %left nodes
```

```
      a(i,i)=-1*((h/(r*cp*dx))+2*kc/(r*cp*dx^2));
      if (i-f)>=1,
            a(i,i-f)=.5*kc/(r*cp*dx^2);
      end;
      if (i+f)<=ef,
            a(i,i+f)=.5*kc/(r*cp*dx^2);
      end;
%reset
      if (i-1)>0,
            a(i,i-1)=0;
      end;
end;
%
%puddle matrix
%right edge column
for k=1:e
      i=(k-1)*f + f;
      a(i,i)=-1*((h/(r*cp*dx))+2*kc/(r*cp*dx^2));
      if(i-f)>=1,
            a(i,i-f)=.5*kc/(r*cp*dx^2);
      end;
      if(i+f)<=ef,
            a(i,i+f)=.5*kc/(r*cp*dx^2);
      end;
%reset
      if (i+1)<(ef+1),
            a(i,i+1)=0;
      end;
end;
%
%puddle matrix
%top row
for k=1:f
      a(k,k) =-1*((h/(r*cp*dx))+2*kc/(r*cp*dx^2));
      if k>1,
            a(k,k-1)=.5*kc/(r*cp*dx^2);
      end;
      if k<f,
            a(k,k+1)=.5*kc/(r*cp*dx^2);
      end;
end;
%
%puddle matrix
%bottom row
for k=2:f-1
      i=e*f-f+k;
      a(i,i+n/2+f/2)=1*kc/(r*cp*dx^2);
end;
%
%puddle matrix
%top left corner
a(1,1) = -1*((h/(r*cp*dx))+1*kc/(r*cp*dx^2));
a(1,1+f)=.5*kc/(r*cp*dx^2);
a(1,2)=.5*kc/(r*cp*dx^2);
```

```
%
%puddle matrix
%top right corner
a(f,f) = -1*((h/(r*cp*dx))+1*kc/(r*cp*dx^2));
a(f,f+f)=.5*kc/(r*cp*dx^2);
a(f,f-1)=.5*kc/(r*cp*dx^2);
%
%puddle matrix
%bottom left corner
i=e*f-f+1;
a(i,i)=-1*((h/(r*cp*dx))+2*kc/(r*cp*dx^2));
a(i,i-f)=.5*kc/(r*cp*dx^2);
a(i,i+n/2+f/2)=.5*kc/(r*cp*dx^2);
%
%puddle matrix
%bottom right corner
i=e*f;
a(i,i)=-1*((h/(r*cp*dx))+2*kc/(r*cp*dx^2));
a(i,i-f)=.5*kc/(r*cp*dx^2);
a(i,i+n/2+f/2)=.5*kc/(r*cp*dx^2);
%%%%%%%%%%%%%%%%%%%%%%%%%%%%%%%%%%%%%%%%%%%%%%%%%%%
%%%%%%%%%%%%%%%%%%%%%%%%%%%%%%%%%%%%%%%%%%%%%%%%%%%
%%%%%%%%%%%%%%%%%%%%%%%%%%%%%%%%%%%%%%%%%%%%%%%%%%%
%
%base
%interior nodes
for i=ef+1:ef+mn;
      a(i,i) = -4*kc/(r*cp*dx^2);
      if (i-(ef+1))>=1,
            a(i,i-1)=1*kc/(r*cp*dx^2);
      end;
      if (i+1)<= ef+mn,
            a(i,i+1)=1*kc/(r*cp*dx^2);
      end;
      if (i-n)>=ef+1,
            a(i,i-n)=1*kc/(r*cp*dx^2) ;
      end;
      if (i+n)<= ef+mn,
            a(i,i+n)=1*kc/(r*cp*dx^2);
      end;
end;
%
%base
%top row under puddle
for k=1:f-2
      i=e*f+n/2-f/2+1+k; %20+k
      a(i,i-(n/2+f/2))=1*kc/(r*cp*dx^2);
end;
%
%base
%top row under puddle left corner
i=e*f+n/2-f/2+1;
a(i,i) = -1*((h/(r*cp*dx))+3*kc/(r*cp*dx^2));
a(i,i-(n/2+f/2))=.5*kc/(r*cp*dx^2);
```

```
a(i,i-1)=.5*kc/(r*cp*dx^2);
%
%base
%top row under puddle right corner
i=e*f+n/2-f/2+f
a(i,i) = -1*((h/(r*cp*dx))+3*kc/(r*cp*dx^2));
a(i,(i-(n/2+f/2)))=.5*kc/(r*cp*dx^2);
a(i,i+1)=.5*kc/(r*cp*dx^2);
%
%base
%top row left of puddle
for k=ef+1:(ef+1+n/2-f/2-1)
      a(k,k) =-1*((h/(r*cp*dx))+2*kc/(r*cp*dx^2));
      if k>=ef+2,
            a(k,k-1)=.5*kc/(r*cp*dx^2);
      end;
      a(k,k+1)=.5*kc/(r*cp*dx^2);
end;
%
%base
%top row right of puddle
for k=ef+1+n/2+f/2:ef+n
      a(k,k) =-1*((h/(r*cp*dx))+2*kc/(r*cp*dx^2));
      a(k,k-1)=.5*kc/(r*cp*dx^2);
      if k<n+ef,
            a(k,k+1)=.5*kc/(r*cp*dx^2);
      end;
end;
%
%base
%left edge
for k=1:m
      i=(k-1)*n+1+ef;
      a(i,i)=-1*((h/(r*cp*dx))+2*kc/(r*cp*dx^2));
      if (i-(1+ef))>=1,
            a(i,i-n)=.5*kc/(r*cp*dx^2);
      end;
      if i<(ef+mn-n+1),
            a(i,i+n)=.5*kc/(r*cp*dx^2);
      end;
%reset
      a(i,i-1)=0;
end;
%
%base
%right edge
for k=1:m
      i=(k-1)*n+n+ef;
      a(i,i)=-1*((h/(r*cp*dx))+2*kc/(r*cp*dx^2));
      if i>(n+ef),
            a(i,i-n)=.5*kc/(r*cp*dx^2);
      end;
      if(i+1)<=(mn+ef),
            a(i,i+n)=.5*kc/(r*cp*dx^2);
```

```
      end;
%reset
      if i<(mn+ef),
            a(i,i+1)=0;
      end;
end;
%
%base
%bottom row
for k=1:n
      i=(m-1)*n+k+ef;
      a(i,i) = -1*((h/(r*cp*dx))+2*kc/(r*cp*dx^2));
      if (i-1)>=(mn-n+1+ef),
            a(i,i-1)=.5*kc/(r*cp*dx^2);
      end;
      if (i+1)<=(mn+ef),
            a(i,i+1)=.5*kc/(r*cp*dx^2);
      end;
end;
%
%base
%top left corner
a(ef+1,ef+1) = -1*((h/(r*cp*dx))+1*kc/(r*cp*dx^2));
a(ef+1,ef+1+n)=.5*kc/(r*cp*dx^2);
a(ef+1,ef+2)=.5*kc/(r*cp*dx^2);
%
%base
%top right corner
a(ef+n,ef+n) = -1*((h/(r*cp*dx))+1*kc/(r*cp*dx^2));
a(ef+n,ef+n+n)=.5*kc/(r*cp*dx^2);
a(ef+n,ef+n-1)=.5*kc/(r*cp*dx^2);
%reset
a(ef+n,ef+n+1)=0;
%
%base
%bottom left corner
a(ef+mn-n+1,ef+mn-n+1) = -1*((h/(r*cp*dx))+1*kc/(r*cp*dx^2));
a(ef+mn-n+1,ef+mn-2*n+1)=.5*kc/(r*cp*dx^2);
a(ef+mn-n+1,ef+mn-n+2)=.5*kc/(r*cp*dx^2);
%reset
a(ef+mn-n+1,ef+mn-n)=0;
%
%base
%bottom right corner
a(ef+mn,ef+mn) = -1*((h/(r*cp*dx))+1*kc/(r*cp*dx^2));
a(ef+mn,ef+mn-1)=.5*kc/(r*cp*dx^2);
a(ef+mn,ef+mn-n)=.5*kc/(r*cp*dx^2);
%%%%%%%%%%%%%%%%%%%%%%%%%%%%%%%%%%%%%%%%%%%%%%%%%%%%%%%%
%%%%%%%%%%%%%%%%%%%%%%%%%%%%%%%%%%%%%%%%%%%%%%%%%%%%%%%%
%%%%%%%%%%%%%%%%%%%%%%%%%%%%%%%%%%%%%%%%%%%%%%%%%%%%%%%%
%
%B,C,D
%
%b matrix
```

```
b=eye(mn+ef,mn+ef);
%c
c=eye(mn+ef,mn+ef);
%d
d=zeros(mn+ef,mn+ef);
%time
time=linspace(.001,.5,500);
%%%%%%%%%%%%%%%%%%%%%%%%%%%%%%%%%%%%%%%%%%%%%%%%%%%
%%%%%%%%%%%%%%%%%%%%%%%%%%%%%%%%%%%%%%%%%%%%%%%%%%%
%%%%%%%%%%%%%%%%%%%%%%%%%%%%%%%%%%%%%%%%%%%%%%%%%%%
%input
input=zeros(500,mn+ef);
for i=1:500;
%top puddle
      for j=1:f;
            input(i,j)=((h*ts)/(dx*r*cp));
      end;
%left side of puddle
      for j=1:(e-1);
            input(i,j*f+1)=((h*ts)/(dx*r*cp));
      end;
%right side of puddle
      for j=1:(e-1);
            input(i,j*f+f)=((h*ts)/(dx*r*cp));
      end;
% base top left
      for j=ef+1:(ef+1+n/2-f/2);
            input(i,j)=((h*ts)/(dx*r*cp));
      end;
%base top right
      for j=(ef+n/2+f/2):(ef+n);
            input(i,j)=((h*ts)/(dx*r*cp));
      end;
%base left side
      for j=1:(m-2);
        input(i,ef+1+j*n)=((h*ts)/(dx*r*cp));
      end;
%base right side
      for j=2:(m-1);
        input(i,ef+j*n)=((h*ts)/(dx*r*cp));
      end;
%base bottom
      for j=ef+((mn-n)+1):ef+mn;
            input(i,j)=((h*ts)/(dx*r*cp));
      end;
end;
%%%%%%%%%%%%%%%%%%%%%%%%%%%%%%%%%%%%%%%%%%%%%%%%%%%
%%%%%%%%%%%%%%%%%%%%%%%%%%%%%%%%%%%%%%%%%%%%%%%%%%%
%%%%%%%%%%%%%%%%%%%%%%%%%%%%%%%%%%%%%%%%%%%%%%%%%%%
%initial conditions
for i=1:ef;
            u0(1,i)=1400;
end;
for i=ef+1:ef+mn;
```

```
            u0(1,i)=t0;
end;
```

Appendix B: Controller Code

```
/*
*********************************************************************
* Program          : controller
* Description      : Controls the temperature and the flow.  The
*                    temperature controller is a PI controller with
*                    anti-windup. The flow controller is a PI controller.
*
* Date             : 2/25/96   K. Amoruso
*********************************************************************
*/

#include <stdio.h>
#include <conio.h>
#include <stdlib.h>
#include <dos.h>
#include <time.h>
#include <bios.h>
#include <math.h>
#include <graph.h>
#include "pclerrs.h"
#include "pcldefs.h"
#define FNAME "teste.dat"
#define gain 1                  /*DT2801-amplification incoming signal*/
#define arcvoltchan 0           /*Arc voltage is hooked to channel 0*/
#define nPyroChannel 2          /*Pyrometer is hooked to channel 2*/

main()
{
      /* Declare variables     */
      /*                       */

      clock_t ti, tf, ti1;
      FILE *tmpread_filename;
      float bias, desired_temp, max_arc, desired_resistance;
      float max_arc_ct, sumdt, voltage;
      float fSum, fPyroVolt, fPyroTemp;
      float t, e, igral, pwr;
      float kpt, kit, uc, u;
      float em1, ant, ant1, kant;
      float ev;
      float vc, v, volt;
      float t_elap_loop, loop, t_elap;
      float kpf, kif;
      float igralv, ev1;
      int ch, done;
      short nI, vi;
      unsigned short analog_data_value, aver;
      unsigned short sAnalogDataVal, sAver;
      unsigned short dac_data[2];
```

```
/*                          */
/*Initialize Parameters */
/*                          */

t=0.5;

/*                                */
/*Temperature PI Parameters   */
/*                                */

kpt=25;
kit=1.25;
kant=2;
ant=0;
igral=0;

/*                          */
/*Flow PI Parameters    */
/*                          */

kpf=200;
kif=6;
igralv=0;
ev1=0;
em1=0;

/*                                */
/*Loop Control Parameters     */
/*                                */

done=0;
loop=0;

/*                                      */
/*Initialize the DT 2801-A Board    */
/*                                      */

initialize();
select_board(1);

/*                                      */
/*Obtain User Specified Values      */
/*                                      */

_clearscreen( _GCLEARSCREEN );
printf("Enter bias voltage: ");
scanf("%f", &bias);
printf("Enter desired Temperature: ");
scanf("%f", &desired_temp);
printf("Enter max arc current: ");
scanf("%f", &max_arc);
printf("Enter desired resistance: ");
scanf("%f", &desired_resistance);
```

```
/*                                    */
/* Obtain pointer for the data file */
/*                                    */

tmpread_filename = fopen(FNAME, "w");

/*                                    */
/* Obtain the initial clock time    */
/*                                    */

ti = clock();
ti1=ti;

/*                                    */
/* Quantizing the max arc current   */
/*                                    */

max_arc_ct = (max_arc/200)*2048+2048;

/*                                          */
/* Exit the program if q was pressed      */
/*                                          */

while (!done)
{

      /*                                                    */
      /* Stop executing control if any key is pressed */
      /*                                                    */

      while(kbhit()==0)
      {

            /*                                */
            /* Obtain the analog voltage  */
            /*                                */

            sumdt=0;
            for (vi=0; vi<10 ; vi++)
            {
                  adc_value(arcvoltchan, gain,
                  &analog_data_value);
                  sumdt += analog_data_value;
            }
            aver = (unsigned short)(sumdt/10);
            analog_to_volts(aver, gain, &voltage);
            voltage=voltage/.24+bias;

            /*                                */
            /* Obtain Pyrometer reading   */
            /*                                */

            fSum = 0.0;
```

```
for (nI=0; nI<10; nI++)
{
      adc_value(nPyroChannel,gain,&sAnalogDataVal);
      fSum += (float)sAnalogDataVal;
}
sAver = (unsigned short)(fSum/10.0);
analog_to_volts(sAver,gain,&fPyroVolt);
fPyroTemp = 500.0+150.*fPyroVolt;

/*                                          */
/* Implement PI Control Law for Temp        */
/*                                          */

e=desired_temp-fPyroTemp;
igral=(t*(e+ant+em1+ant1))/2+igral;
pwr=(kpt*e+kit*igral);
uc=pwr/14;
u=(uc/200)*2048+2048;
em1=e;
ant1=ant;

/*                                    */
/* Check Control Current Value        */
/*                                    */

if(u<2250)
{
      ant=kant*(20-uc);
      uc=20;
      dac_data[0]=2253;
      dac_value(1,&dac_data[0]);
}
if(u>max_arc_ct)
{
      ant=kant*(max_arc-uc);
      uc=max_arc;
      dac_data[0]=(unsigned short)(max_arc_ct);
      dac_value(1, &dac_data[0]);
}
if(u<=max_arc_ct && u>=2250)
{
      ant=0;
      dac_data[0]=(unsigned short)(u);
      dac_value(1,&dac_data[0]);
}

/*                                    */
/*Implement PI Control Law for Flow */
/*                                    */

ev=desired_resistance-(voltage/.24/uc);
igralv=(t*(ev+ev1))/2+igralv;
v=(kpf*ev+kif*igralv);
vc=2048+2048/10*v;
```

```
ev1=ev;

/*                        */
/*Check Voltage Value     */
/*                        */

if(v<=0)
{
      dac_data[0]=2048;
      dac_value(0,&dac_data[0]);
      volt=0;
}
if(v>10)
{
      dac_data[0]=4096;
      dac_value(0,&dac_data[0]);
      volt=10;
}
if(v>0 && v<=10)
{
      dac_data[0]=(unsigned short)(vc);
      dac_value(0,&dac_data[0]);
      volt=v;
}

/*                 */
/*End of Loop      */
/*                 */

while (!loop)
{
      tf = clock();
      t_elap_loop=(float)(tf-ti1)/1000;
      if(t_elap_loop>=0.5)
      {
            loop=1;
      }
}
ti1=tf;
loop=0;
t_elap = (float)(tf-ti)/1000;

/*                 */
/*Output data      */
/*                 */

_clearscreen( _GCLEARSCREEN );
printf("Time(seconds): %4.1f \n",t_elap);
printf("\n");
printf("Desired Temperature (C): %4.0f\n",
desired_temp);
printf("Pyrometer output (C): %4.0f\n",fPyroTemp);
printf("\n");
printf("Arc Current: %3.0f\n",uc);
```

```
            printf("Arc Voltage: %2.1f\n",voltage);
            printf("Arc Power (Watts): %3.0f\n",uc*voltage);
            printf("\n");
            printf("Desired Resistance: %2.3f\n",
            desired_resistance);
            printf("Actual Resistance:%2.3f\n",voltage/uc);
            printf("\n");
            printf("Voltage to valve (V): %4.2f\n",volt);
            printf("\n");
            printf("Press q to stop program.")
            printf("\n");
            printf("Press space to change desired Temp.")
            printf("\n");
            printf("Press r to change desired resistance.")
            printf("\n");
            fprintf(tmpread_filename,"%4.3f %2.4f %2.4f %4.0f %f
                  %2.3f %2.3f %2.2f\n", t_elap, voltage, uc,
                  desired_temp, fPyroTemp, desired_resistance,
                  voltage/uc, volt);

      }

      /*                */
      /*Check Keyboard  */
      /*                */

      if (( ch=getch())=='q')
      {
            done=1;
      }
      else if (ch==' ')
      {
            printf("Enter New Desired Temperature: ");
            scanf("%f", &desired_temp);
            _clearscreen( _GCLEARSCREEN );
      }
      else if (ch=='r')
      {
            printf("Enter New Desired Resistance: ");
            scanf("%f", &desired_resistance);
            _clearscreen( _GCLEARSCREEN );
      }
}

/*                                        */
/*if q is pressed the program will stop   */
/*                                        */

fclose(tmpread_filename);
dac_data[0]=(unsigned short)(0);
dac_value(0, &dac_data[0]);
dac_data[1]=(unsigned short)(0);
dac_value(1, &dac_data[1]);
terminate();
```

```
}     /*end of main*/
```

References

1 Budiman, B. Welding Process Control, Seminar. Massachusetts Institute of Technology. January 1995.

2 Campbell, I.E. High Temperature Materials and Technology. Wiley, New York, NY. 1967.

3 Data Translation. User Manual for DT2801. Data Translation Inc., Marlboro, MA. Document UM-00666-D-1855. 1985.

4 Data Translation. PCLAB User Manual: Data Acquisition Subroutine Library. Data Translation Inc., Marlboro, MA. Document UM-02899-F. 1991.

5 Doumanidis, C.C. Modeling and Control of Thermal Phenomena in Welding, Ph.D. Thesis. Massachusetts Institute of Technology. February 1988.

6 Fay, J. A. Introduction to Fluid Mechanics. MIT Press, Cambridge, MA. 1994.

7 Franklin, G. F., Powell, J.D., Emami-Naeini, A. Feedback Control of Dynamic Systems. Addison-Wesley, Reading, MA. 1986.

8 Hale, M.B. Multivariable Dynamic Modeling and Control of GMAW Weld Pool Geometry, Ph.D. Thesis. Massachusetts Institute of Technology. September 1989.

9 Hardt, D. E. Welding Process Modeling and Re-Design for Control. Proceedings Japan/USA Symposium on Flexible Automation, Kobe. July 1994.

10 Horowitz, P., Hill, W. The Art of Electronics, 2nd Ed. Cambridge University Press, New York, NY. 1989.

11 Incropera, F. P., DeWitt, D.P. Introduction to Heat Transfer, 2nd Ed. Wiley, New York, NY. 1990.

12 Lee, S. Development of a Continuous Flow Arc Furnace for Welding Applications, S. M. Thesis. Massachusetts Institute of Technology. September 1993.

13 Luxtron Corporation. Users Manual Accufiber Model 100C. Accufiber Division of the Luxtron Corporation, Beaverton, OR. 1990.

14 Masmoudi, R. A. Modeling and Control of Geometric and Thermal Properties in Arc Welding, Ph.D. Thesis. Massachusetts Institute of Technology. September 1992.

15 The Math Works. Simulink: Dynamic System Simulation Software. The Math Works Inc., Natick, MA. 1993.

16 O'Brien, R. L. Welding Handbook, 8th Ed. American Welding Society, Miami, FL. 1991.

17 Ogata, K. Modern Control Engineering, 2nd Ed. Prentice Hall, Englewood Cliffs, NJ. 1990.

18 Passow, C. H. A Study of Spray Forming Using Uniform Droplet Sprays, S.M. Thesis. Massachusetts Institute of Technology. 1992.

19 Ratliff, C. Development of a Stream Welding Process, S. M. Thesis. Massachusetts Institute of Technology. September 1993.

20 Samsonov, G. V. Plenum Press Handbook of High-Temperature Materials No. 2 Properties Index. Plenum Press, New York, NY. 1964.

21 Singer. U.K. Patent Application GB 2142858A. 1985.

22 Song, J. Multivariable Adaptive Control in GMA Welding Using a Thermally Based Depth Estimator, Ph.D. Thesis. Massachusetts Institute of Technology. February 1992.

23 Stein, G. Limitations on Achievable Performance of Feedback Systems, Multivariable Control Systems Lecture Notes Ref. No. 850429/6232. Massachusetts Institute of Technology. April 1985.